

NACA TM 1360

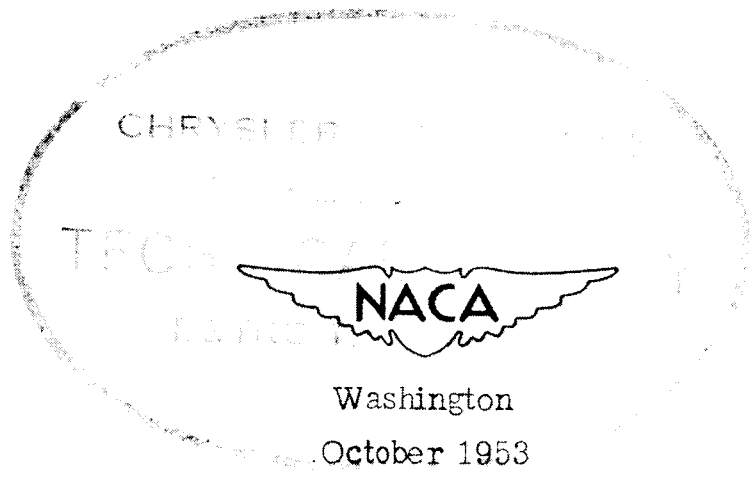
NATIONAL ADVISORY COMMITTEE FOR AERONAUTICS

TECHNICAL MEMORANDUM 1360

CONCERNING THE FLOW ABOUT RING-SHAPED COWLINGS
PART XII - TWO NEW CLASSES OF CIRCULAR COWLS

By Dietrich Küchemann and Johanna Weber

Translation of "ZWB Untersuchungen und Mitteilungen No. 3111."



TM 1360

NATIONAL ADVISORY COMMITTEE FOR AERONAUTICS

TECHNICAL MEMORANDUM 1360

CONCERNING THE FLOW ABOUT RING-SHAPED COWLINGS

PART XII - TWO NEW CLASSES OF CIRCULAR COWLS*

By Dietrich Küchemann and Johanna Weber

Abstract: For application in practice for annular radiator fairings and similar arrangements, two new classes of circular cowls are developed by theoretical method, and investigated in a systematic test series regarding their behavior under various working conditions.

Outline:

- I. STATEMENT OF THE PROBLEM
- II. DESCRIPTION OF THE CIRCULAR COWLS
 - 1. The Two New Classes
 - 2. Supplement to Class I of Circular Cowl
- III. TEST PERFORMANCE
- IV. RESULTS
 - 1. The Two New Classes
 - 2. Supplement to Class I of Circular Cowl
- V. SUMMARY

SYMBOLS

x, r rectangular coordinates; x in direction of the axis of rotation

R_E radius of the cowl in the entrance cross section (narrowest cross section in the inlet part)

R_a maximum outer radius of the cowl

R_N radius of the hub in the entrance cross section

ρ_N radius of curvature of the inlet lip

$$F_E = \pi R_E^2 - \pi R_N^2$$

*"Über die Strömung an ringförmigen Verkleidungen. XII Mitteilung: Zwei neue Klassen von Ringhauben." Untersuchungen und Mitteilungen No. 3111. (ZWB).

$$F_a = \pi R_a^2$$

F_E/F_a contraction of cowl

$F_E'/F_a = \frac{R_E^2}{R_a^2}$, contraction of circular cowl without hub

α angle of attack

v_o undisturbed free-stream velocity

v_E mean value of velocity in the entrance cross section

v_E/v_o inlet velocity ratio

v_{E_o}/v_o inlet velocity ratio for $\alpha = 0^\circ$ for same position of the sliding throttle valve

v_{max} maximum velocity on the outside of the circular cowl

p local static pressure

p_o static pressure in the undisturbed flow

q_o dynamic pressure of approach flow, $\frac{\rho}{2}v_o^2$

p_{ges} local total pressure

η_E	inlet efficiency; mean value of $\frac{p_{ges} - p_0}{q_0}$ over the entrance cross section*
ζ_E	loss factor; mean value of $\frac{p_{ges} - p}{p_0 - p}$ over the entrance cross section*

I. STATEMENT OF THE PROBLEM

The basic phenomena concerning the inlet problem in fairings of propulsion units may be regarded today as clarified to a high degree.¹ Still lacking is the systematic investigation of different forms for the use in practice. On our part, there exist so far only two classes of symmetrical circular cowls¹ which are chiefly visualized for application in inlets of special propulsion units. Due to their relatively considerable contraction and their slenderness, they are, however, less suitable for fairings of circular radiators or radial engines. It is the aim of the present report to prepare usable cowls to include these application purposes and to indicate their properties at least for the incompressible case.

In the practical use of such cowls, it has always been found expedient to indicate certain classes of cowls, the individual shapes of which are related to each other so that an interpolation is directly possible. This corresponds to a custom which proved very successful also for standard wing profiles. Thus, we shall indicate, for the application of circular cowls for radiator fairings, two new classes of circular cowls in the form of geometrical systematics, and shall determine their properties for various flow quantities and angles of attack with the aid of wall pressure-distribution measurements. Moreover, the class I of cowls which has already been set up is to be supplemented by further forms of particularly pronounced contraction.

*NACA reviewer's footnote: The symbols η_E and ζ_E are used in figures 57 and 58 of the present paper and are not area weighted quantities as is indicated in the definition under the symbols. As used in figure 57 η_E appears to be the arithmetic mean of the maximum and minimum value of $\frac{p_{ges} - p_0}{q_0}$. As used in figure 58 ζ_E appears to be one minus the arithmetic mean of the maximum and minimum value of $\frac{p_{ges} - p}{p_0 - p}$.

¹Compare D. Küchemann and J. Weber: Das Einlaufproblem bei Triebwerksverkleidungen. Mitteilungen der Deutschen Akademie der Luftfahrtforschung, 1943.

II. DESCRIPTION OF THE CIRCULAR COWLS

1. The Two New Classes

Like the cowls previously set up, those of the two new classes also have resulted from a theoretical calculation. Without discussing in detail the actual calculation which is based on the method of singularities, we shall describe here only the goal we aimed at.

The previous cowls of classes I and II had a relatively pronounced contraction ($F_E/F_a \leq 0.4$) and were slender (the cylindrical piece on which the maximum diameter was attained began at a distance $2R_a$ or $1R_a$, respectively, from the entrance plane); the new cowls therefore had to include the range of lesser contraction and, moreover, were to be shorter. In the class III, the maximum diameter is attained at a distance $1.R_a$ from the entrance plane and the values of F_E/F_a are between 0.3 and 0.5, whereas, the cowls of class IV are still shorter (maximum diameter at $0.5R_a$) and show still lesser contraction (F_E/F_a between 0.4 and 0.6). A further shortening and further lessening of the contraction is hardly of interest for applications at present since then the aerodynamic properties become too unfavorable as we shall see below. Due to these slight contractions, it is not always possible to round off the inlet lip to such a degree that even when nonmoving air is sucked in (static conditions) no more flow losses in the interior occur. However, this severe condition need no longer be set generally, since we shall deal with engine or radiator cowls where such a state of flow hardly occurs. Thus, the radius of curvature is considerably smaller than would be required for the static condition; on the other hand, it was, of course, kept as large as possible: for many application purposes (for instance, drum radiator) a lip rounded as much as possible, if only for reasons of space economy, is desirable; moreover, the aerodynamic properties generally deteriorate considerably with decreasing radius of curvature, also for high-speed flight and oblique approach flow, as we shall see later.

As a measure for the aerodynamic load on the cowl, we had to depend on the maximum excess velocity occurring, although at high speeds it by no means necessarily characterizes the Mach sensitivity unequivocally.² Nevertheless, the value of v_{\max}/v_0 can convey a good comprehensive view of the behavior of the separate cowls and show, for instance, the sensitiveness to variations of the working conditions, and the possibility of an increase in drag by separation phenomena,

²Compare H. Ludwig: Widerstandsmessungen an zwei Ringhauben bei hohen Geschwindigkeiten. UM 3026, 1943.

particularly in incompressible flow. In the calculation, which was performed only for one state of operation, high-speed flight with symmetrical approach flow, we endeavored to keep the value of v_{\max}/v_0 constant in this state within one class of cowls. Thus, v_{\max}/v_0 was to be about 1.3 for class III for a v_E/v_0 of about 0.3 (which generally is approximately the case for radiator fairings), and about 1.4 for class IV with the same flow quantity. As a consequence, the cowls with lesser contraction also will have a smaller radius of curvature which agrees with the geometrical facts.

The forms of the two new classes of circular cowls are plotted in figures 1 and 2, the coordinates are given in the numerical tables 1 and 2. Since it will almost always be necessary to interpolate a cowl for a special purpose, diagrams which facilitate this interpolation have been indicated in figures 3 and 4. The shapes of the insides of the cowls have been shown in every case only up to the junction with a cylindrical piece. At this point, one has to adjoin the inner contour corresponding to the purpose; its shape may be assumed as highly independent of the outer flow.

2. Supplement to Class I of Circular Cowls

Class I of circular cowls which is developed particularly for the inlets of special propulsion units was indicated so far only up to a $F_E/F_a = 0.25$; however, since it frequently occurs that the cowl in certain installation arrangements can be considerably more contracted at least over part of the circumference, we supplemented class I in this respect and indicated it up to values $F_E/F_a = 0.10$. Shapes, interpolation diagrams, and coordinates may be found in figures 5 and 6 and in numerical table 3.

III. TEST PERFORMANCE

We investigated three cowls of each of the two new classes: of class III those with $F_E/F_a = 0.3, 0.4, 0.5$, and of class IV those with $F_E/F_a = 0.4, 0.5, 0.6$ so that in every case the entire range is included. In the model, all cowls had the same outer diameter $2R_a = 200$ mm and were continued cylindrically toward the rear corresponding to the sketch in figure 7. By throttle valves at the rear portion cut-off at an obtuse angle or, respectively, by a built-in blower, the flow quantity which we indicate in the form of a ratio v_E/v_0 was varied; in every case, the wall pressure distribution on the cowl as well as the total

pressure and the static pressure in the inlet inside were measured. The measuring plane was at a distance of 50 mm from the entrance plane; the cross section showing the most extreme conditions in case of variation of the angle of attack was singled out; measurement of the entire circular cross section was omitted.

For the following results, the wall pressure distributions have been indicated in every case for the various inlet velocity ratios for $\alpha = 0^\circ$ and for $v_E/v_0 = 0$ and also for various angles of attack, since for this state the most extreme values occur. For the other inlet velocity ratios too, series of angles of attack have been measured but not indicated in detail. The results, if desired, may be had from the AVA. We merely determined and plotted the occurring maximum excess velocities.

The flow quantity was determined from the measurement in the inner cross section and, due to the simplification in the measurement, is correct only for the case $\alpha = 0^\circ$. We kept the throttling position constant for angles of attack different from zero and indicated, for characterization of the flow quantity, the corresponding value for $\alpha = 0^\circ$ which is denoted by v_{E_0}/v_0 .

Furthermore, we should like to point out a certain dubiousness in the measurements with angle of attack which is caused by the body shape used behind the inlet cowl (compare fig. 7). Since, in case of oblique position, the entire body is subject to a lateral flow which is the reason for the dissymmetry on the cowl, and since this lateral flow in turn depends partly on the body shape, the variation of the excess velocity with α also will be influenced by the body shape, for this reason. It would therefore be more accurate to introduce also for these measurements a number corresponding to the lift curve slope for standard wing profiles, and thus to correct the results. Anyway, the results can give a good comprehensive view in the form indicated. We evaluated the measurement in the inner cross section also as to the losses occurring in the inflow; we indicated it in the form of an inlet efficiency

$$\eta_E = \frac{p_{ges} - p_0}{q_0}$$

Especially for the static condition, where this definition fails, we used a loss factor

$$\zeta_E = \frac{p_{ges} - p}{p_0 - p}$$

which sets up a relation between the actual kinetic energy of the flow and the energy to be expected theoretically. For both quantities, the mean values have to be taken over the entrance cross section.

For the circular cowls investigated, one may assume that they frequently are used in combination with a projecting hub. Thus, we investigated all cowls also with hub. In order not to increase the number of parameters prohibitively, we used only similar hub shapes which all obstruct exactly half the entrance cross section of the cowl and one developed as ellipsoids of revolution of the axis ratio 2:1 the small axis of which lies in the entrance plane of the cowl. In proportion with the outer diameter of the cowl, the hubs are thus different for the different contractions of the cowls (compare figs. 8 and 9).

The tests were carried out in the wind tunnel of the KWJ (0.7×1 m free jet).

IV RESULTS

1. The Two New Classes

The measured results obtained on the classes III and IV of circular cowls are given in figures 10 to 46. The cowls with the largest contraction of each class have a pressure distribution with a flat minimum lying relatively far to the rear. Due to the pronounced rounding of their lips, these cowls are rather insensitive to variations in flow quantity as well as in angle of attack. The presence of a hub - on which there appears, particularly for small flow quantities, the known boundary-layer separation - also produces only a very slight drop in the excess velocities.

With decreasing contraction, the excess velocities do not rise at first, in contrast to the experience with cowl class I. The reason lies in the simultaneously reduced rounding of the lip whereby the pressure distribution flattens noticeably without the minimum assuming a lower position. These phenomena can be observed in the models of even the least contracted cowls of both classes which becomes particularly clear in the comparative plots of figures 47 to 56. It is true that these cowls, especially those of class III with $F_E/F_a = 0.5$, then are extremely sensitive to every change in working conditions. In the wall pressure distributions, one can find, even for $\alpha = 0^\circ$ and small flow quantity, at least local separation phenomena with a very steep rise of the excess velocities; the same occurs in case of small variations in angle of attack. Although these processes need not

absolutely make themselves felt in an increase in drag, such an increase, to a considerable degree, is to be expected for the separation phenomena which are clearly recognizable in the figures. In the plotting of v_{max}/v_0 the regions with local separations have been drawn in dashed lines, those with complete separation in dotted lines.

Since the cowls with slight contraction possess a very pronounced narrow pressure minimum directly at the inlet lip, this pressure minimum can be noticeably influenced by the welling over of the flow made turbulent by the hub separation. An already existing local separation in the case without hub thus frequently may be made to disappear completely; the drop in excess velocities also may be considerable.

Entrance losses generally do not occur in case of the cowl without hub. Only for very large angles-of-attack do separation phenomena appear on the inside of the less rounded cowls. Of importance though is the loss factor for static condition which rises continuously with decreasing radius of the lip. The development of a region of separation in the interior space for static condition is, naturally, noticeably impeded by a hub. In high-speed flight, however, the projecting hub may cause considerable flow losses, the effect of which can be very noticeable for instance on the radiator lying behind the hub.

On the whole, we can state that the theory has yielded a number of usable circular cowls, and that the theoretical predictions have been satisfactorily fulfilled. It is now possible for the designer to select without delay a cowl useful for his purposes, the properties of which are known to a great extent. For the application in annular radiators and radial engines, generally, a cowl of class IV will best meet the requirements under present standard conditions. In a later report, we shall discuss what conclusions may be drawn from the existing measurements quite generally for the design of annular radiators.

2. Supplement to Class I of Circular Cowls

In the newly added cowls of class I, the very pronounced rounding of the lip is particularly striking; at first glance, it appears almost clumsy. This is, however, to a great extent, a corrigible matter of habit since the aerodynamic properties of these cowls must be denoted as very favorable. A pressure distribution measurement on a nonrotationally symmetrical cowl (this is the application they are predominantly meant for) may serve as evidence. The cowl measured was of circular cross section in its lower part (class I with $F_E/F_a = 0.3$) and in the upper part continuously thickened up to the ridge where it attains a (local) F_E/F_a of 0.1. The wall pressure distributions in the state of most extreme stress ($v_E = 0$) for various oblique approach flows show

a favorable course so that such an inlet form seems suitable, especially for the wing installation of special propulsion units. The related problems will be discussed in detail in a later report.

V. SUMMARY

Two new classes of circular cowls are indicated for use in practice which are particularly suitable as fairings of annular radiators and radial engines. For any existing purpose, a cowl may be interpolated from completed diagrams in the simplest manner; the aerodynamic properties of each cowl may be largely ascertained from a systematic test series. Thus, the maximum excess velocities on the outside of the cowl and the certain losses for the various inlet velocity ratios and angles of attack are given. Furthermore, the states for which separation phenomena occur can be recognized.

The already existing class I of cowls is supplemented by cowls of particularly strong contraction as are needed in some cases for installation in special propulsion units.

Translated by Mary L. Mahler
National Advisory
Committee for Aeronautics

NUMERICAL TABLE 1
CLASS III OF CIRCULAR COWLS

$F_E/F_a =$	0.3	0.35	0.4	0.45	0.5
x/R_E	r/R_E	r/R_E	r/R_E	r/R_E	r/R_E
Coordinates of the outsides					
0	1.190	1.136	1.091	1.056	1.030
.05	1.351	1.267	1.203	1.155	1.116
.1	1.420	1.327	1.255	1.201	1.156
.15	1.473	1.373	1.295	1.236	1.187
.2	1.515	1.410	1.328	1.265	1.213
.25	1.550	1.441	1.356	1.290	1.235
.3	1.580	1.468	1.381	1.313	1.255
.4	1.628	1.512	1.421	1.350	1.288
.5	1.665	1.547	1.453	1.379	1.315
.6	1.695	1.575	1.479	1.403	1.337
.7	1.720	1.598	1.501	1.423	1.355
.8	1.741	1.618	1.519	1.439	1.370
.9	1.759	1.635	1.535	1.453	1.382
1.0	1.774	1.649	1.548	1.465	1.393
1.1	1.786	1.660	1.558	1.475	1.402
1.2	1.797	1.669	1.566	1.482	1.408
1.3	1.806	1.677	1.572	1.487	1.412
1.4	1.813	1.683	1.577	1.490	1.414
1.5	1.818	1.687	1.580	1.491	1.414
1.6	1.822	1.689	1.581	1.491	1.414
1.7	1.825	1.690	1.581	1.491	1.414
1.8	1.826	1.690	1.581	1.491	1.414
1.9	1.826	1.690	1.581	1.491	1.414
2.0	1.826	1.690	1.581	1.491	1.414
Coordinates of the insides					
0.05	1.067	1.032	1.011	1.001	1.000
.1	1.031	1.008	1.000	1.000	1.000
.15	1.010	1.000	1.000	1.000	1.000
.2	1.001	1.000	1.000	1.000	1.000
.25	1.000	1.000	1.000	1.000	1.000
Radius of curvature ρ_N/R_E		(Coordinates of the center of curvature: $x = \rho_N$; $r = r$ for $x = 0$)			
$\rho_N/R_E =$	0.180	0.132	0.090	0.056	0.030

NUMERICAL TABLE 2
 CLASS IV OF CIRCULAR COWLS

$F_E/F_a =$	0.4	0.45	0.5	0.55	0.6
x/R_E	r/R_E	r/R_E	r/R_E	r/R_E	r/R_E

Coordinates of the outsides

0	1.130	1.105	1.083	1.063	1.045
.05	1.290	1.245	1.203	1.164	1.127
.1	1.354	1.301	1.251	1.206	1.165
.15	1.400	1.341	1.286	1.237	1.193
.2	1.437	1.372	1.313	1.261	1.215
.25	1.467	1.397	1.335	1.280	1.232
.3	1.492	1.418	1.353	1.296	1.246
.35	1.513	1.436	1.369	1.310	1.258
.4	1.530	1.451	1.382	1.321	1.268
.45	1.544	1.463	1.392	1.330	1.276
.5	1.555	1.473	1.400	1.337	1.282
.55	1.564	1.480	1.406	1.342	1.287
.6	1.570	1.485	1.410	1.345	1.290
.65	1.575	1.488	1.412	1.347	1.291
.7	1.578	1.490	1.414	1.348	1.291
.75	1.580	1.491	1.414	1.348	1.291
.8	1.581	1.491	1.414	1.348	1.291
.85	1.581	1.491	1.414	1.348	1.291
.9	1.581	1.491	1.414	1.348	1.291
.95	1.581	1.491	1.414	1.348	1.291
1.0	1.581	1.491	1.414	1.348	1.291

Radius of curvature ρ_N/R_E (Coordinates of the center of curvature: $x = \rho_N$; $r = r$ for $x = 0$)

$\rho_N/R_E =$	0.125	0.100	0.078	0.058	0.040
----------------	-------	-------	-------	-------	-------

NUMERICAL TABLE 3

CLASS I OF CIRCULAR COWLS

$F_E/F_a =$	0.1	0.15	0.2	0.25	0.3	0.35	0.4
x/R_E	r/R_E	r/R_E	r/R_E	r/R_E	r/R_E	r/R_E	r/R_E
Coordinates of the outsides							
0	1.312	1.241	1.195	1.170	1.163	1.158	1.155
.05	1.442	1.369	1.322	1.291	1.265	1.247	1.239
.1	1.528	1.443	1.386	1.345	1.310	1.284	1.269
.2	1.660	1.558	1.478	1.417	1.371	1.334	1.309
.3	1.769	1.645	1.547	1.473	1.418	1.374	1.342
.4	1.861	1.718	1.604	1.518	1.457	1.407	1.369
.5	1.941	1.781	1.653	1.557	1.491	1.435	1.392
.6	2.011	1.836	1.696	1.592	1.521	1.460	1.413
.7	2.074	1.885	1.735	1.623	1.548	1.483	1.432
.8	2.132	1.930	1.771	1.652	1.573	1.503	1.449
.9	2.186	1.971	1.804	1.679	1.596	1.521	1.464
1.0	2.238	2.010	1.834	1.704	1.616	1.537	1.477
1.2	2.332	2.080	1.890	1.750	1.651	1.564	1.499
1.4	2.415	2.143	1.940	1.790	1.681	1.587	1.517
1.6	2.489	2.200	1.983	1.825	1.707	1.607	1.532
1.8	2.557	2.250	2.021	1.855	1.730	1.624	1.544
2.0	2.619	2.293	2.054	1.881	1.750	1.639	1.554
2.2	2.676	2.331	2.082	1.904	1.768	1.652	1.562
2.4	2.728	2.366	2.107	1.925	1.783	1.663	1.569
2.6	2.775	2.397	2.130	1.943	1.796	1.672	1.574
2.8	2.818	2.425	2.150	1.958	1.806	1.679	1.578
3.0	2.857	2.450	2.167	1.970	1.814	1.684	1.580
3.2	2.893	2.473	2.181	1.980	1.820	1.688	1.581
3.4	2.926	2.493	2.194	1.988	1.824	1.690	1.581
3.6	2.957	2.510	2.206	1.994	1.826	1.690	
3.8	2.985	2.526	2.216	1.998	1.826		
4.0	3.010	2.540	2.224	2.000			

NUMERICAL TABLE 3 - Concluded

CLASS I OF CIRCULAR COWLS

$F_E/F_a =$	0.1	0.15	0.2	0.25	0.3	0.35	0.4
x/R_E	r/R_E	r/R_E	r/R_E	r/R_E	r/R_E	r/R_E	r/R_E
4.2	3.033	2.552	2.230				
4.4	3.055	2.562	2.234				
4.6	3.075	2.570	2.236				
4.8	3.092	2.576					
5.0	3.107	2.580					
5.2	3.120	2.582					
5.4	3.132						
5.6	3.142						
5.8	3.150						
6.0	3.156						
6.2	3.160						
6.4	3.162						

Coordinates of the insides

0.05	1.063	1.063	1.063	1.063	1.063	1.063	1.063
.10	1.032	1.032	1.032	1.032	1.032	1.032	1.032
.15	1.015	1.015	1.015	1.015	1.015	1.015	1.015
.20	1.006	1.006	1.006	1.006	1.006	1.006	1.006
.30	1.000	1.000	1.000	1.000	1.000	1.000	1.000

Radius of curvature ρ_N/R_E (Coordinates of the center of curvature:
 $x = \rho_N$; $r = r$ for $x = 0$)

$\rho_N/R_E =$	0.205	0.180	0.157	0.135	0.115	0.110	0.090
----------------	-------	-------	-------	-------	-------	-------	-------

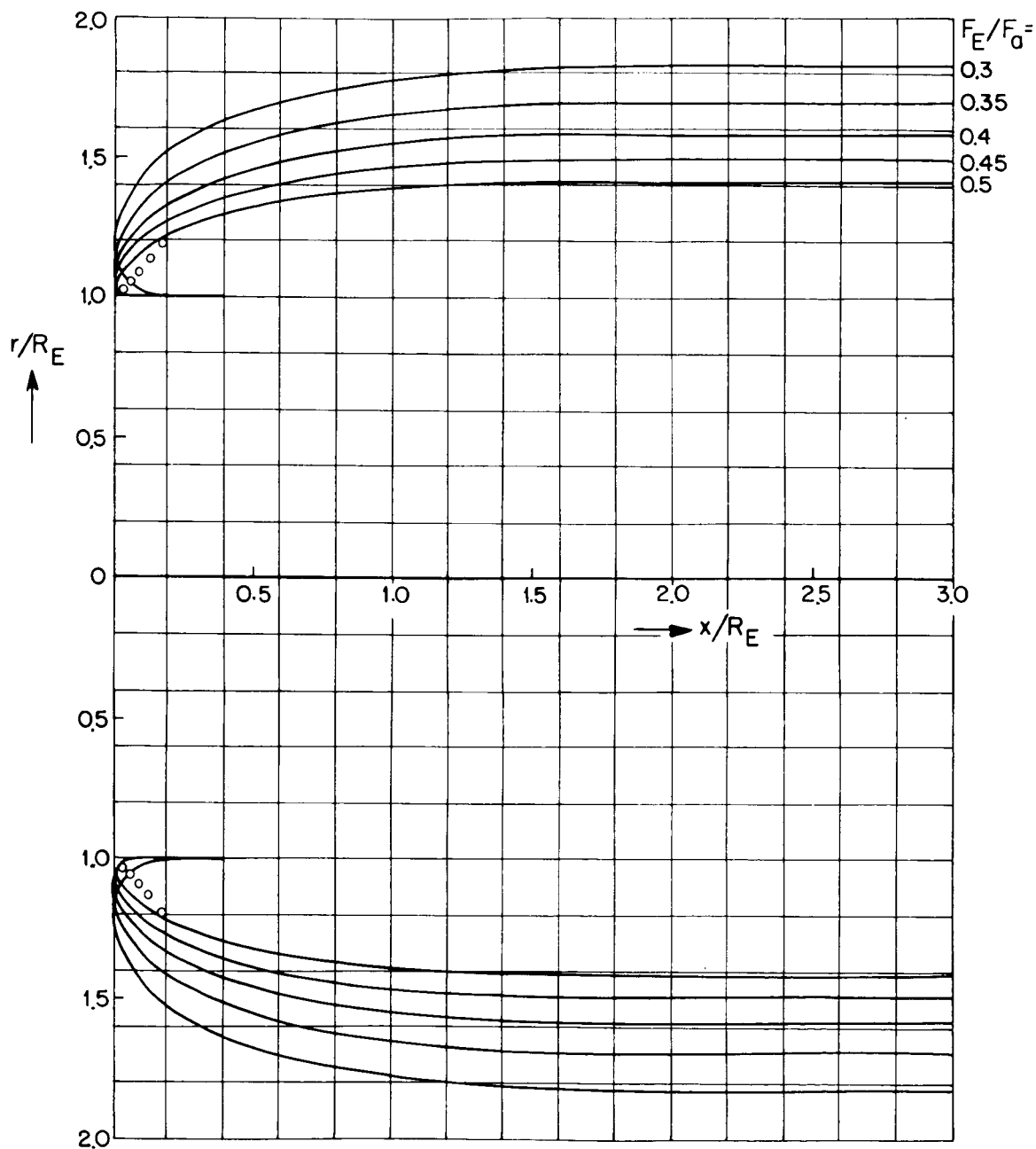


Figure 1.- Class III of circular cowls.

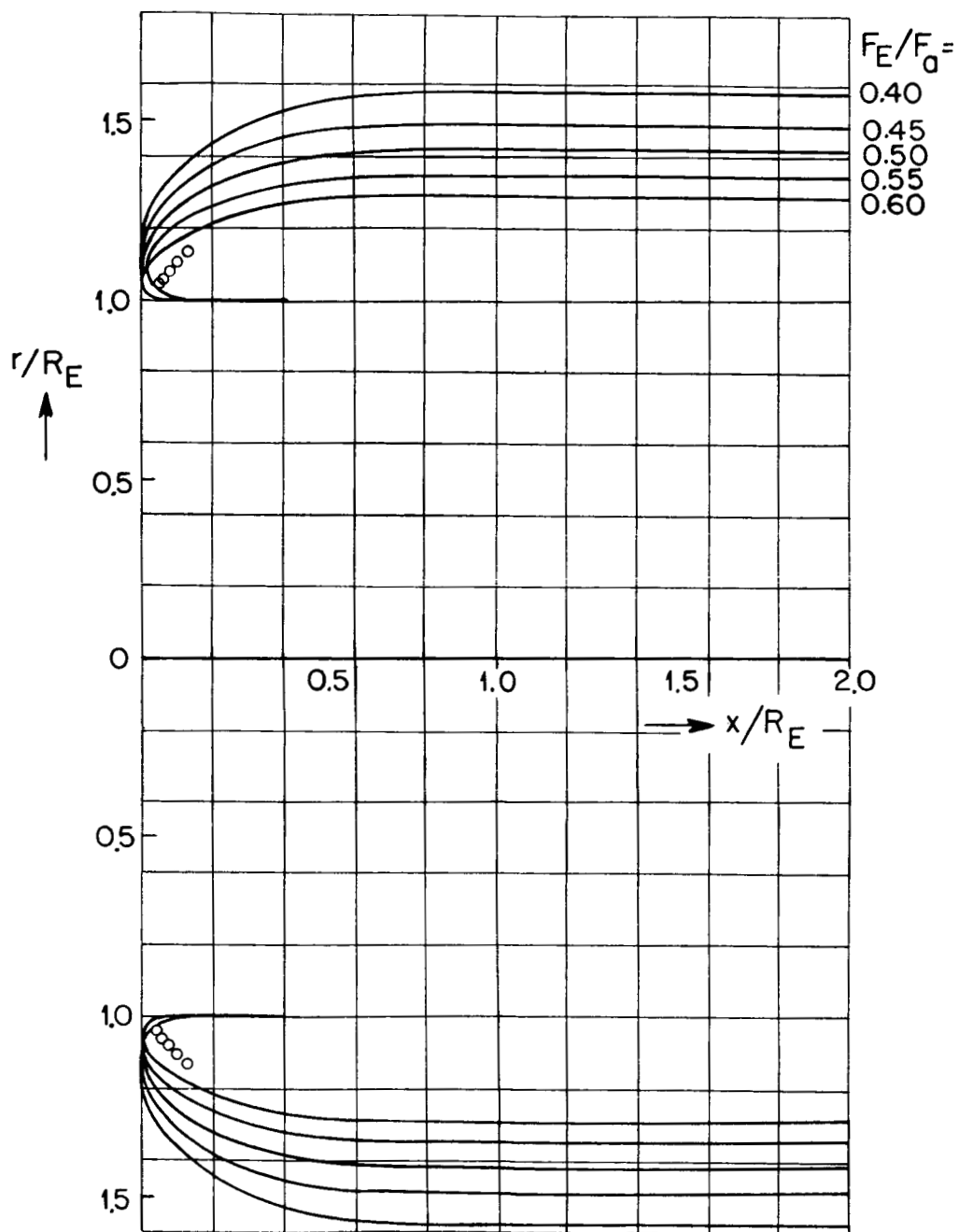


Figure 2.- Class IV of circular cowls.

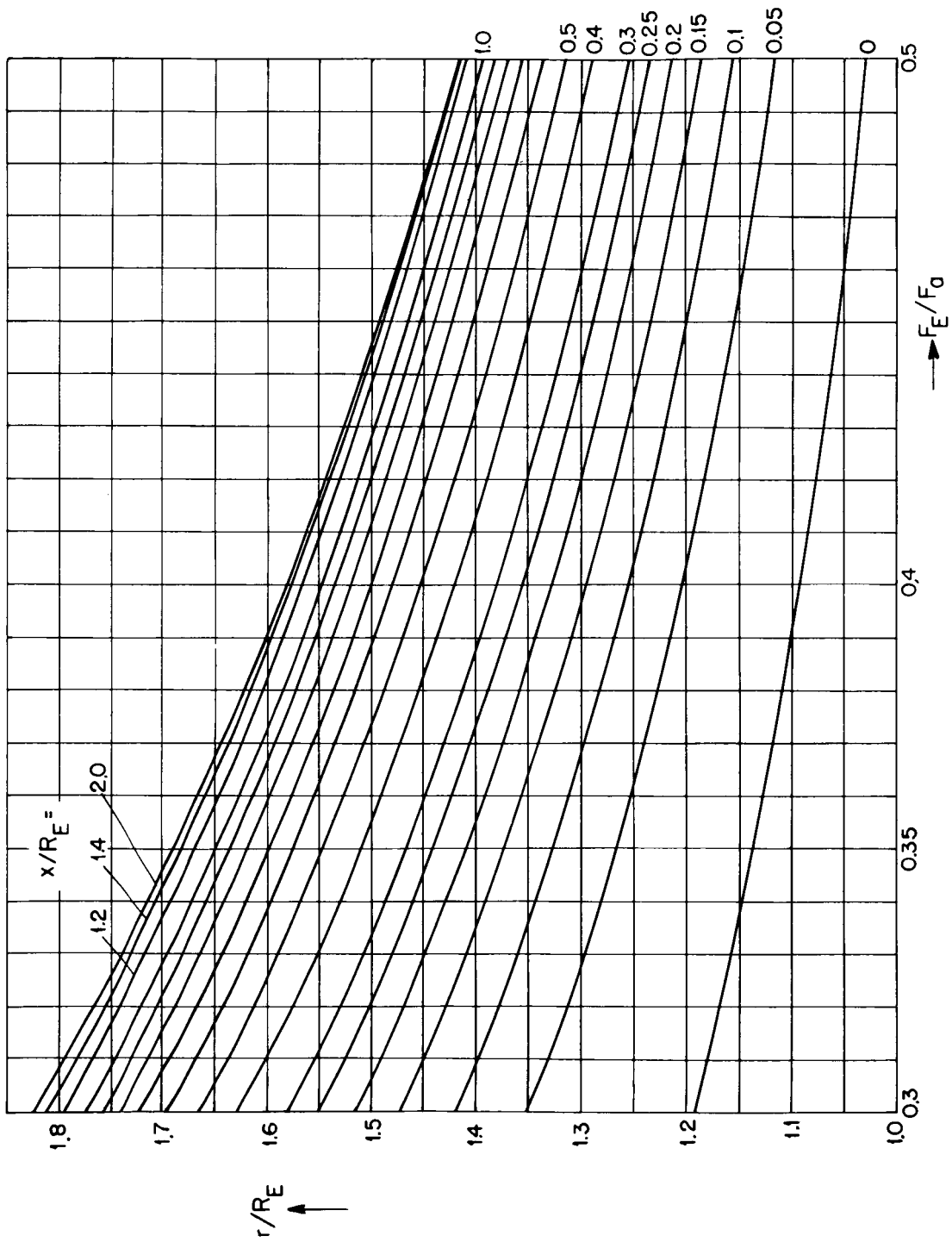


Figure 3.- Class III of circular cowls.

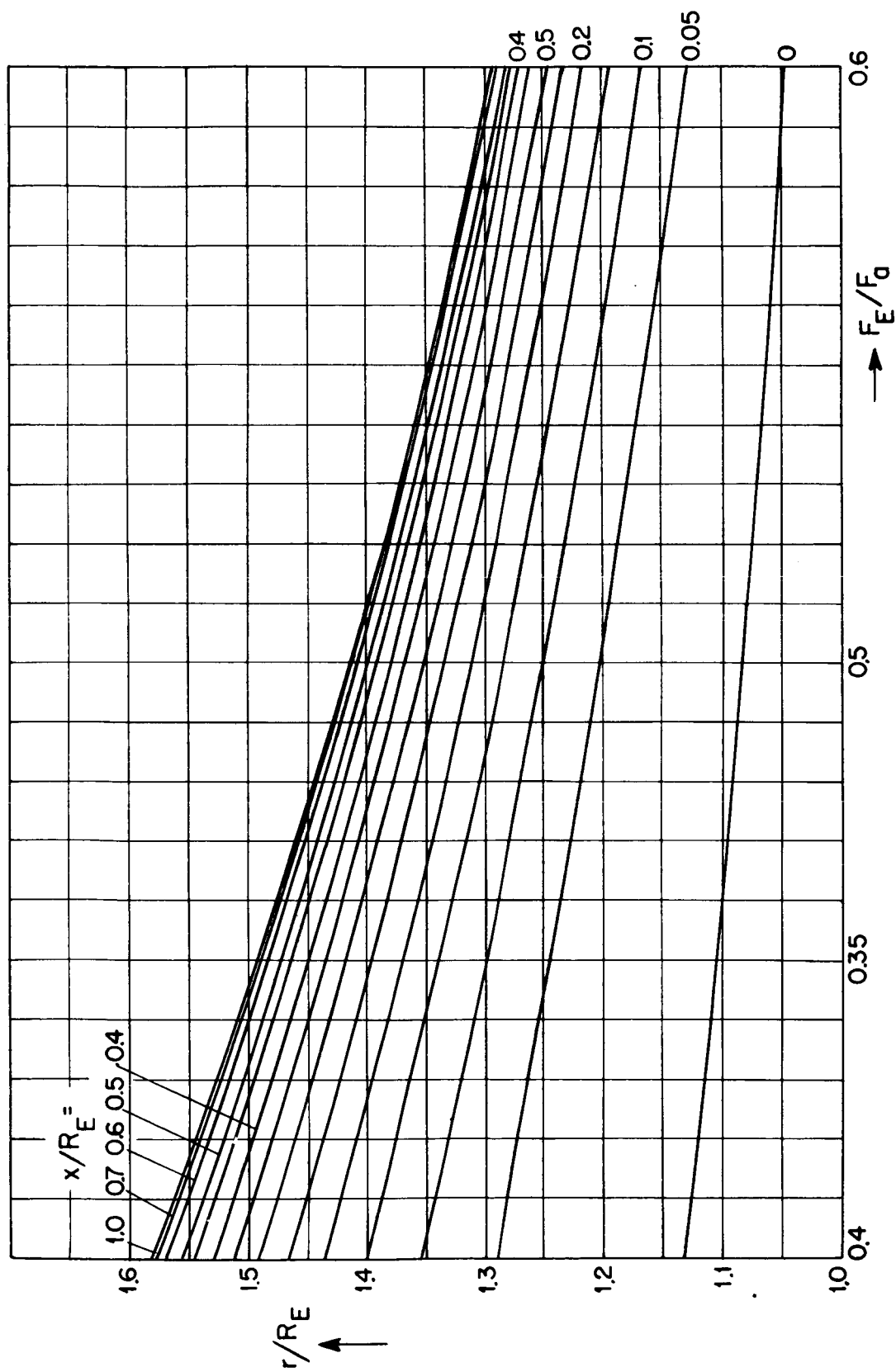


Figure 4.- Class IV of circular cowls.

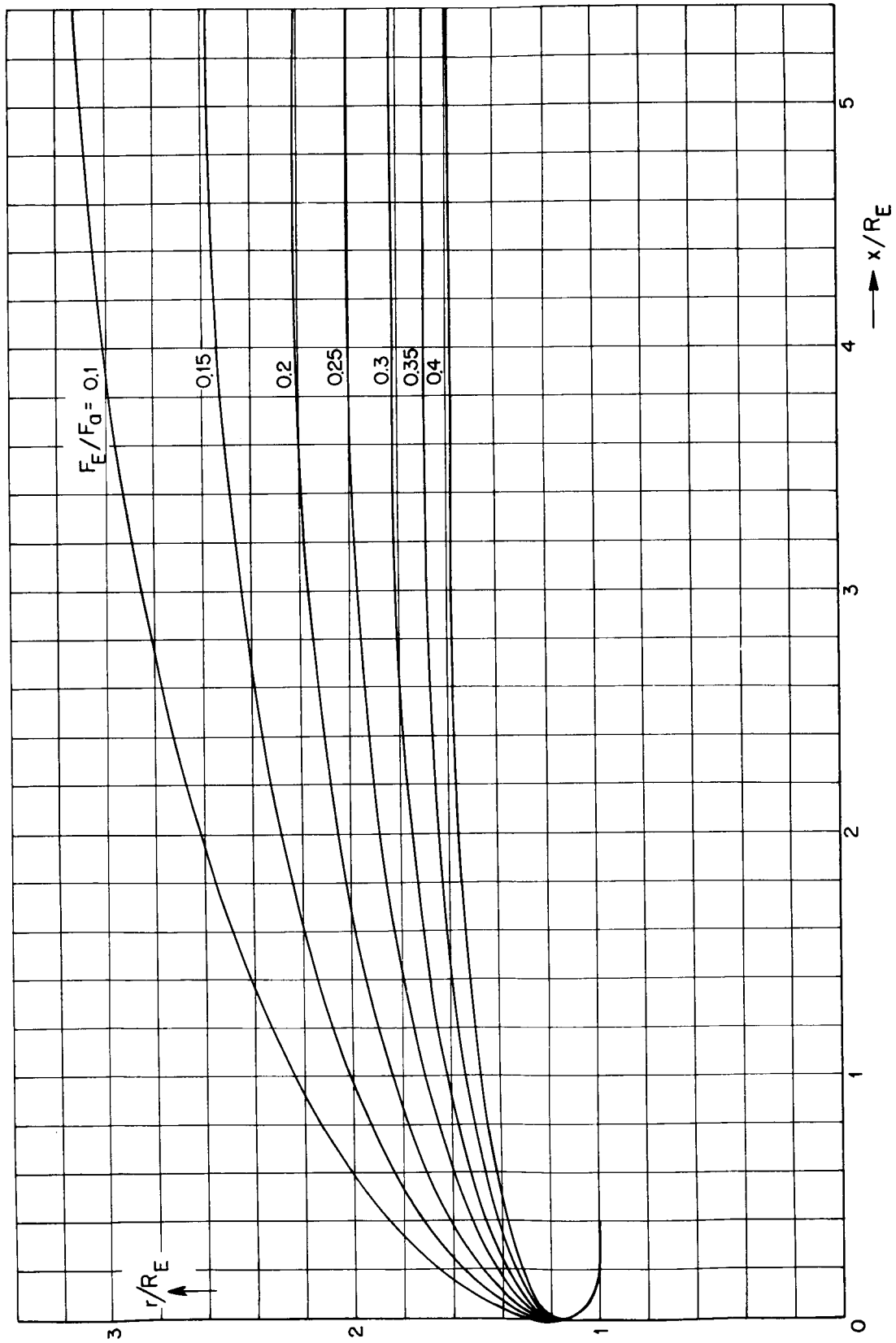


Figure 5.- Class I of circular cowls.

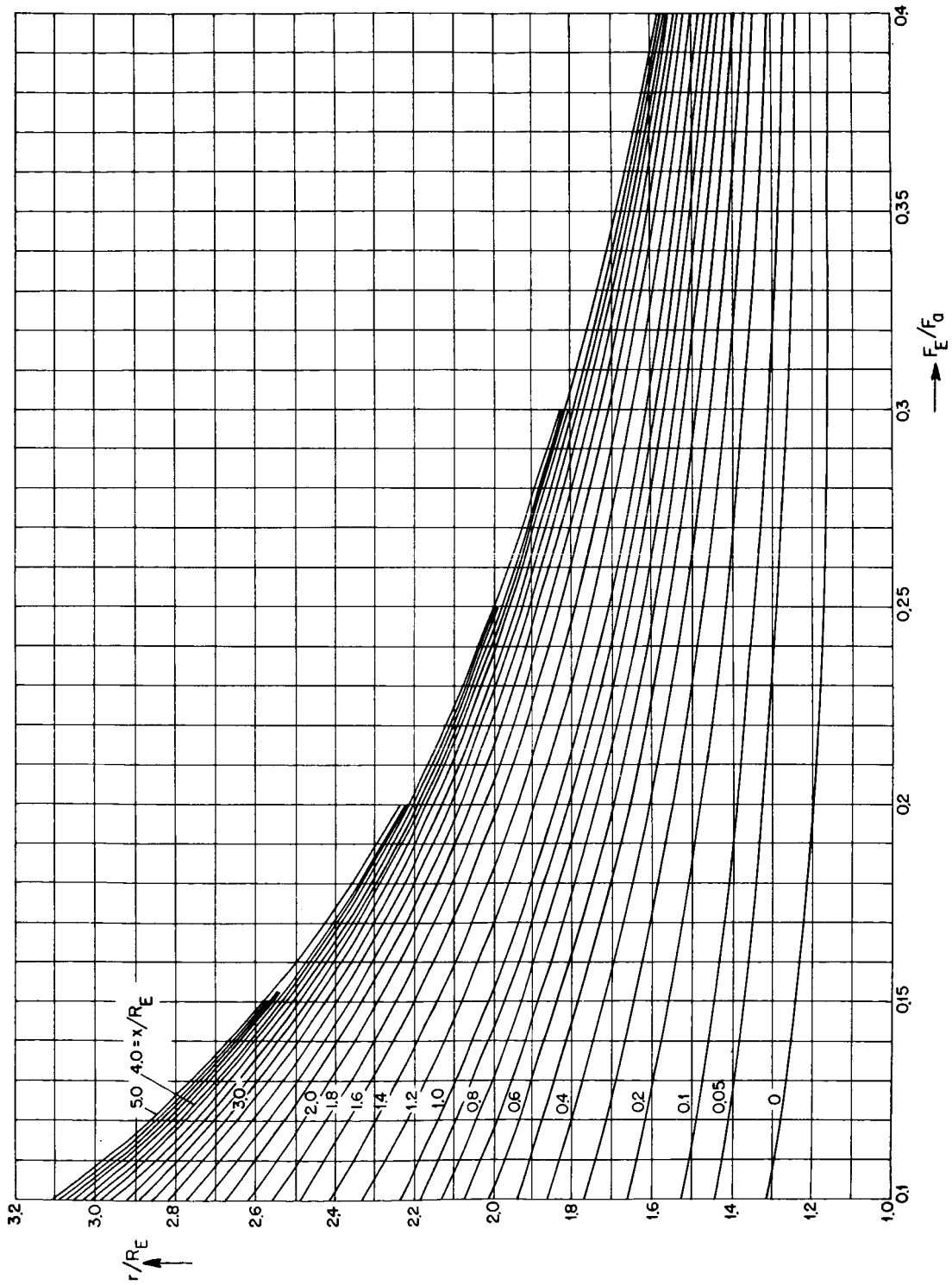


Figure 6.- Class I of circular cowls.

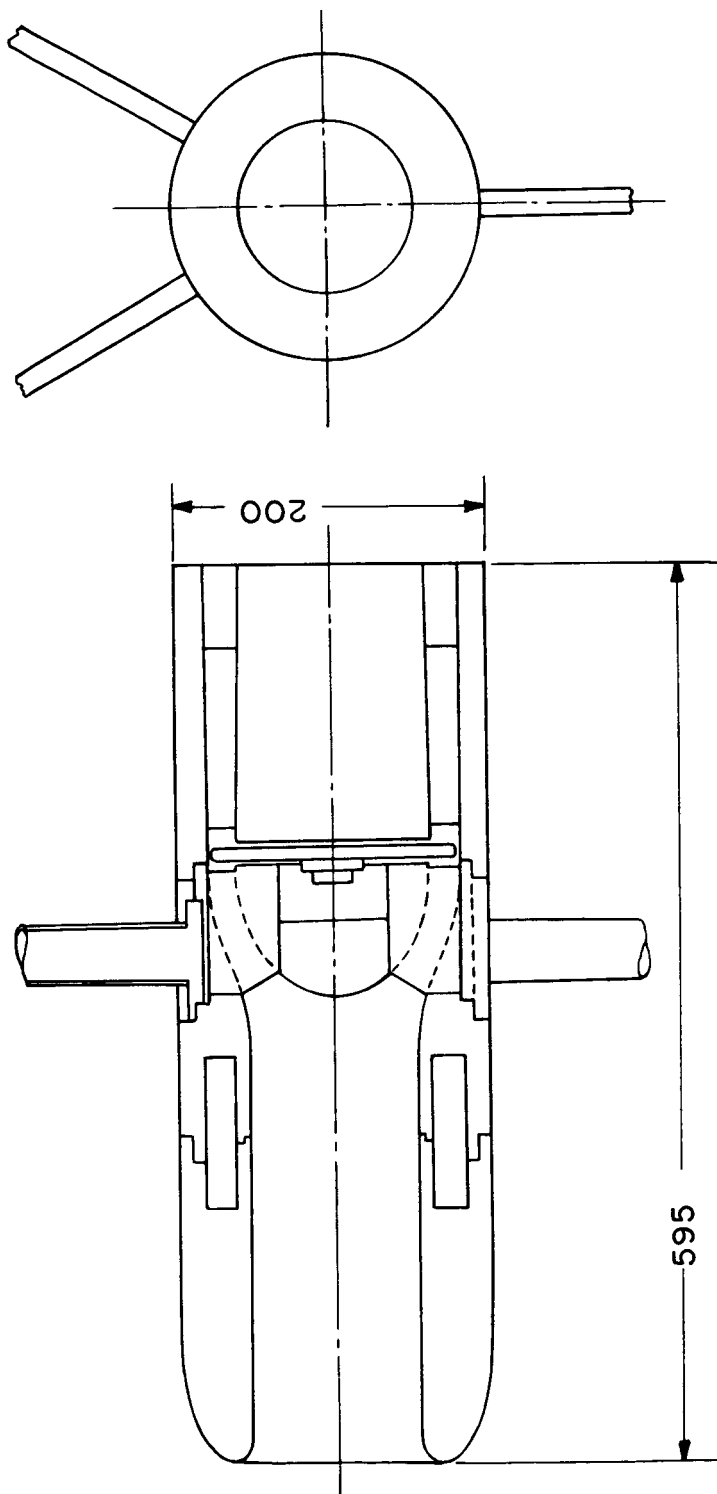


Figure 7.- Model arrangement, comprehensive view M 1:5.

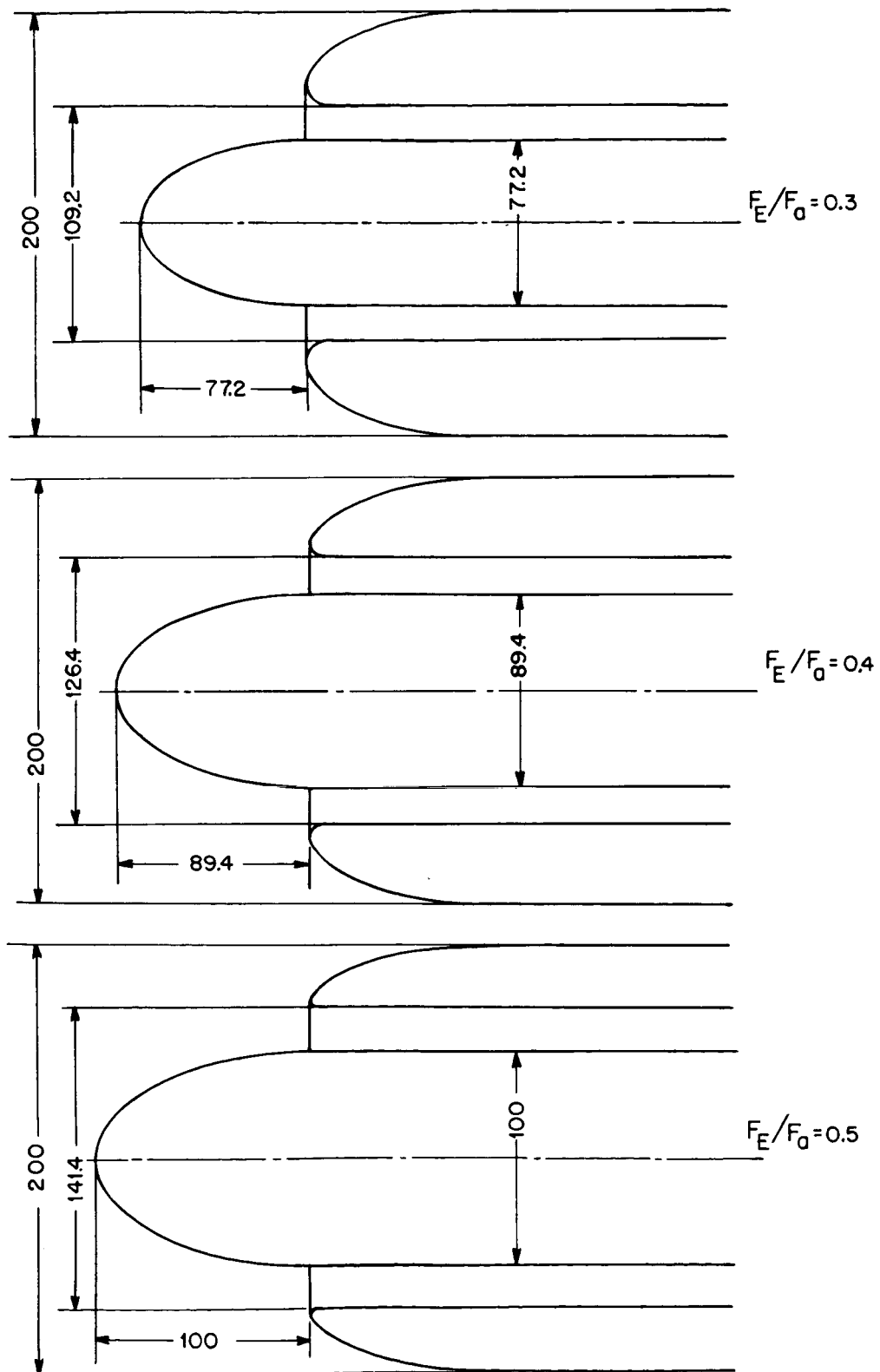


Figure 8.- Class III of circular cowls.

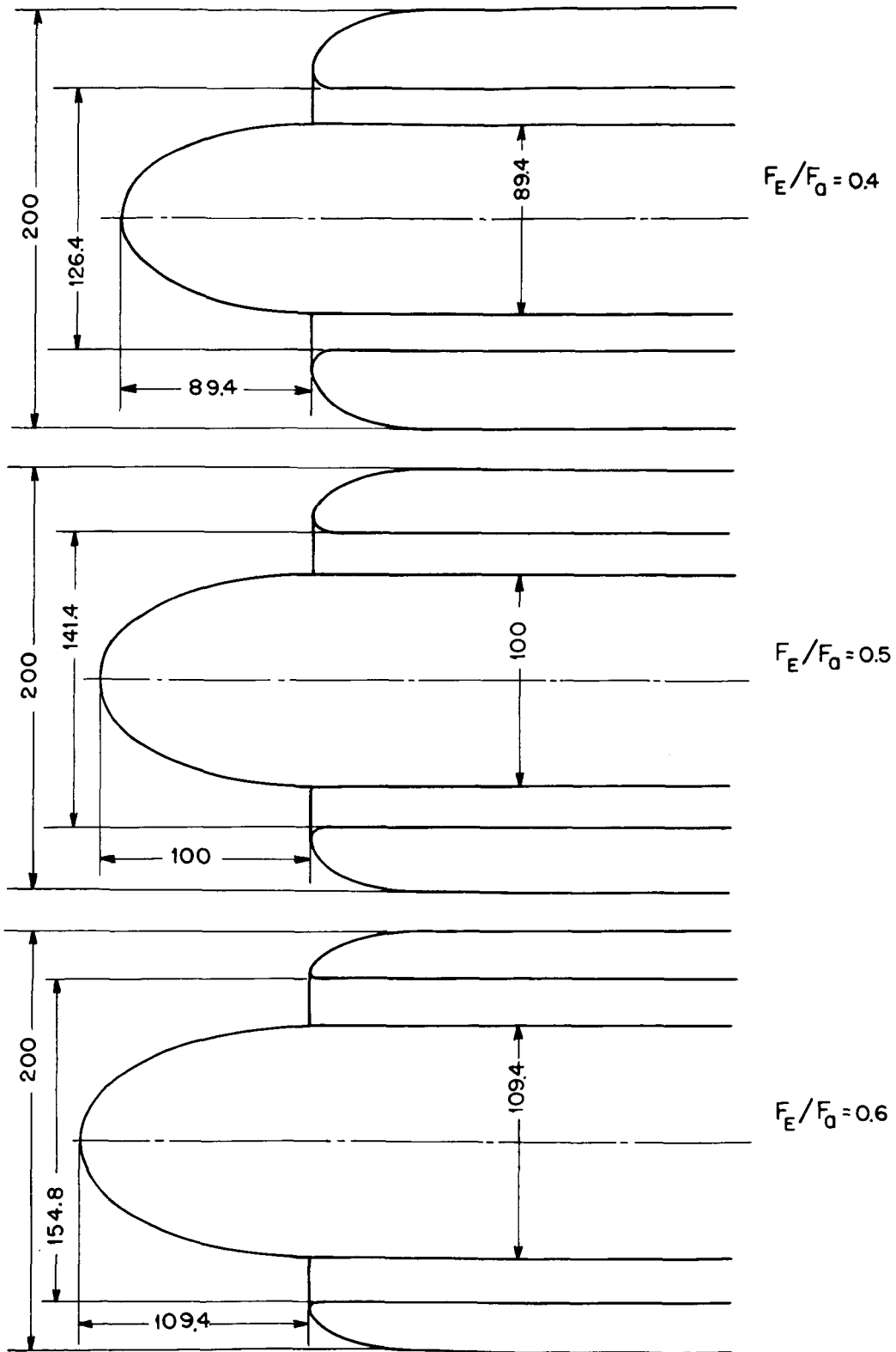


Figure 9.- Class IV of circular cowls.

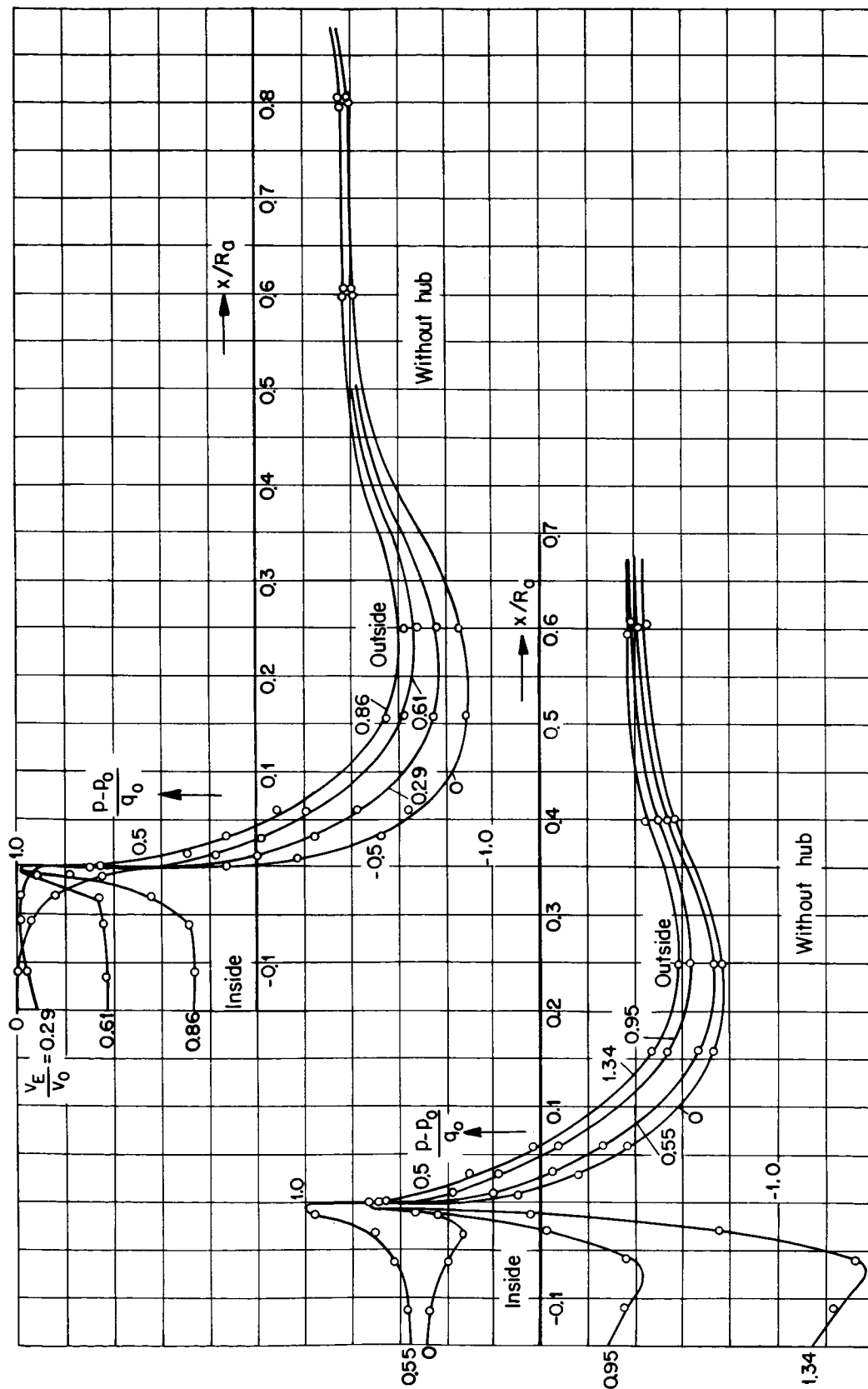


Figure 10.- Class III of circular cowls; $F_E/F_a = 0.3$, $\alpha = 0^\circ$.

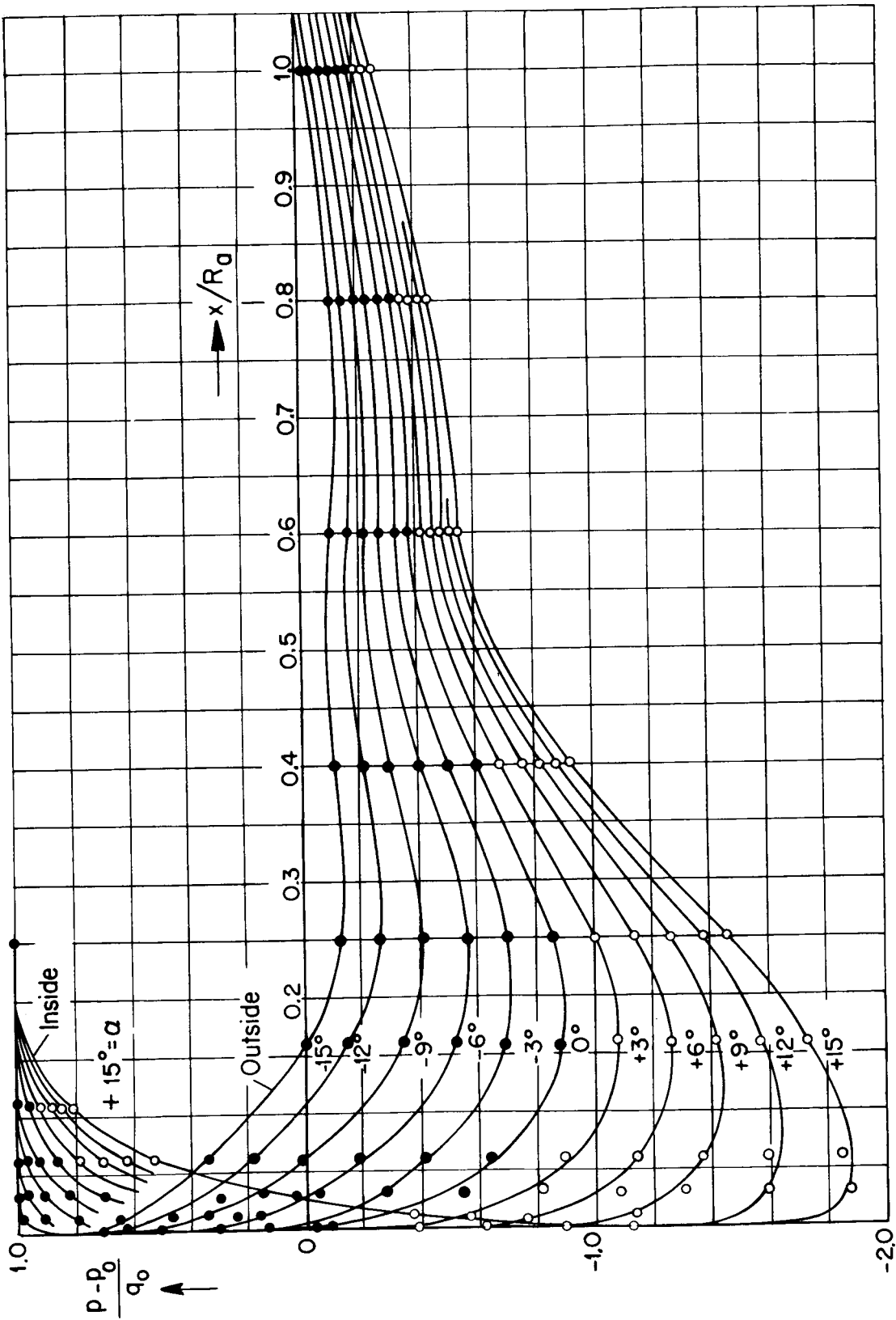


Figure 11.- Class III of circular cowls (without hub); $F_E/F_a = 0.3$, $v_E/v_0 = 0$.

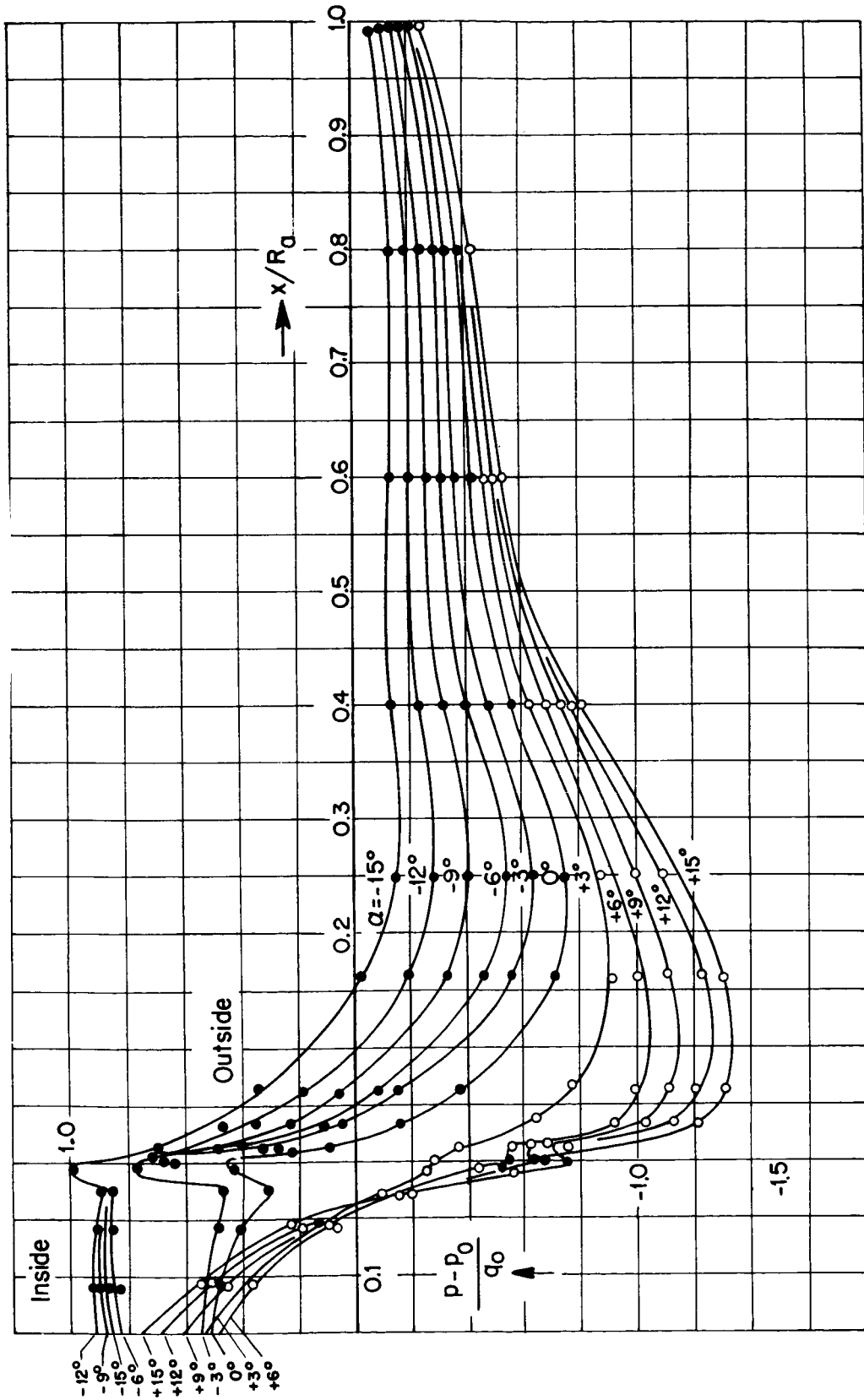


Figure 12.- Class III of circular cowls (with hub); $F_{E'} / F_a = 0.3$,
 $v_{E'} / v_0 = 0$.

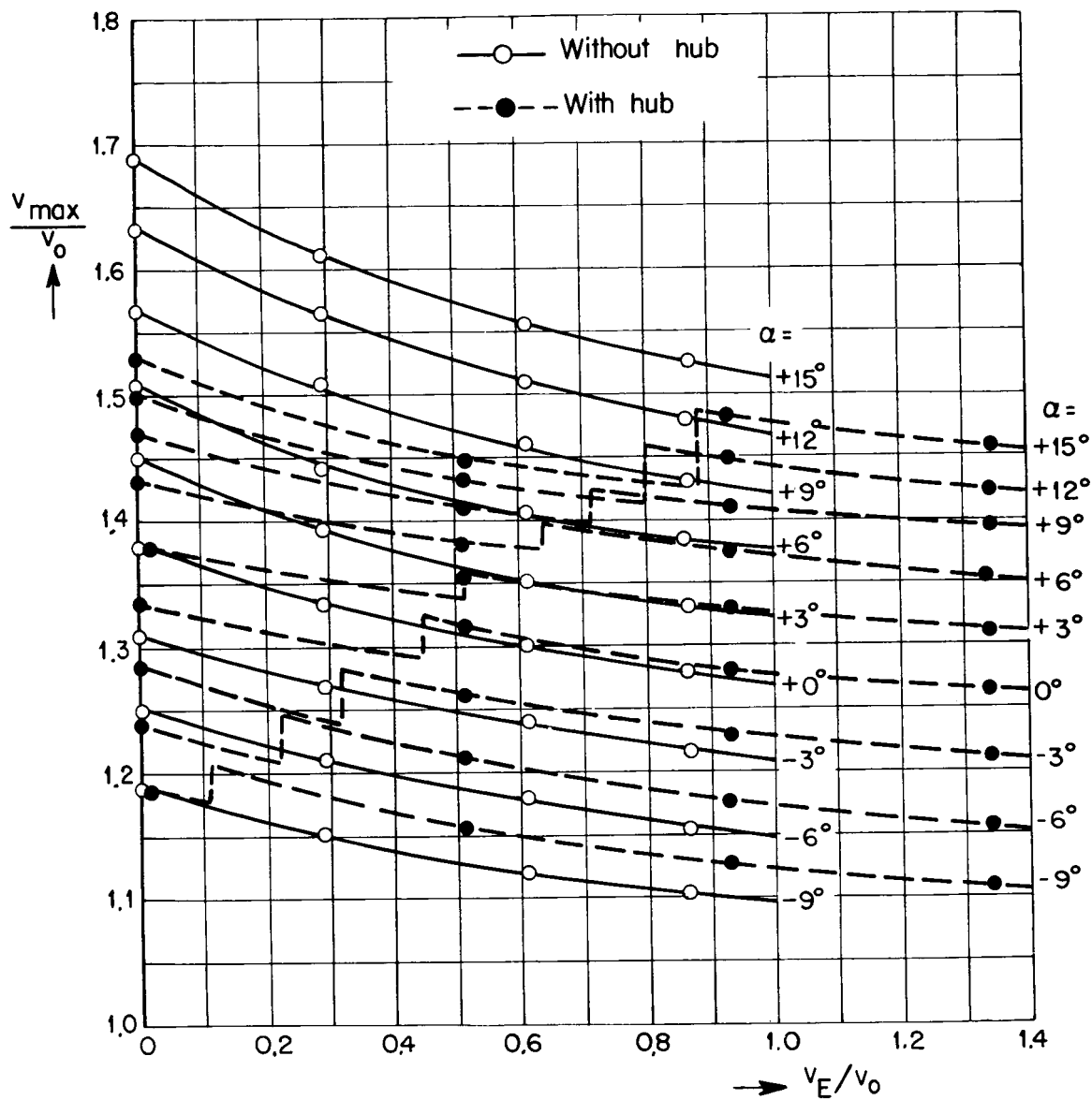


Figure 13.- Class III of circular cowls; $F_E/F_a = 0.3$.

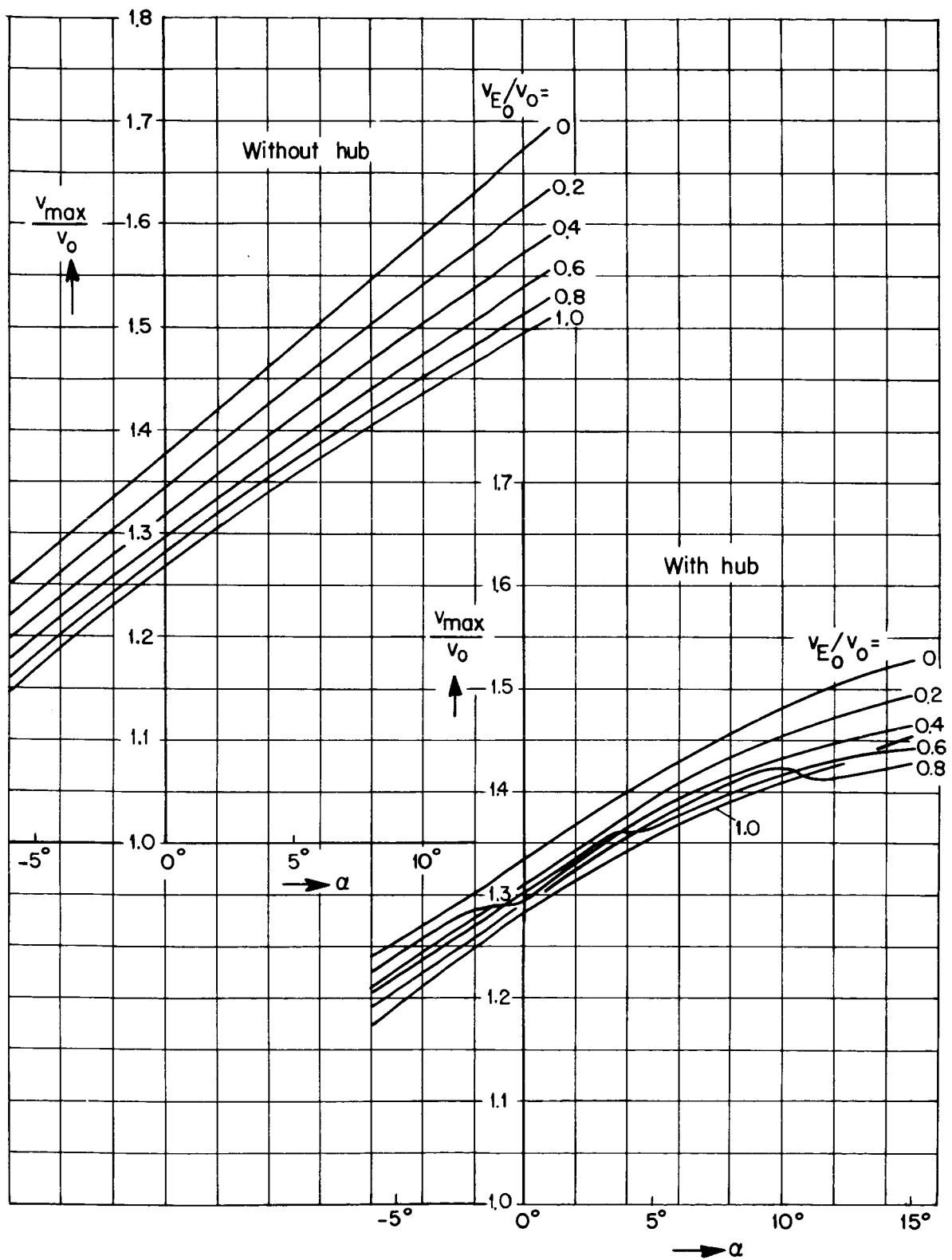


Figure 14.- Class III of circular cowls; $F_E/F_a = 0.3$.

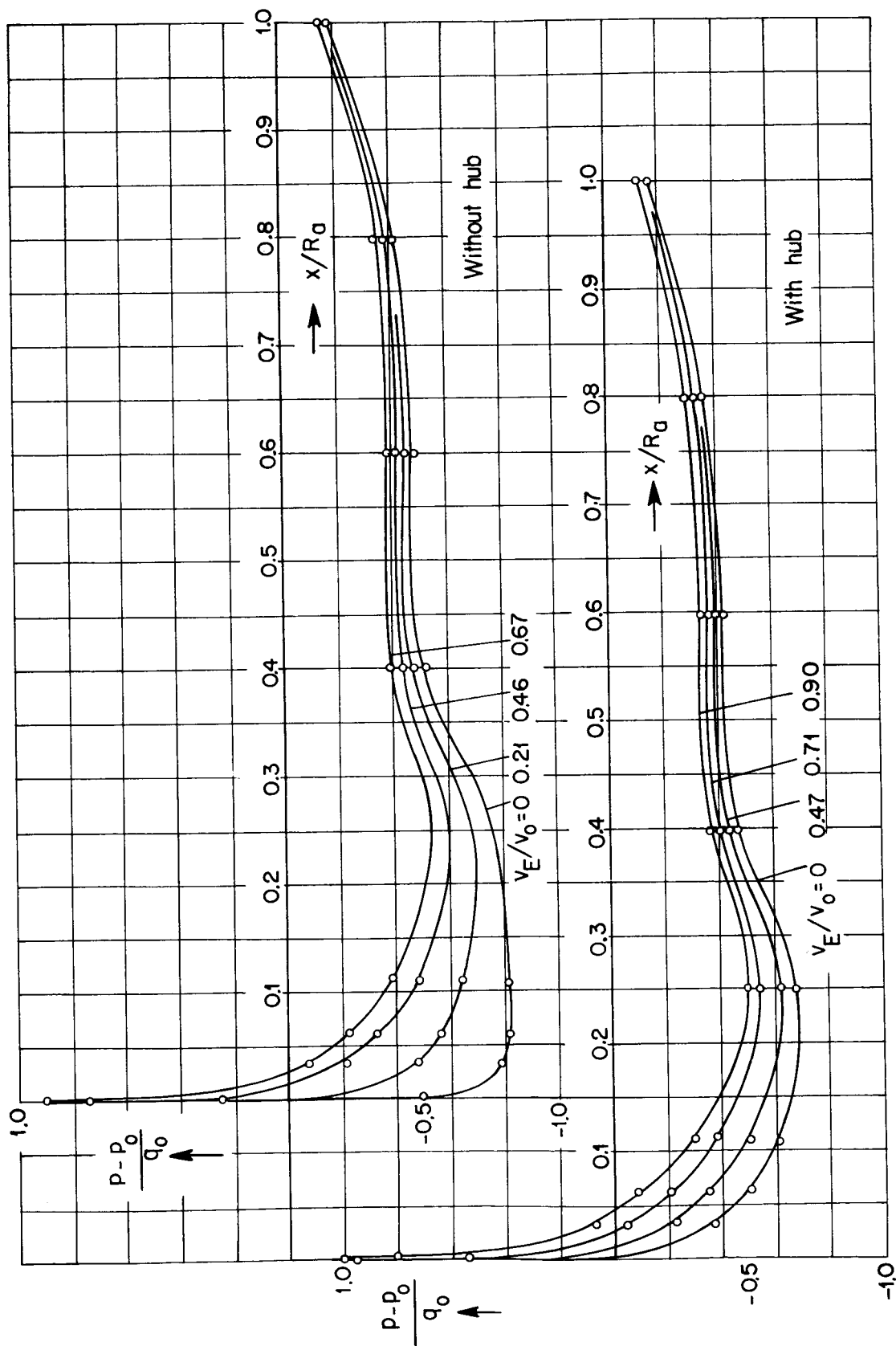


Figure 15.- Class III of circular cowls; $F_E/F_a = 0.4$, $\alpha = 0^\circ$.

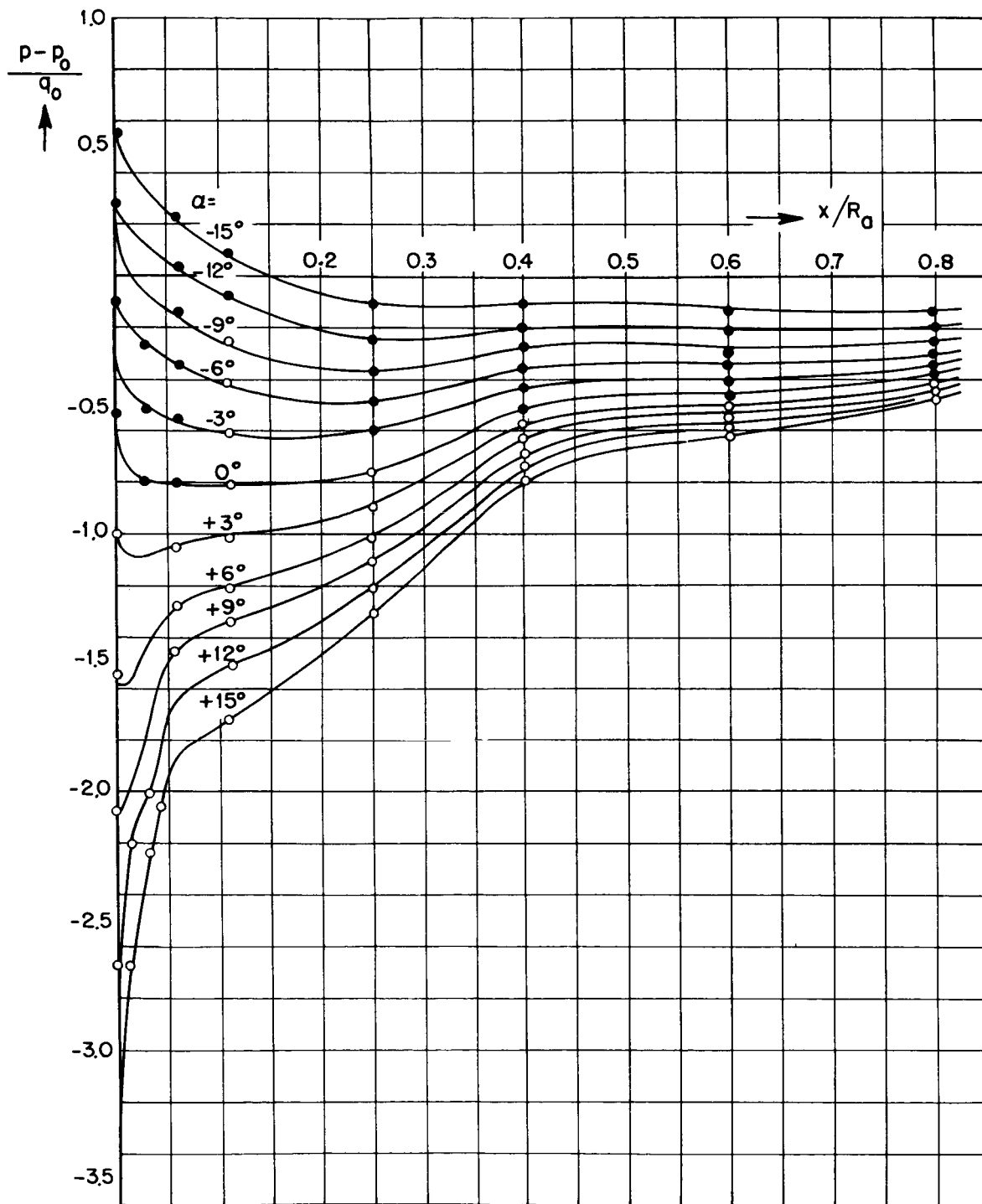


Figure 16.- Class III of circular cowls (without hub); $F_E/F_a = 0.4$,
 $v_E/v_0 = 0$.

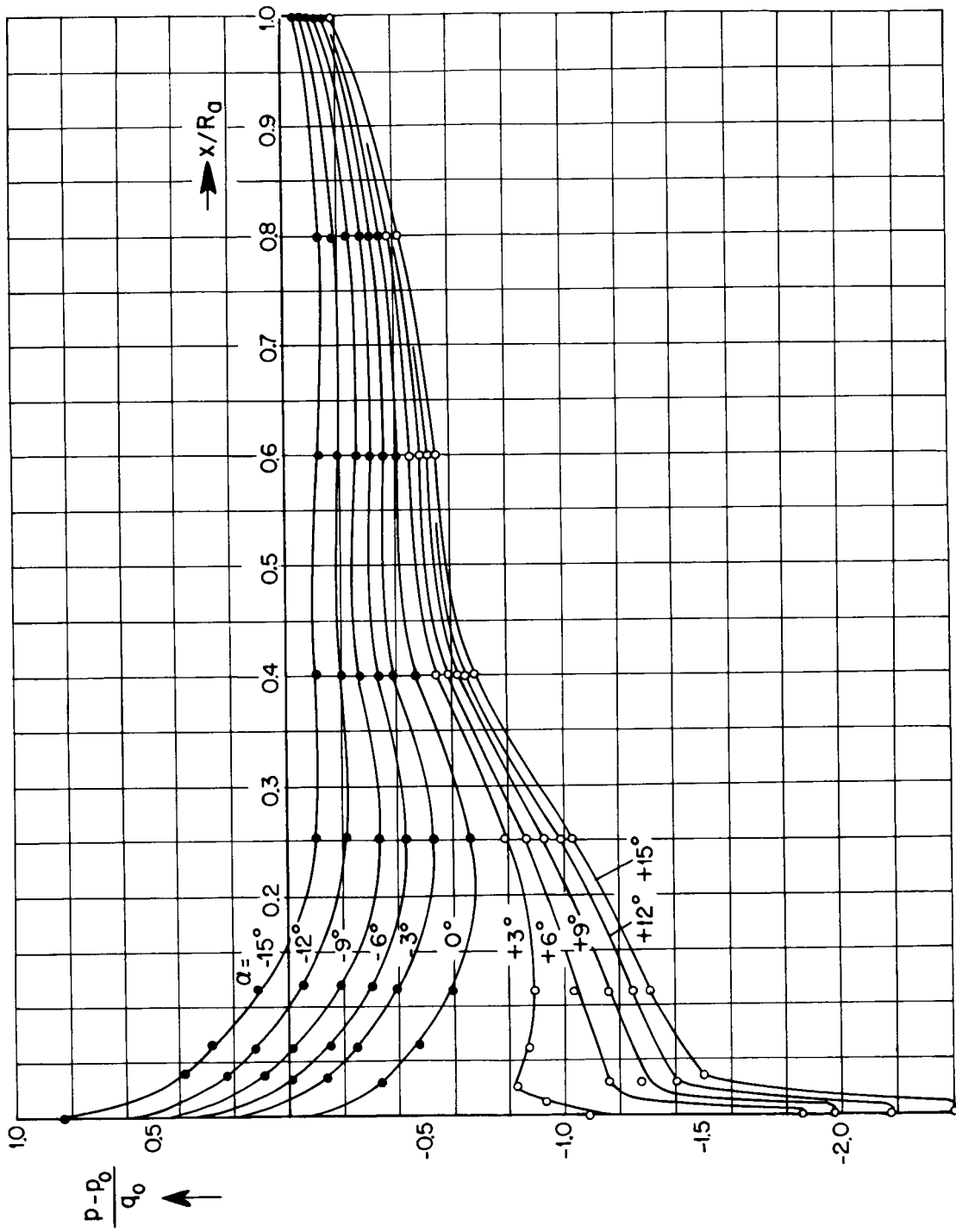


Figure 17.- Class III of circular cowls (with hub); $F_E'/F_a = 0.4$,
 $v_E/v_0 = 0$.

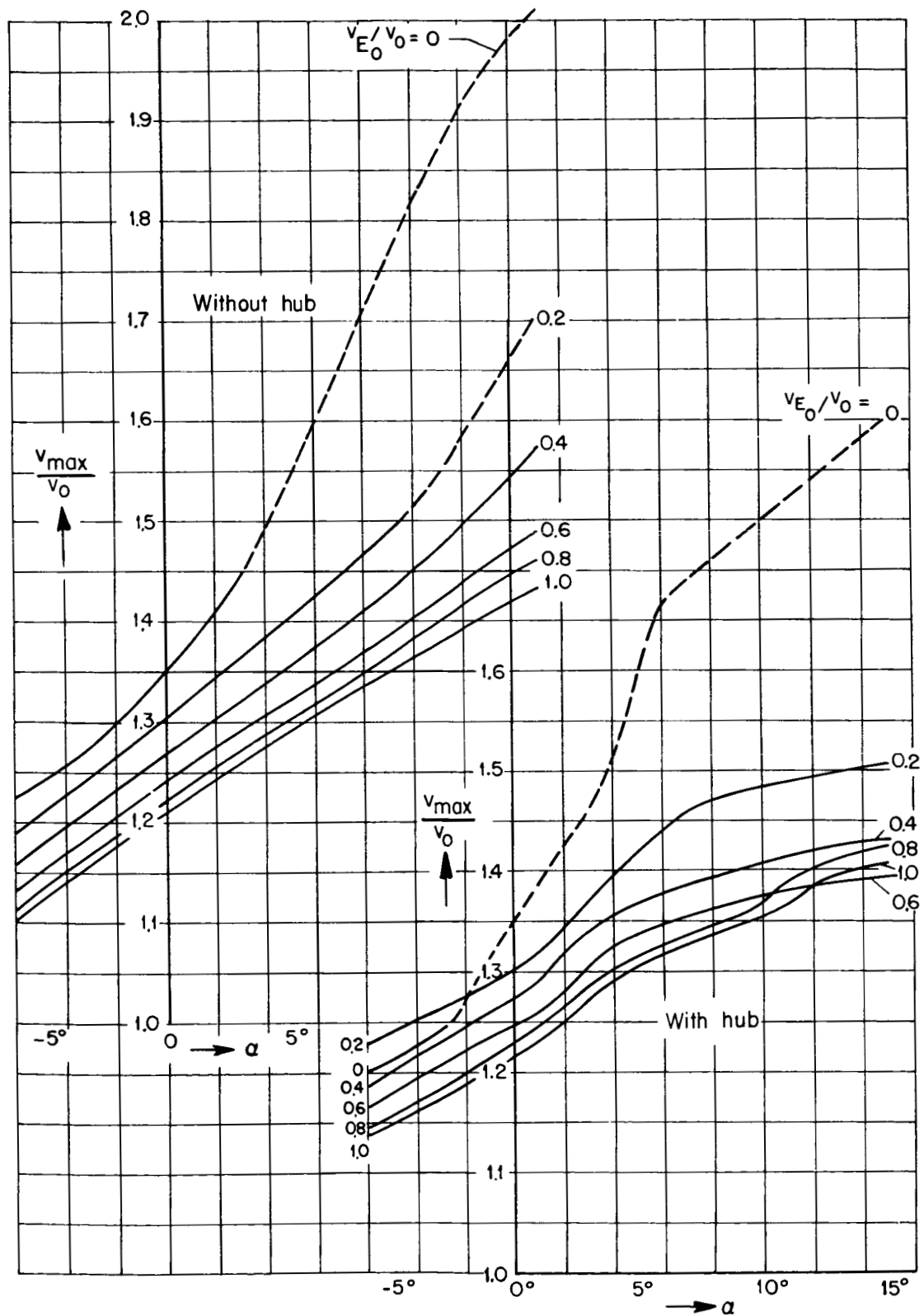


Figure 18.- Class III of circular cowls; $F_E/F_a = 0.4$; $v_{E0}/v_0 = 0$.

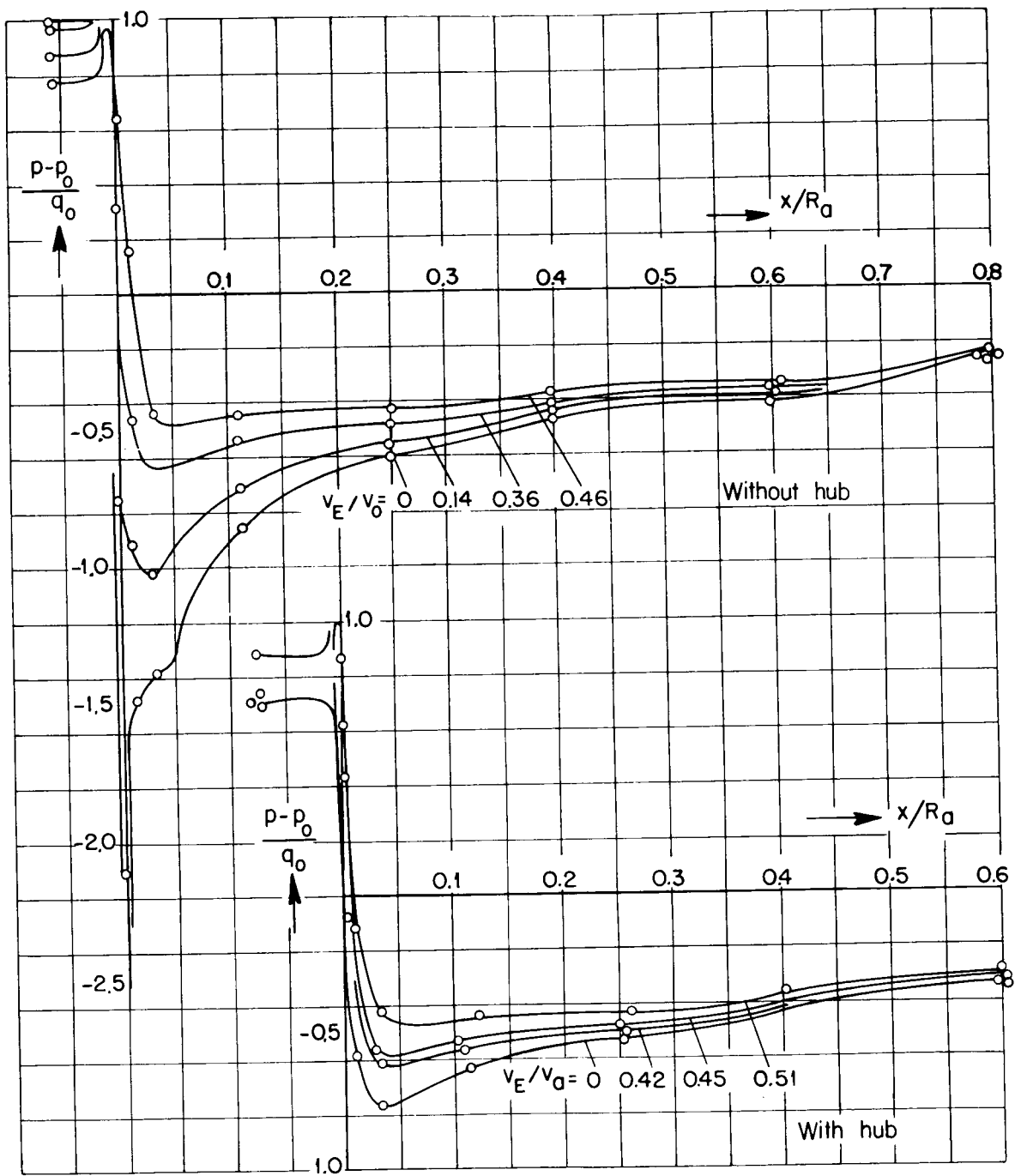


Figure 19.- Class III of circular cowls; $F_E/F_a = 0.5$, $\alpha = 0^\circ$.

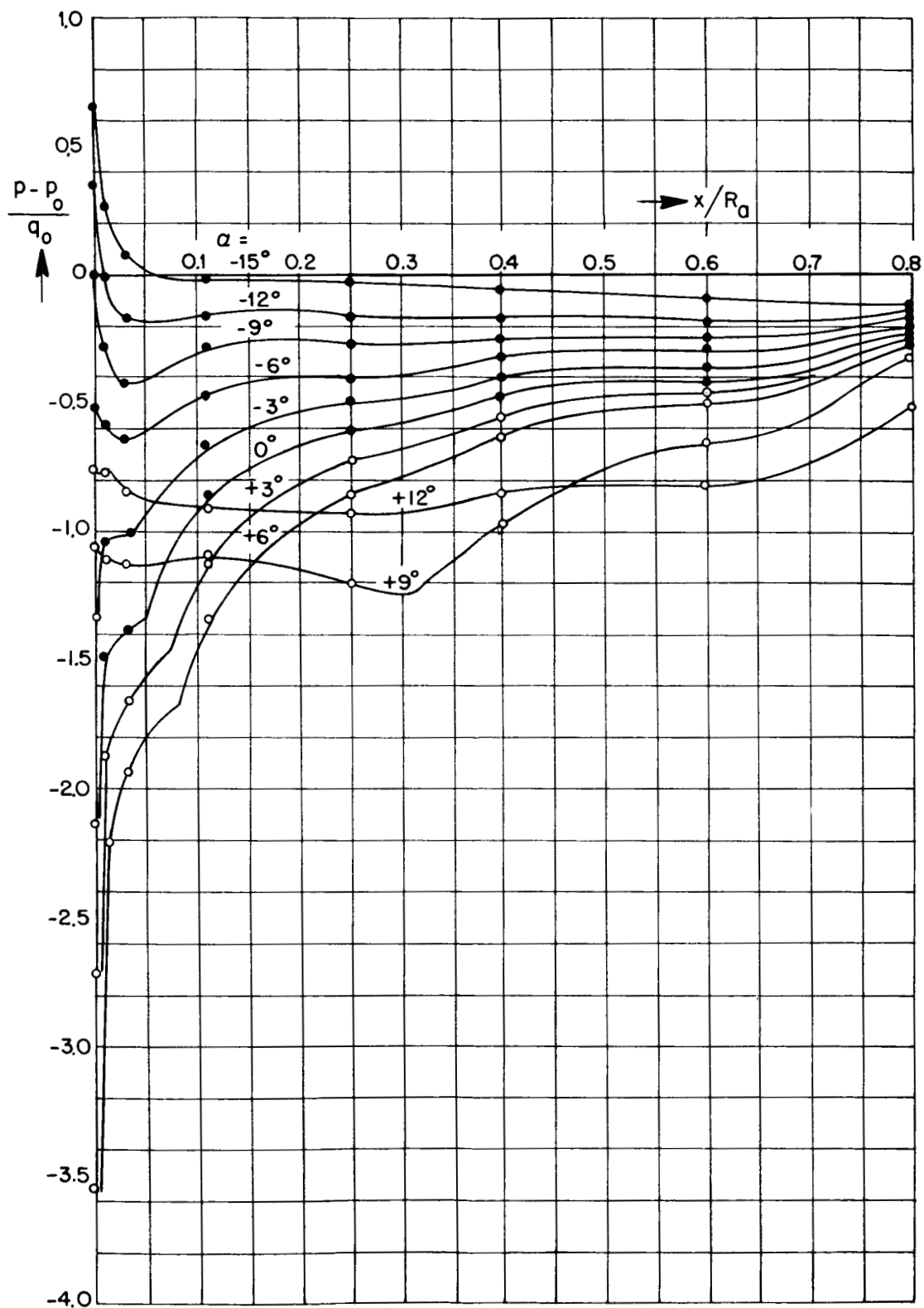


Figure 20.- Class III of circular cowls (without hub); $F_E/F_a = 0.5$,
 $v_E/v_0 = 0$.

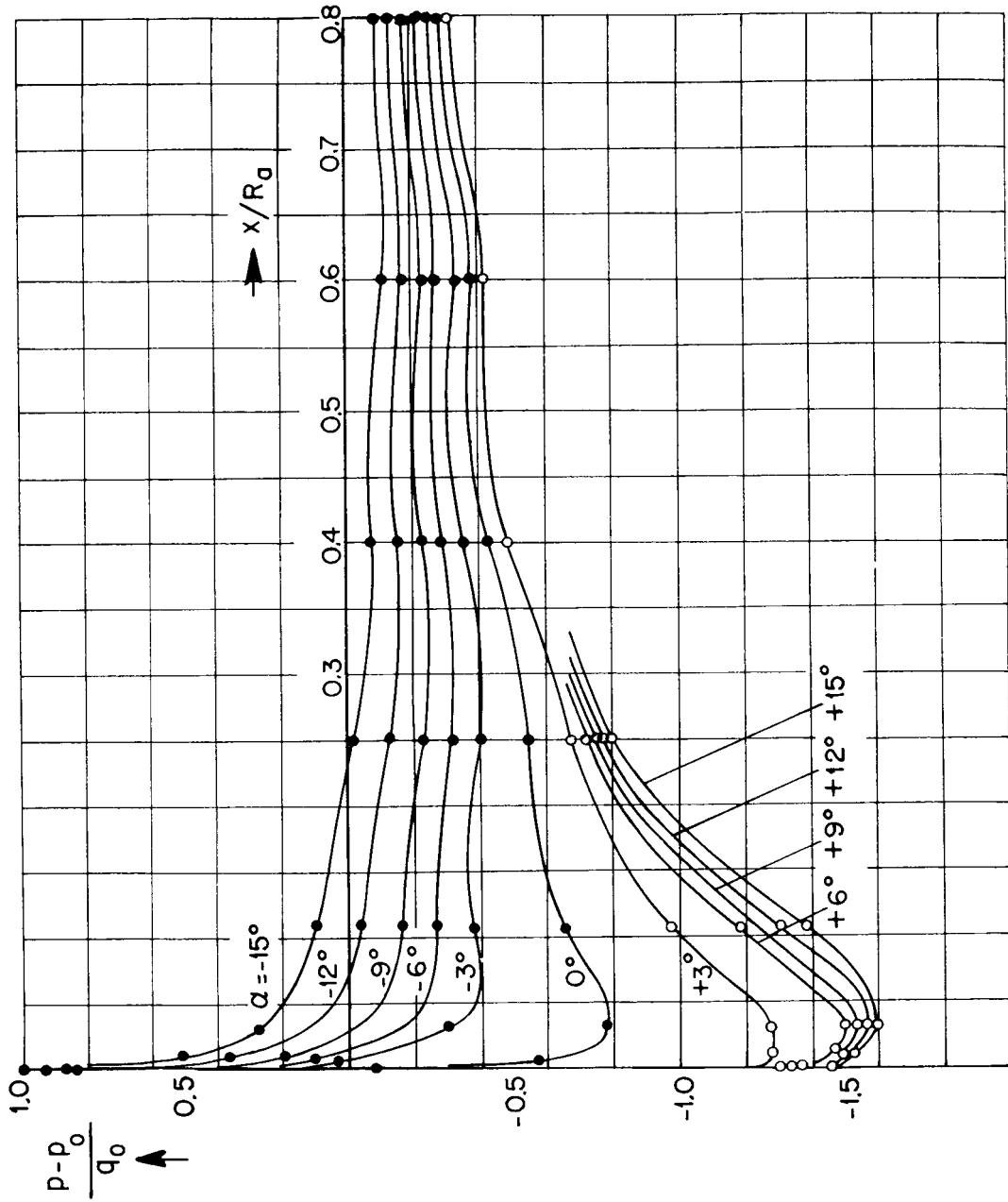


Figure 21.- Class III of circular cowls (with hub); $F_E'/F_a = 0.5$,
 $v_E'/v_0 = 0$.

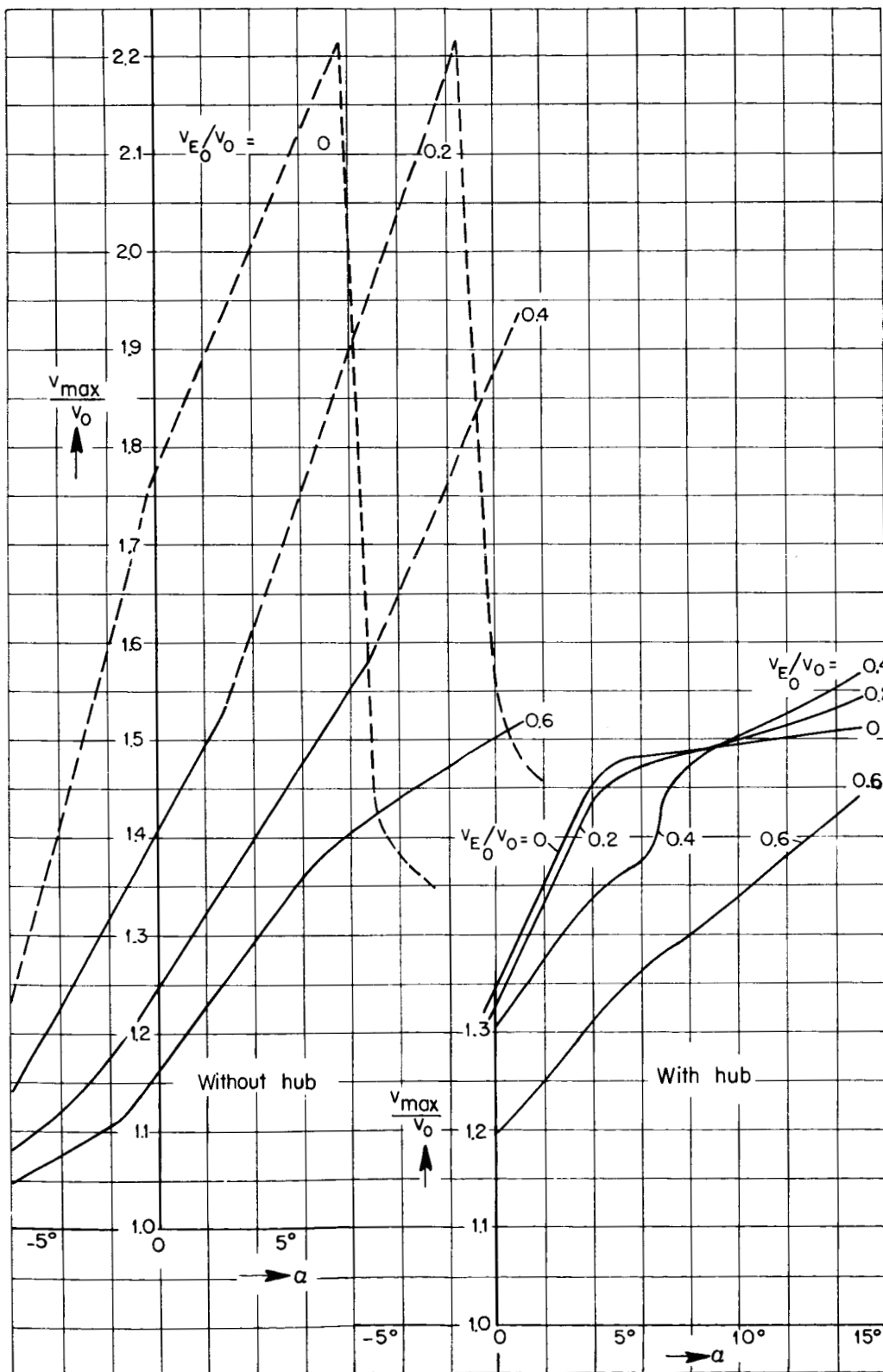


Figure 22.- Class III of circular cowls; $F_E/F_a = 0.5$.

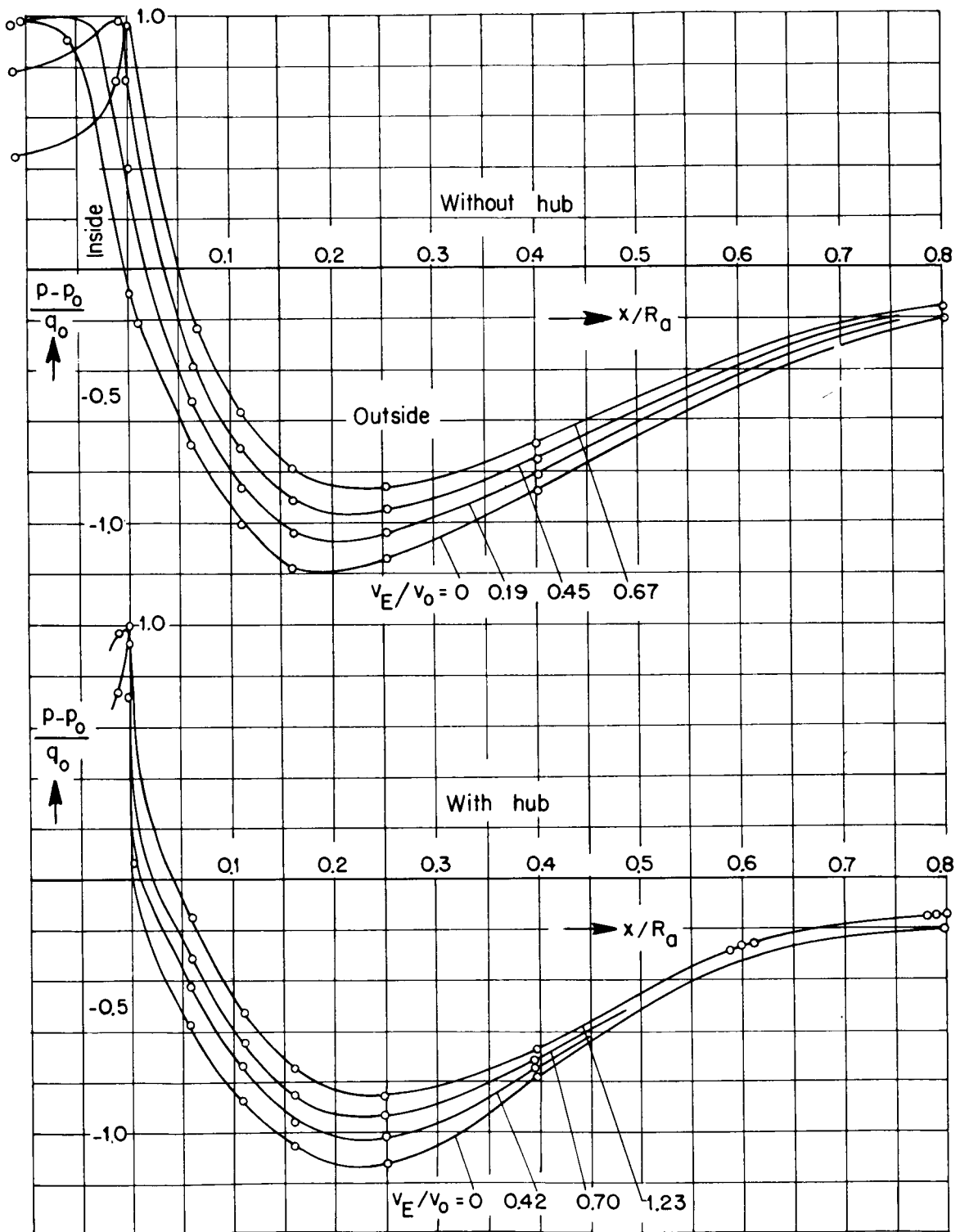


Figure 23.- Class IV of circular cowls; $F_E/F_a = 0.4, \alpha = 0^\circ$.

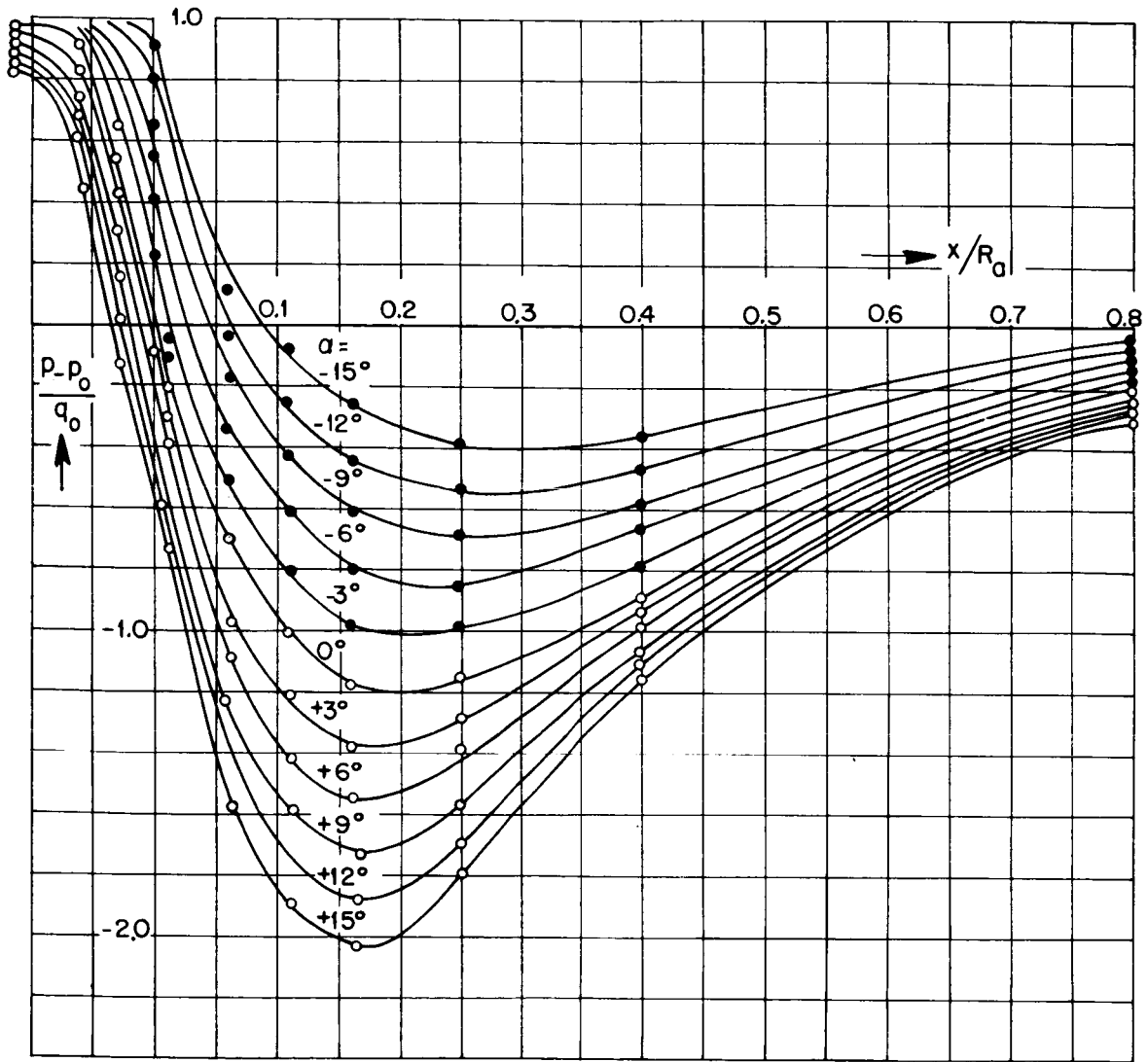


Figure 24.- Class IV of circular cowls (without hub); $F_E/F_a = 0.4$,
 $v_E/v_0 = 0$.

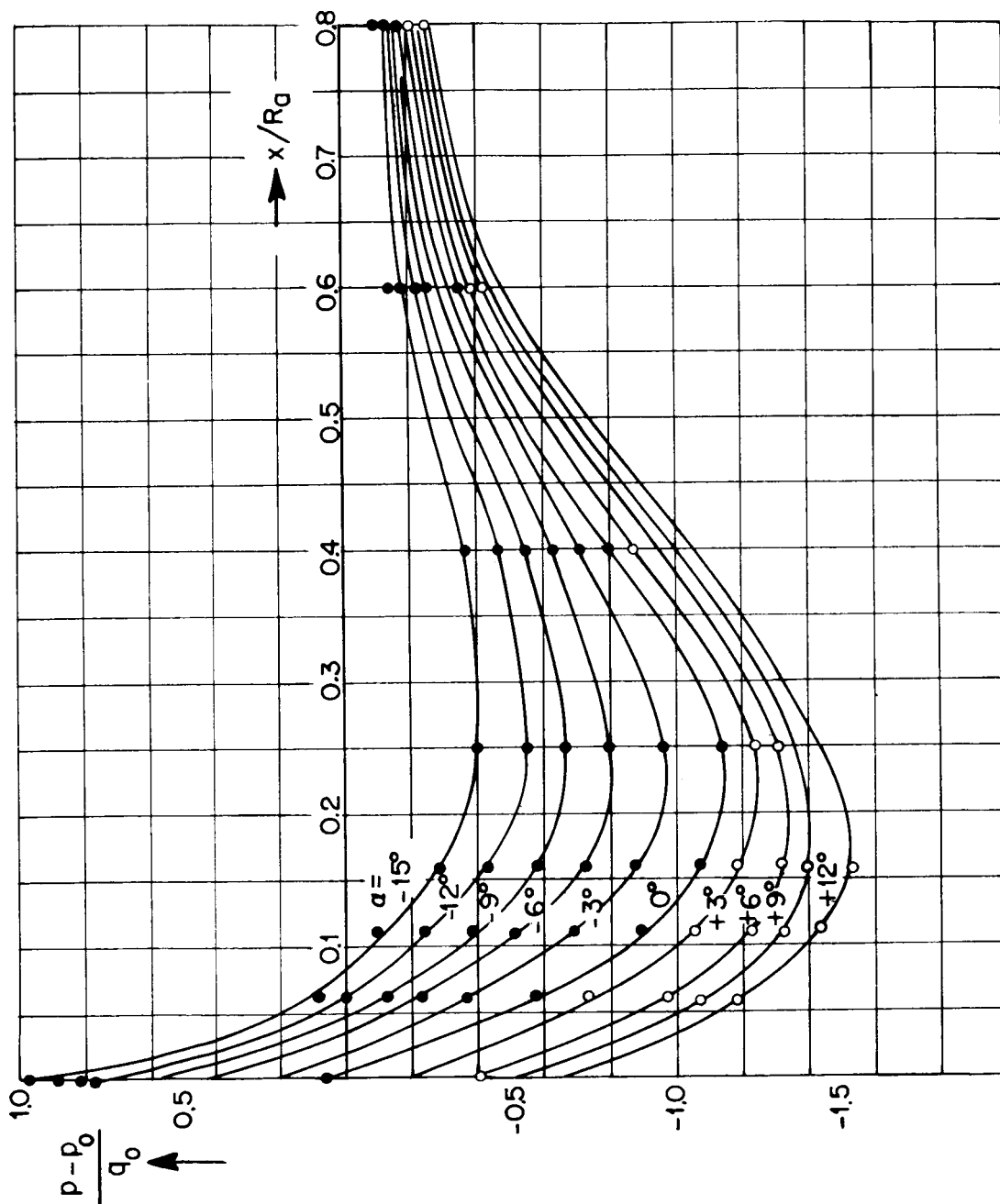


Figure 25.- Class IV of circular cowls (with hub); $F_E'/F_a = 0.4$,
 $v_E/v_0 = 0$.

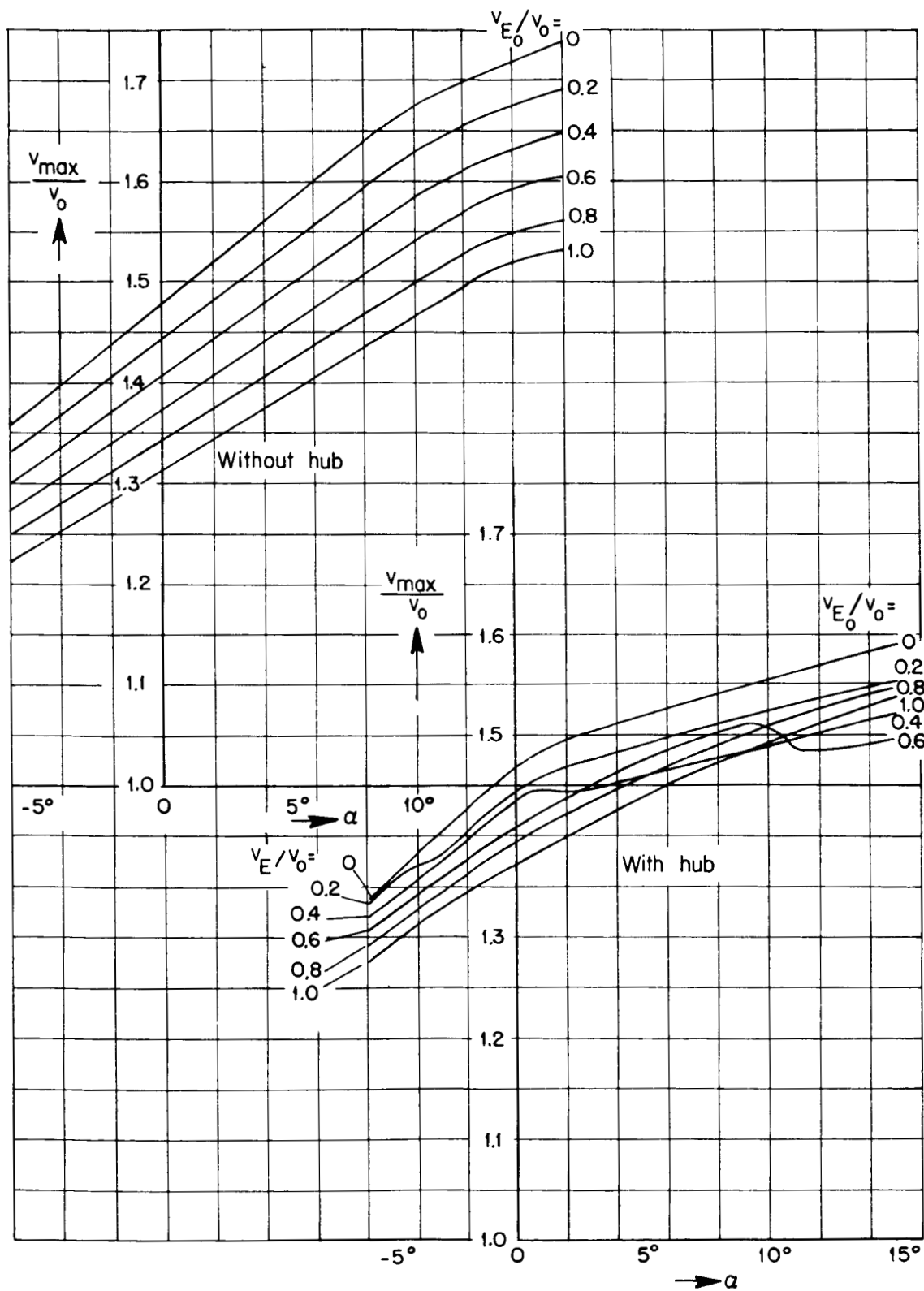


Figure 26.- Class IV of circular cowls; $F_E/F_a = 0.4$.

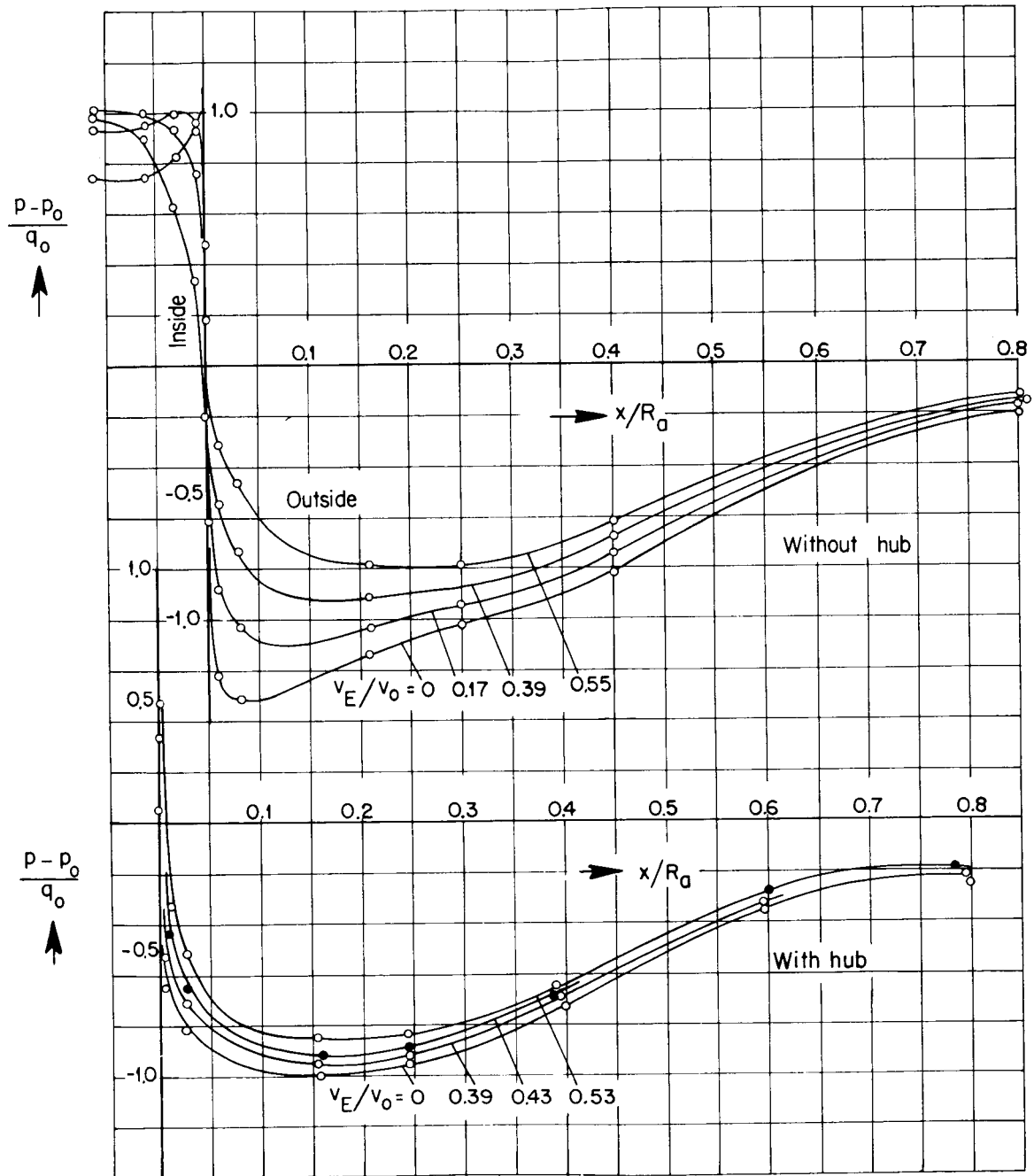


Figure 27.- Class IV of circular cowls; $F_E/F_a = 0.5$, $\alpha = 0^\circ$.

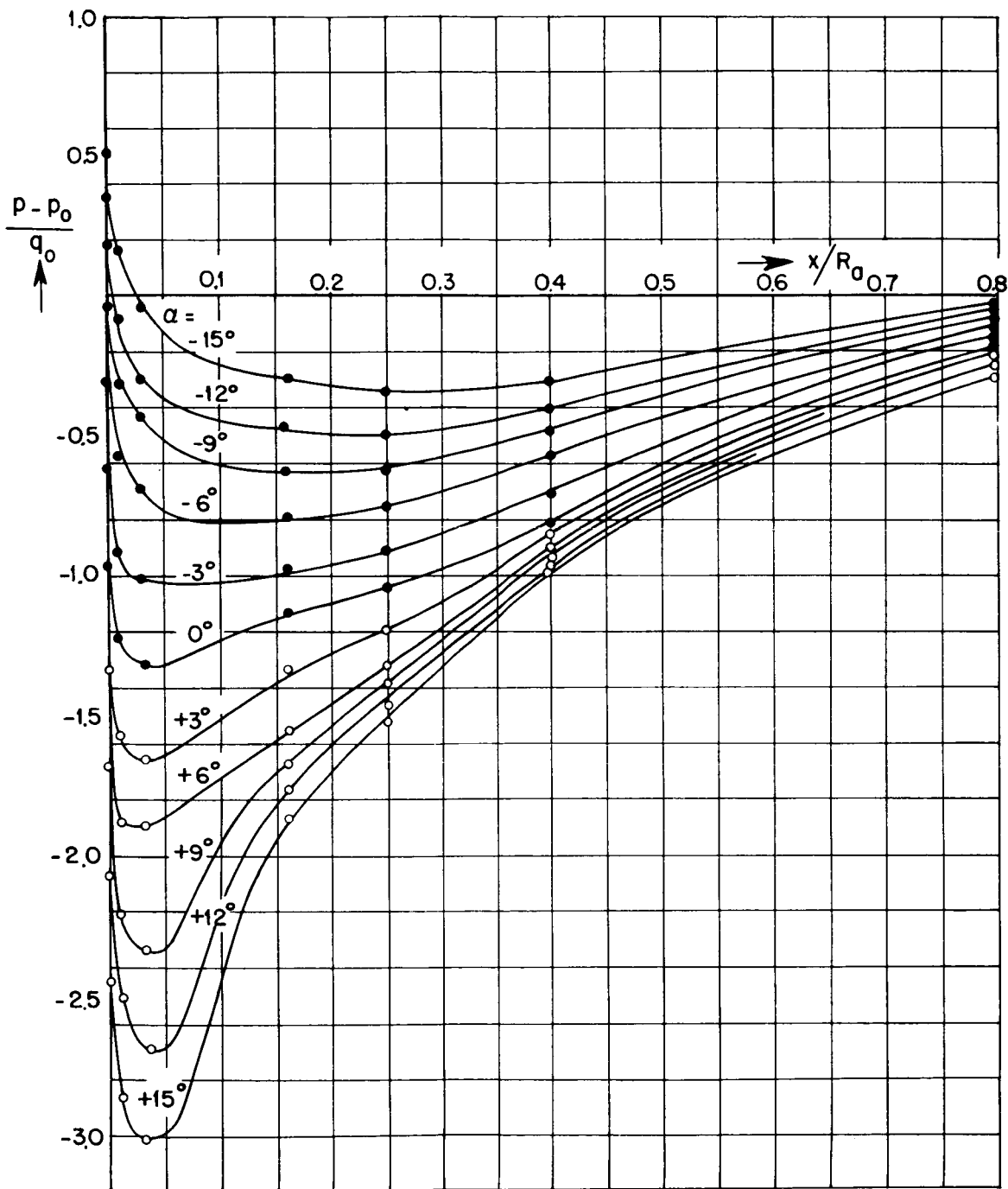


Figure 28.- Class IV of circular cowls (without hub); $F_E/F_a = 0.5$,
 $v_E/v_0 = 0$.

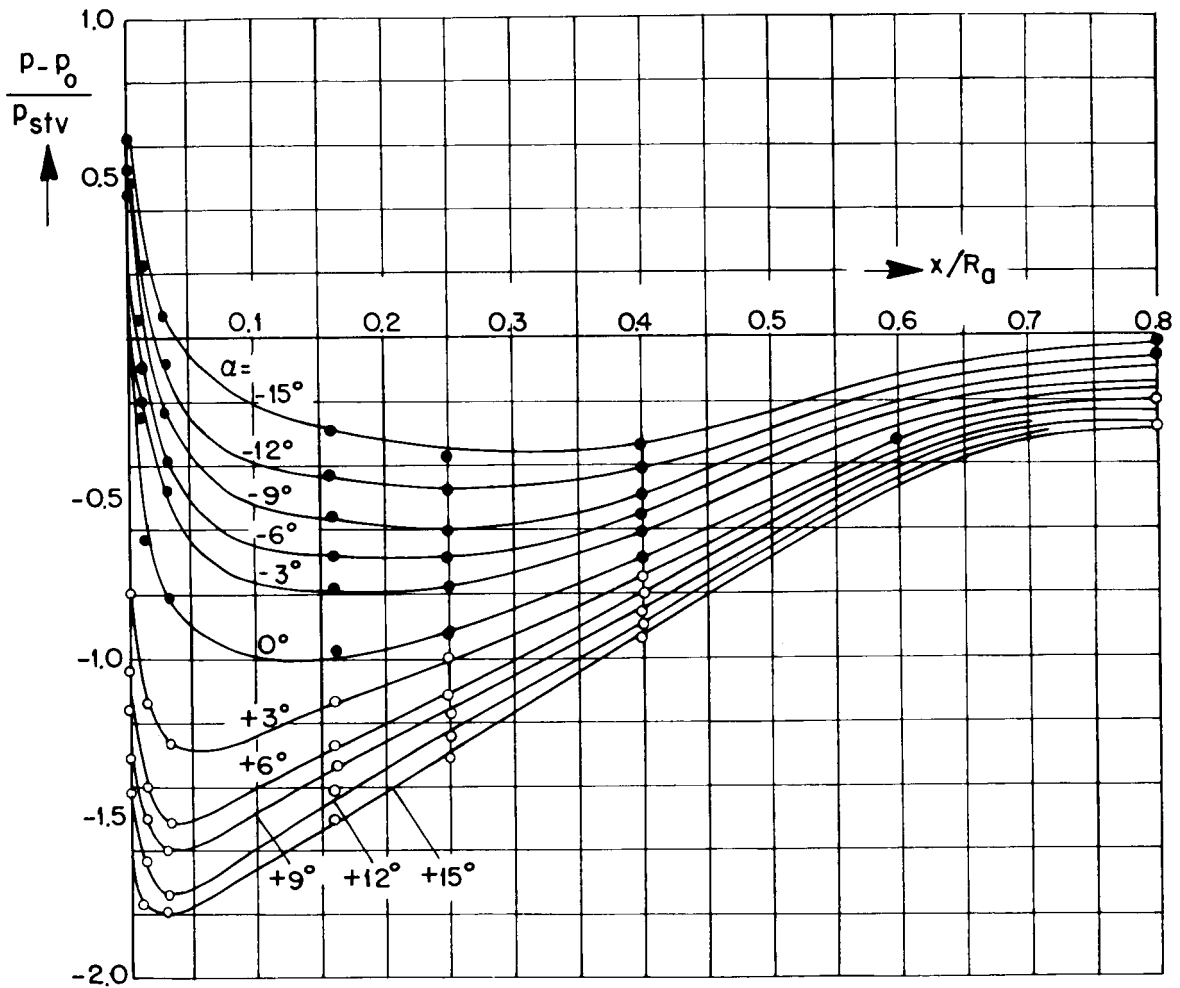


Figure 29.- Class IV of circular cowls (with hub); $F_E'/F_a = 0.5$,
 $v_E/v_O = 0$.

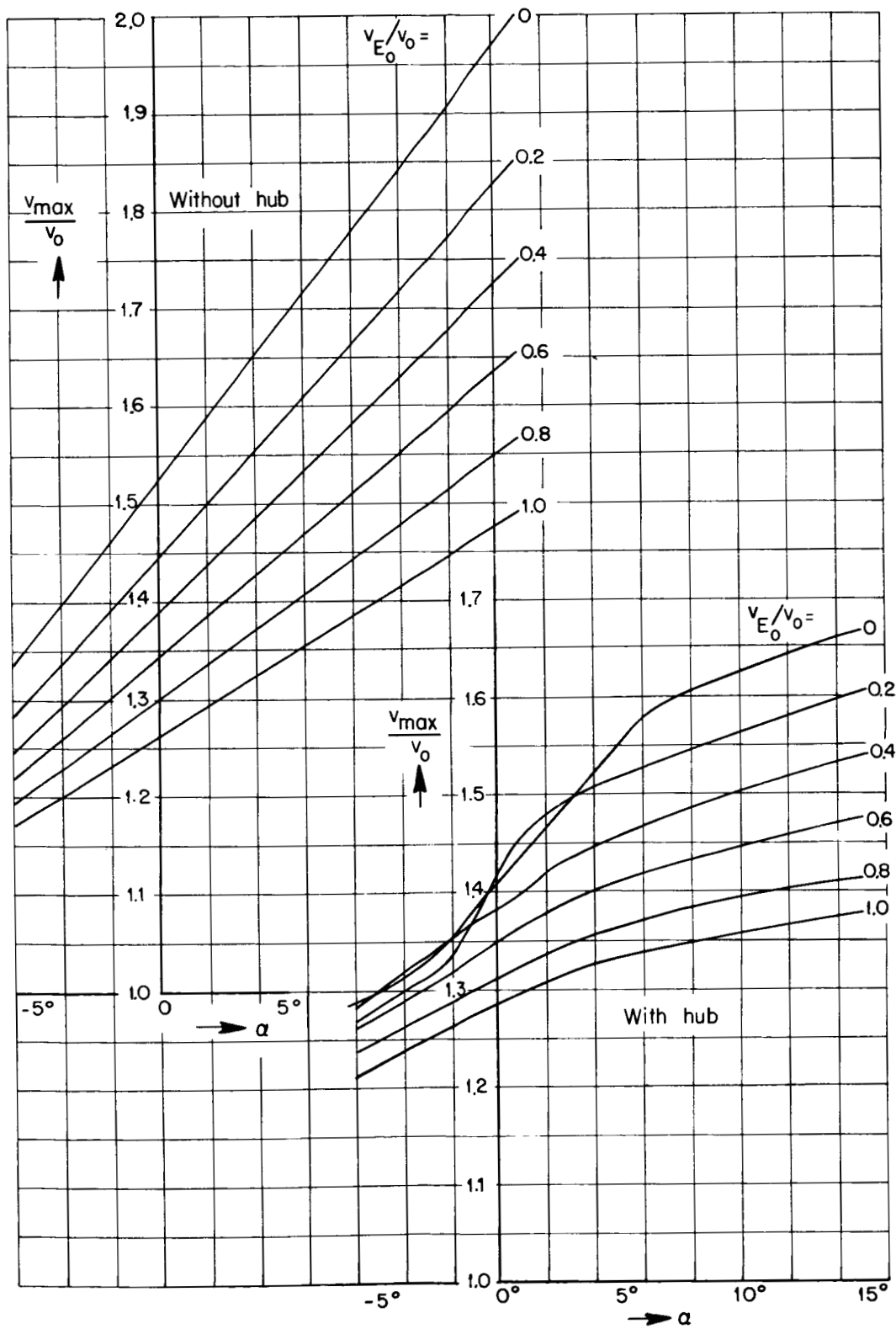


Figure 30.- Class IV of circular cowls; $F_E/F_a = 0.5$.

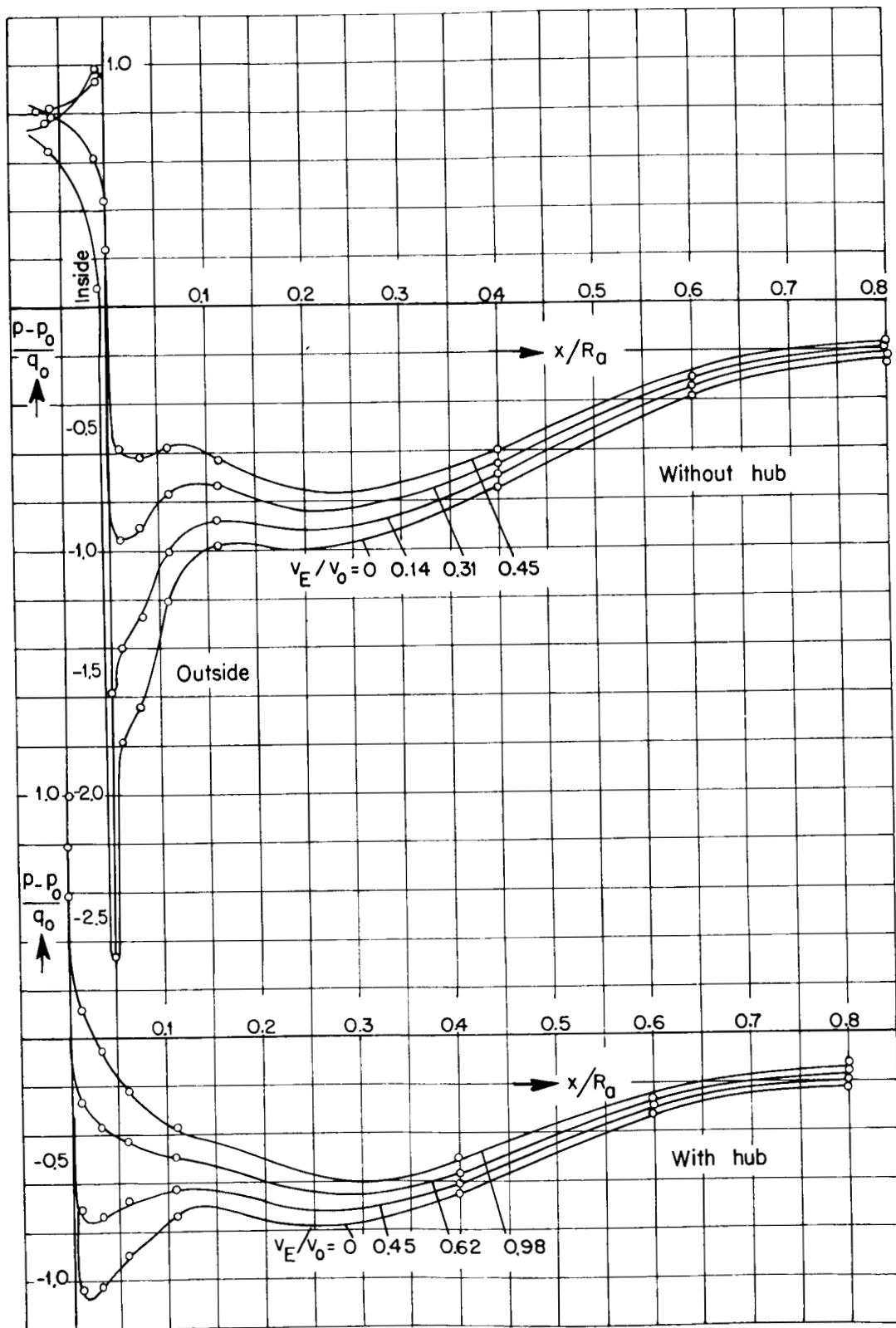


Figure 31.- Class IV of circular cowls; $F_E/F_a = 0.6$, $\alpha = 0^\circ$.

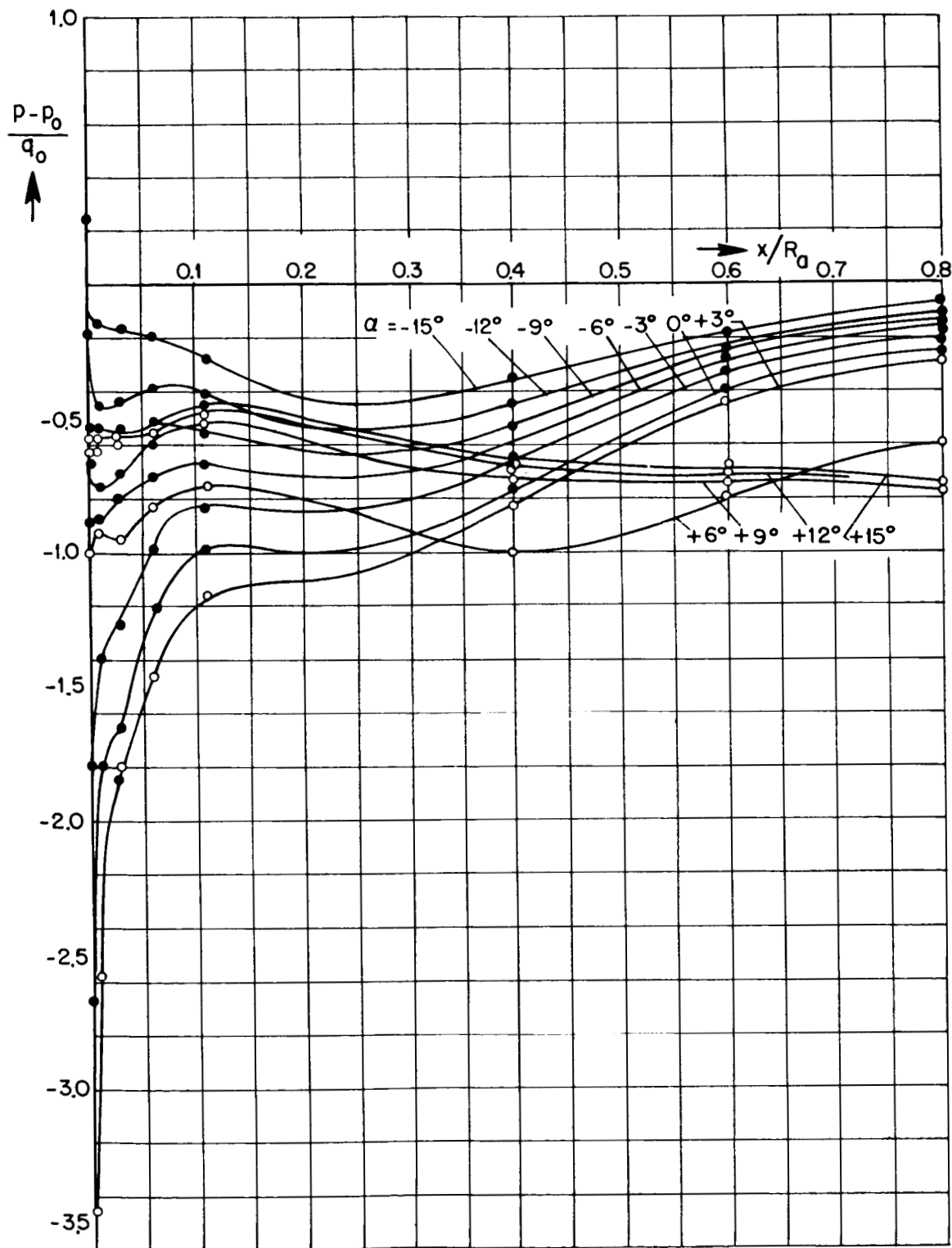


Figure 32.- Class IV of circular cowls (without hub); $F_E/F_a = 0.6$,
 $v_E/v_0 = 0$.

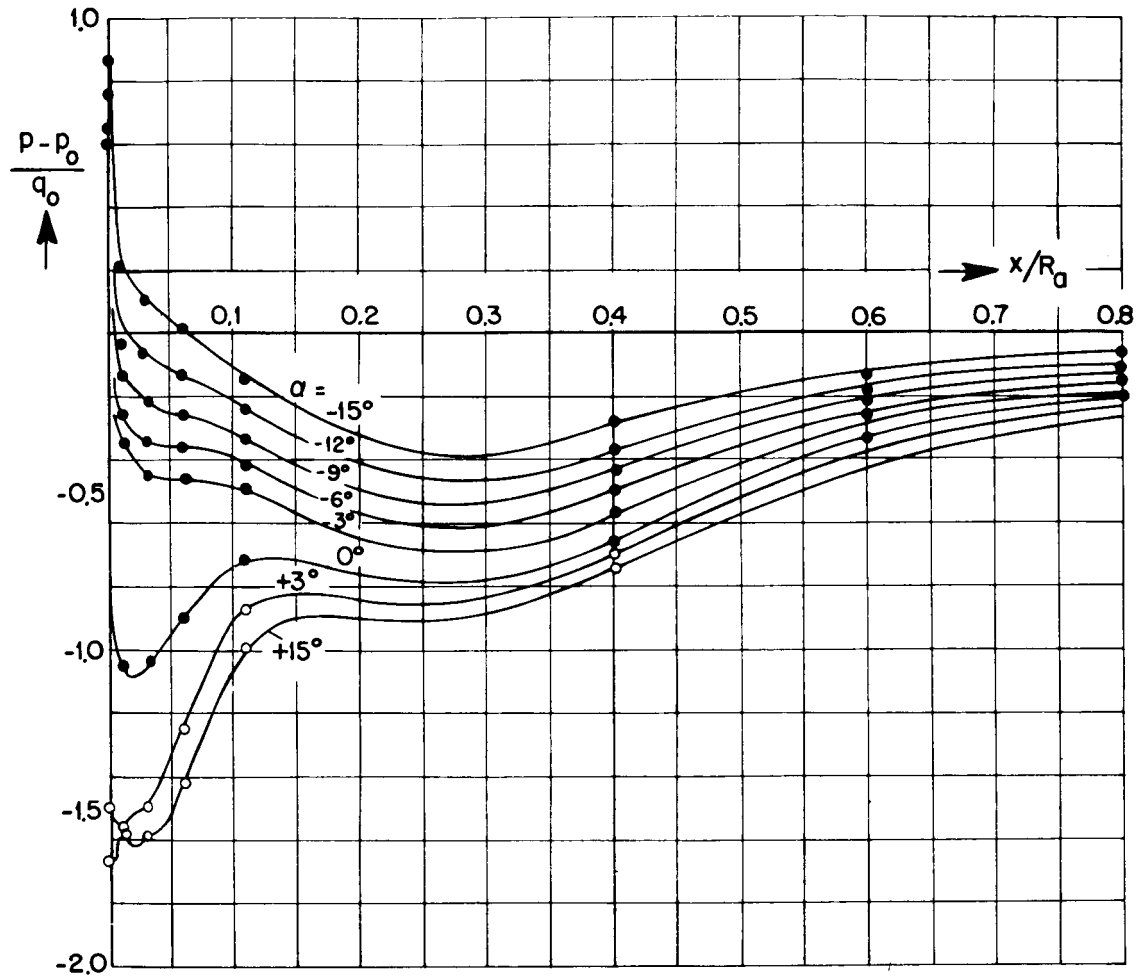


Figure 33.- Class IV of circular cowls (with hub); $F_E'/F_a = 0.6$,
 $v_E/v_0 = 0$.

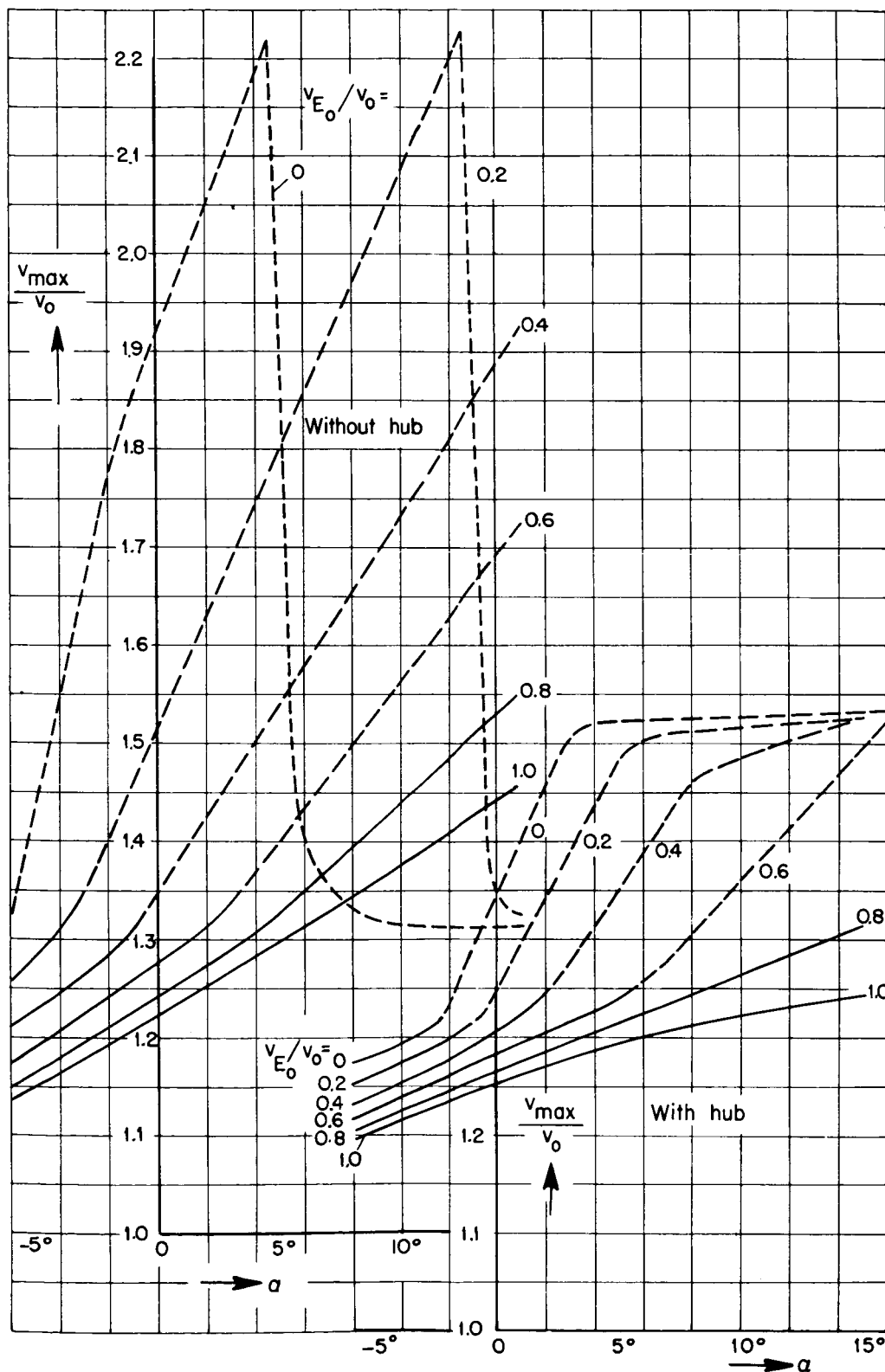


Figure 34.- Class IV of circular cowls; $F_E/F_a = 0.6$.

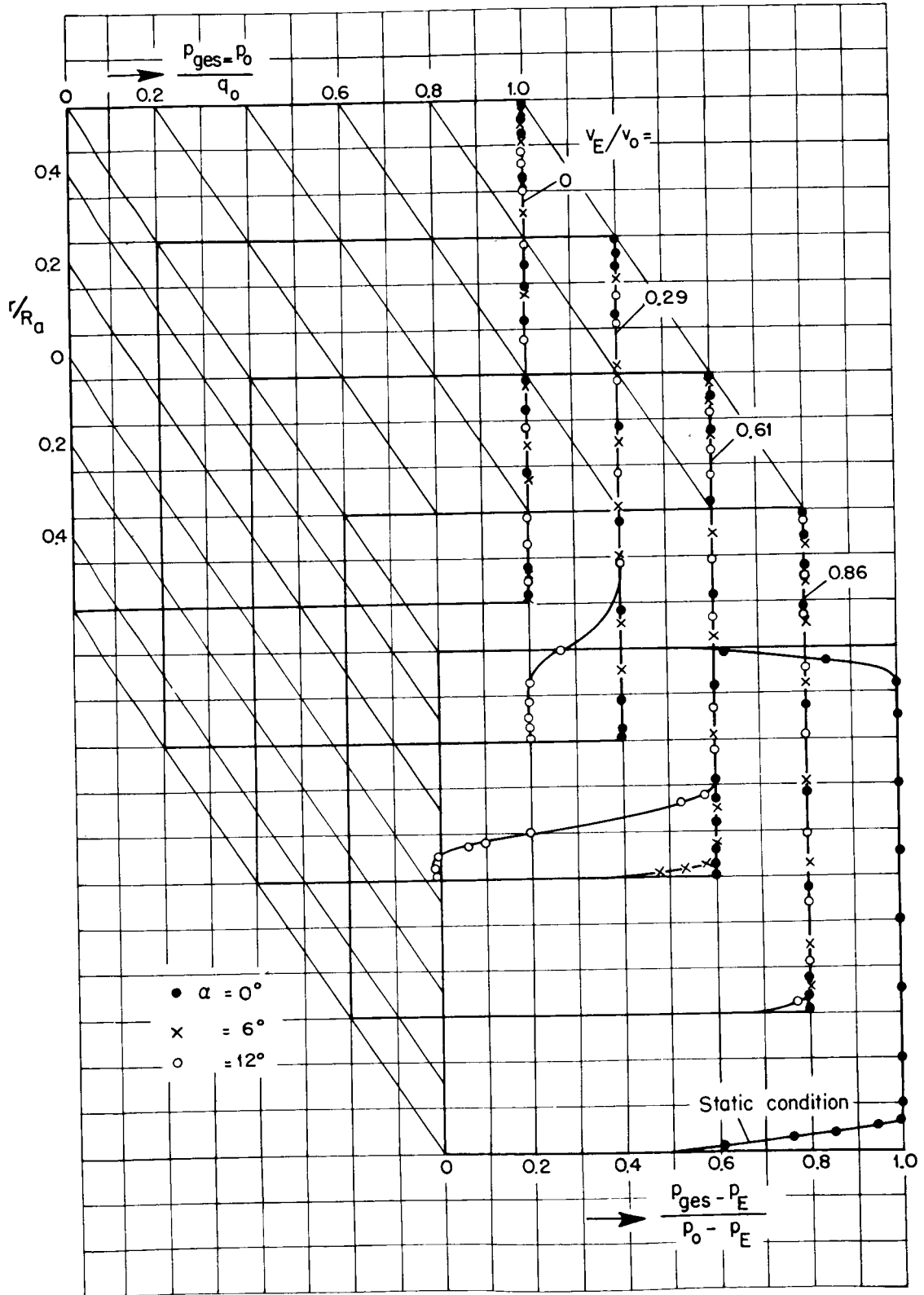


Figure 35.- Class III of circular cowls (without hub); $F_E/F_a = 0.3$.

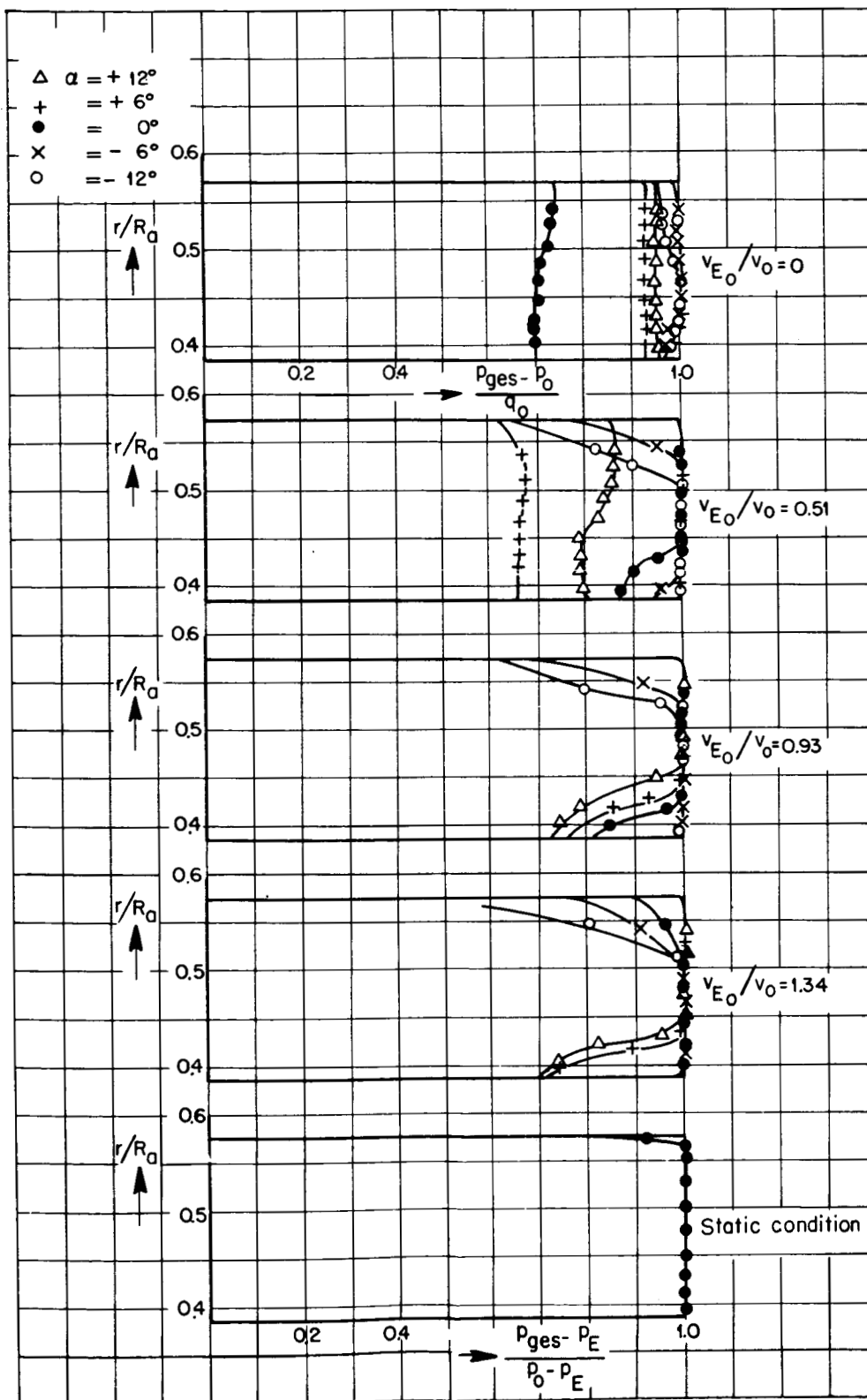


Figure 36.- Class III of circular cowls (with hub); $F_{E'}/F_a = 0.3$.

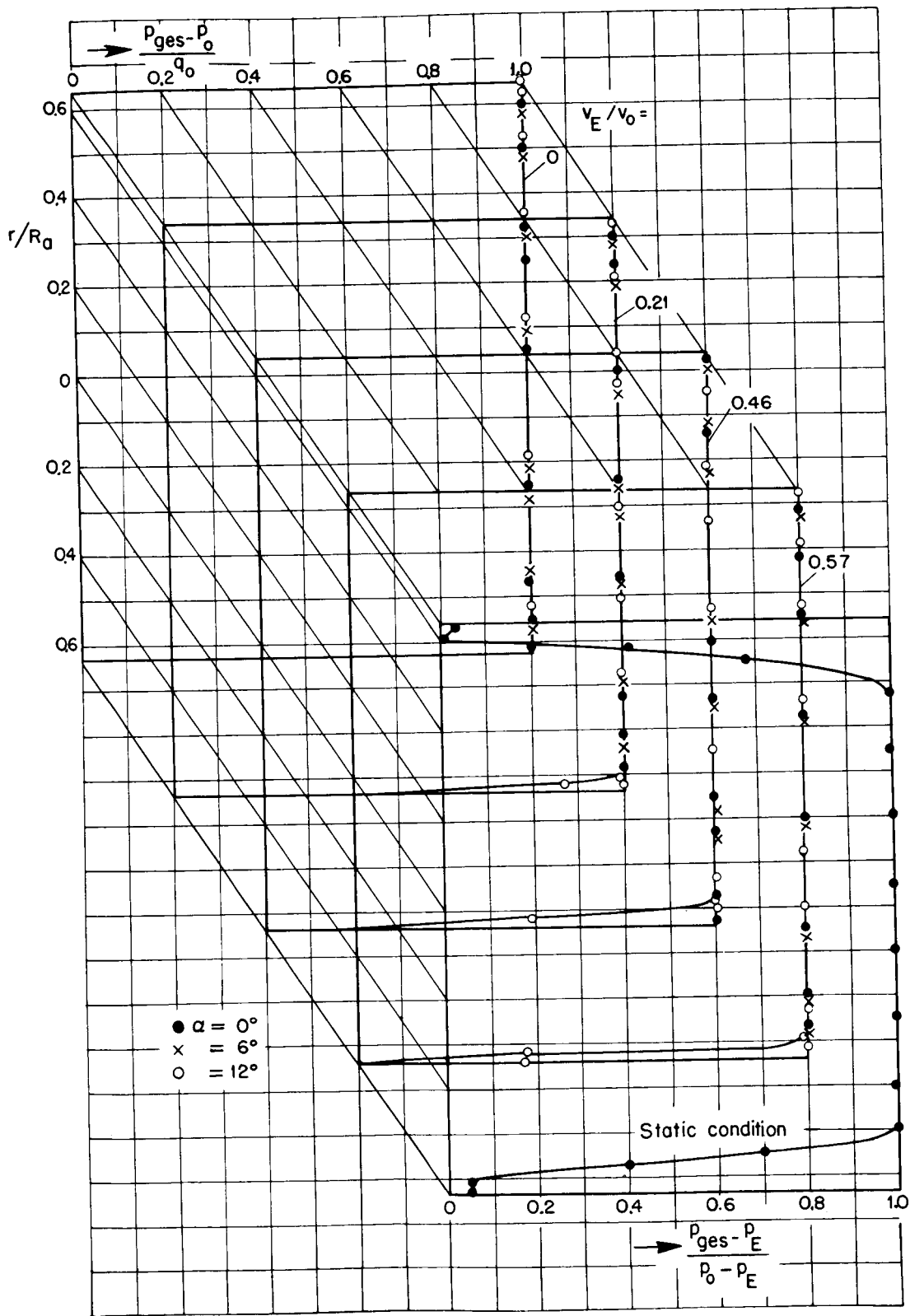


Figure 37.- Class III of circular cowls (without hub); $F_E/F_a = 0.4$.

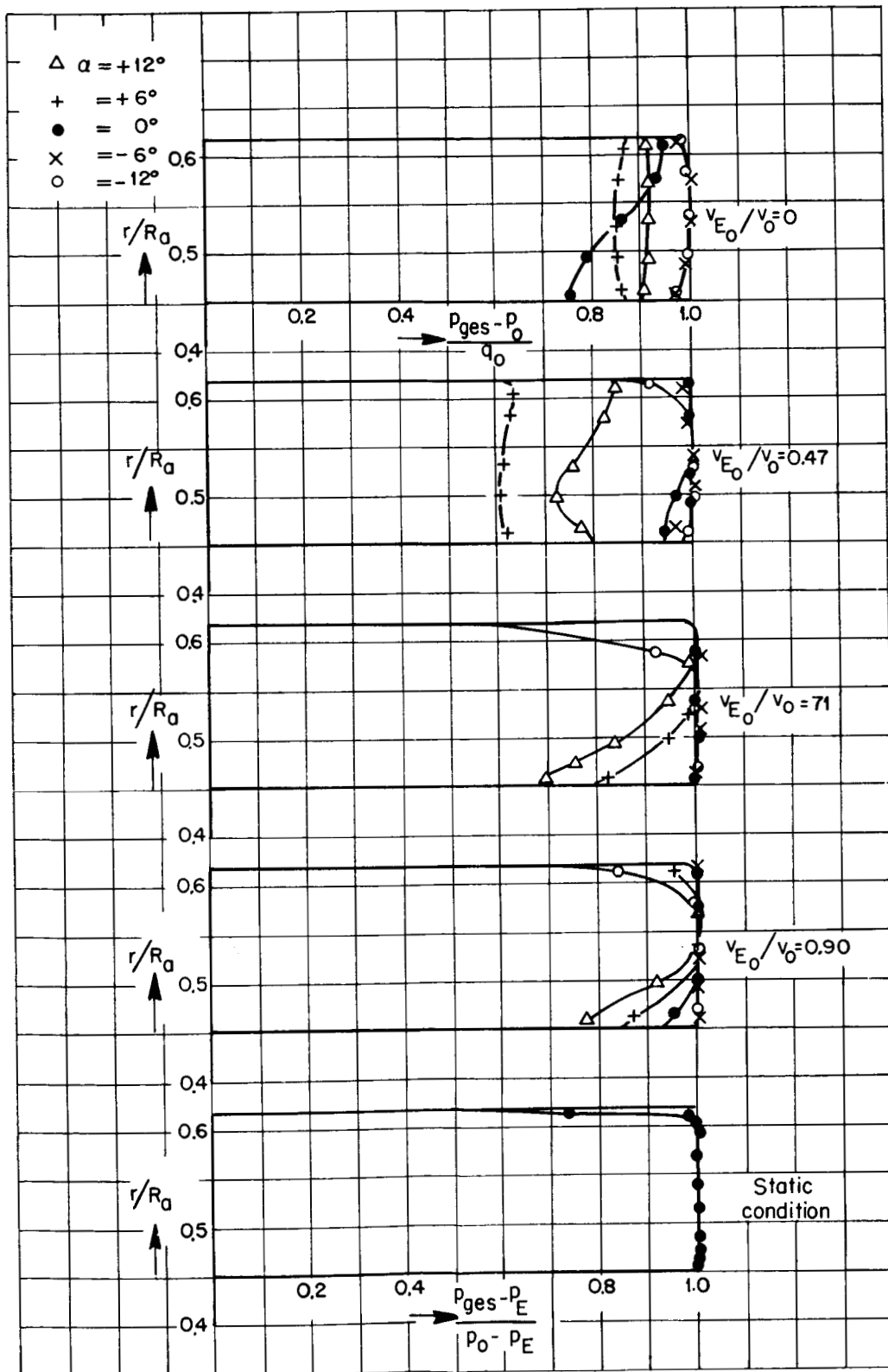


Figure 38.- Class III of circular cowls (with hub); $F_E'/F_a = 0.4$.

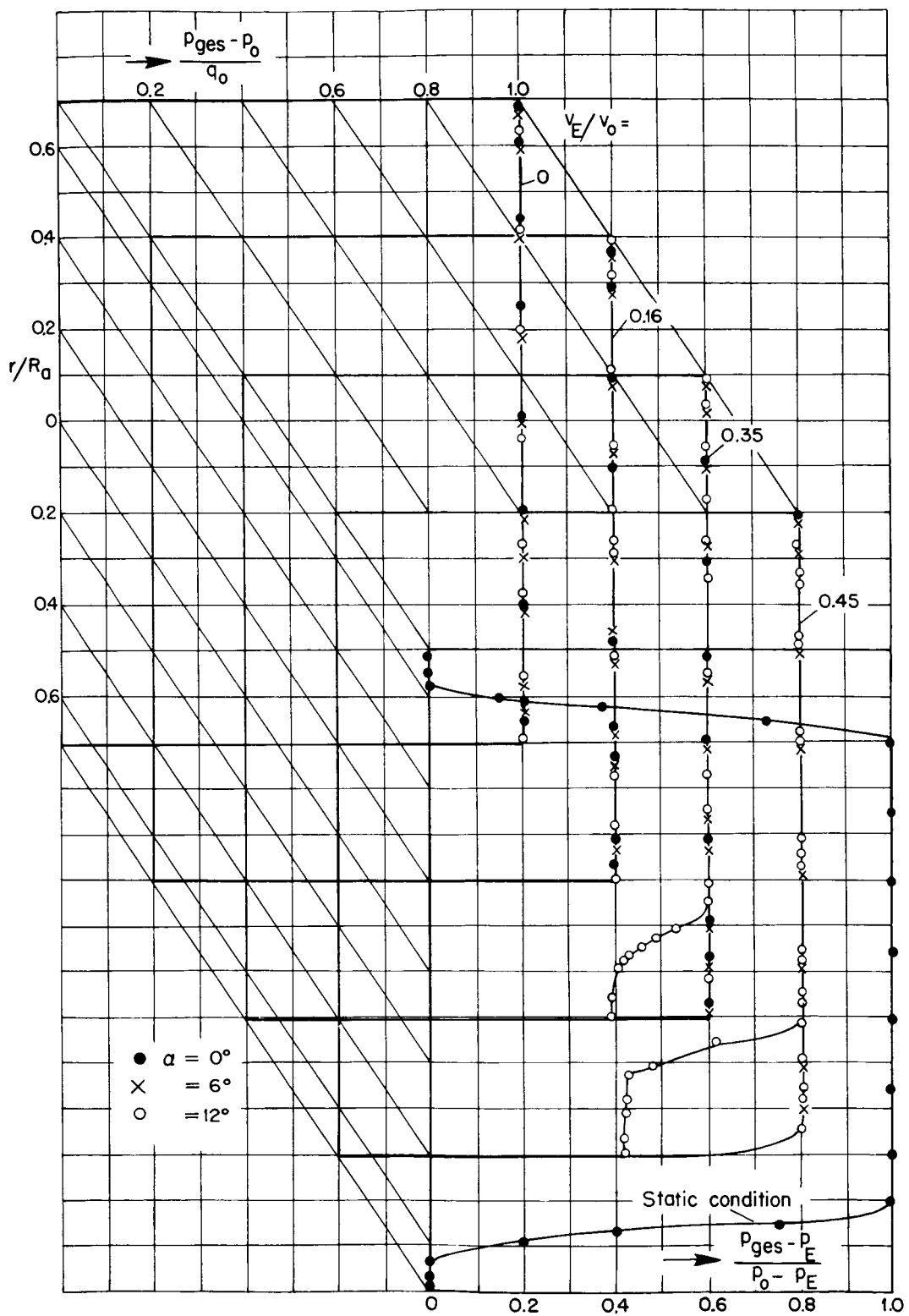


Figure 39.- Class III of circular cowls (without hub); $F_E/F_a = 0.5$.

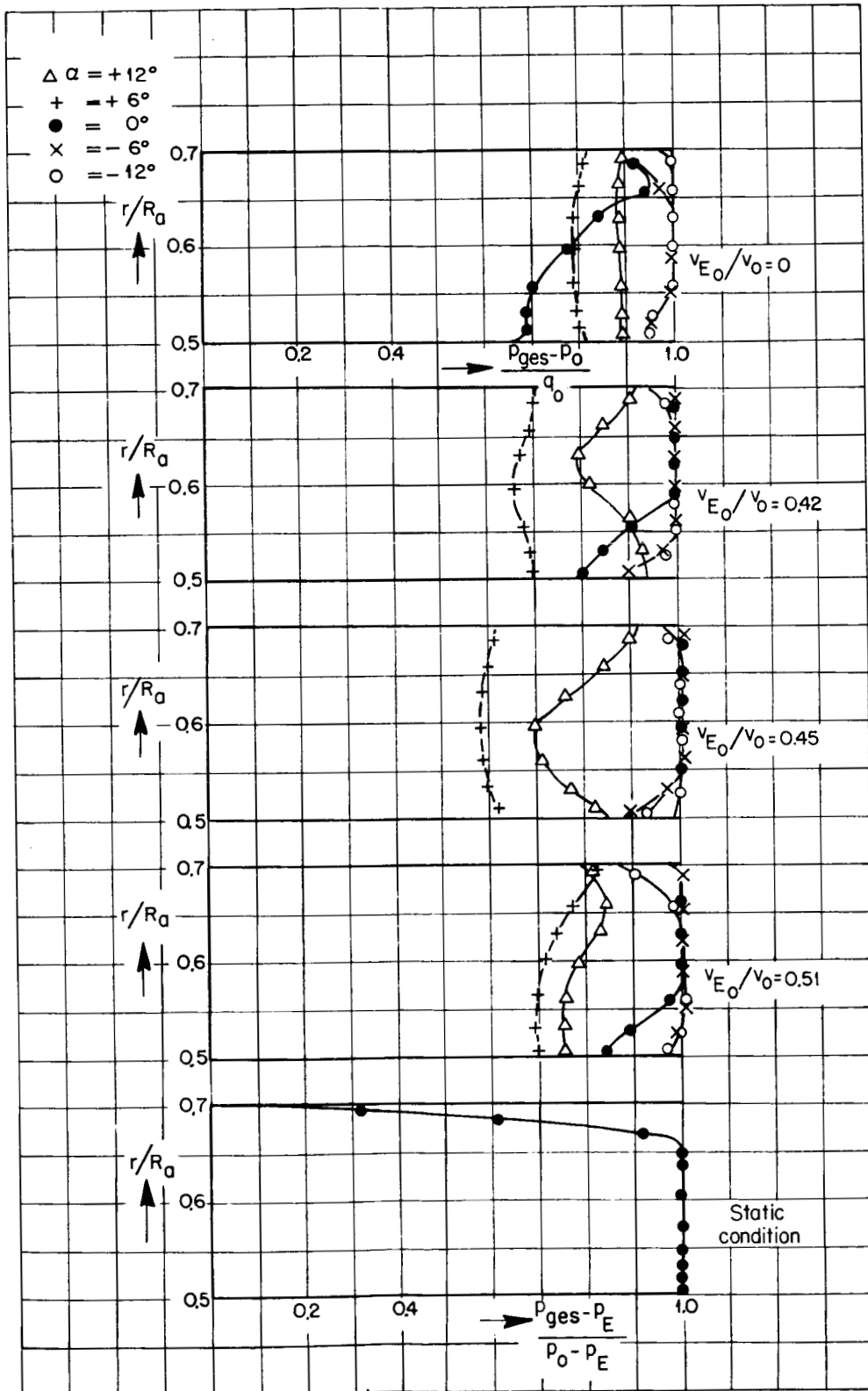


Figure 40.- Class III of circular cowls (with hub); $F_{E'}/F_a = 0.5$.

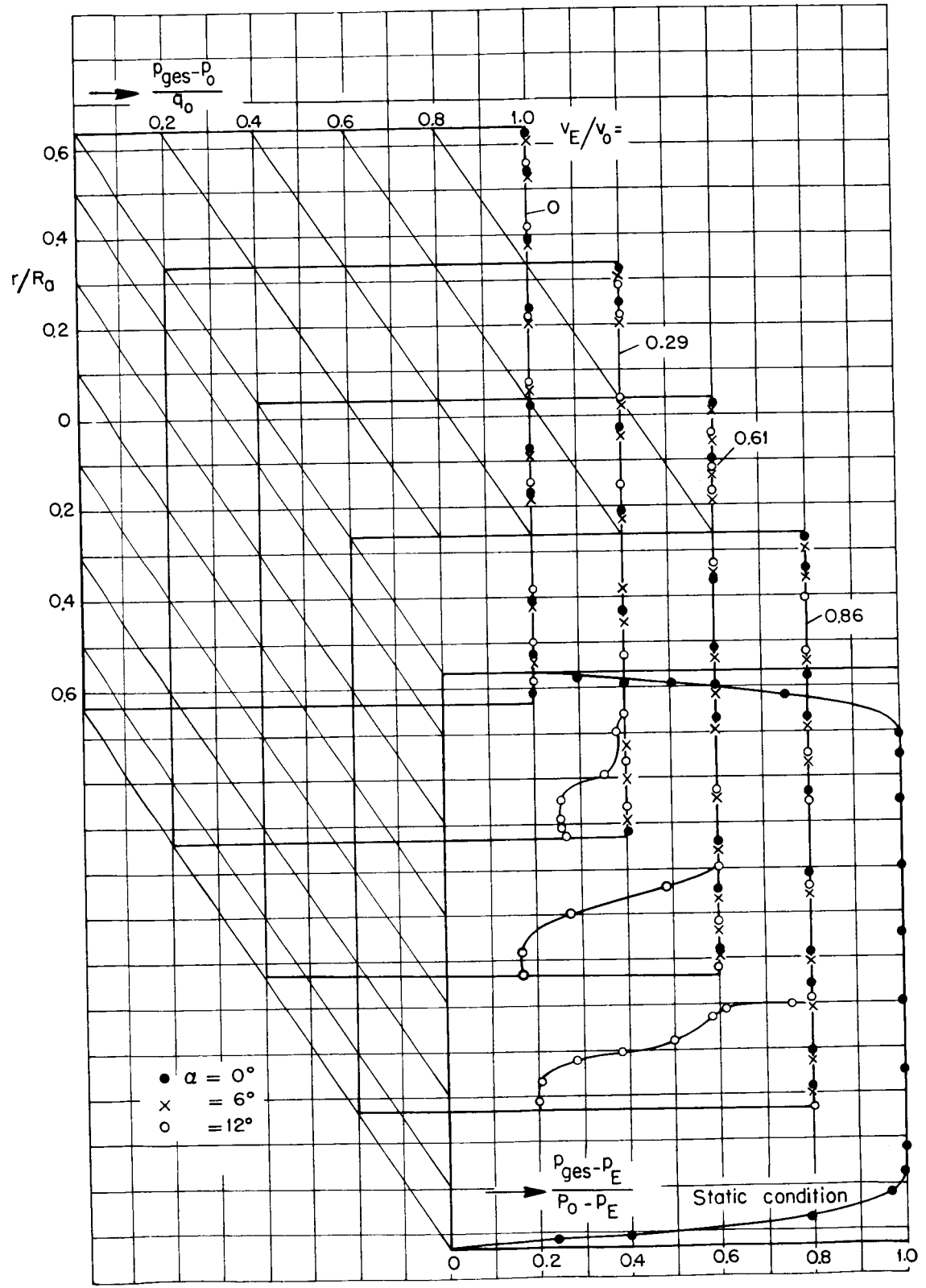


Figure 41.- Class IV of circular cowls (without hub); $F_E/F_a = 0.4$.

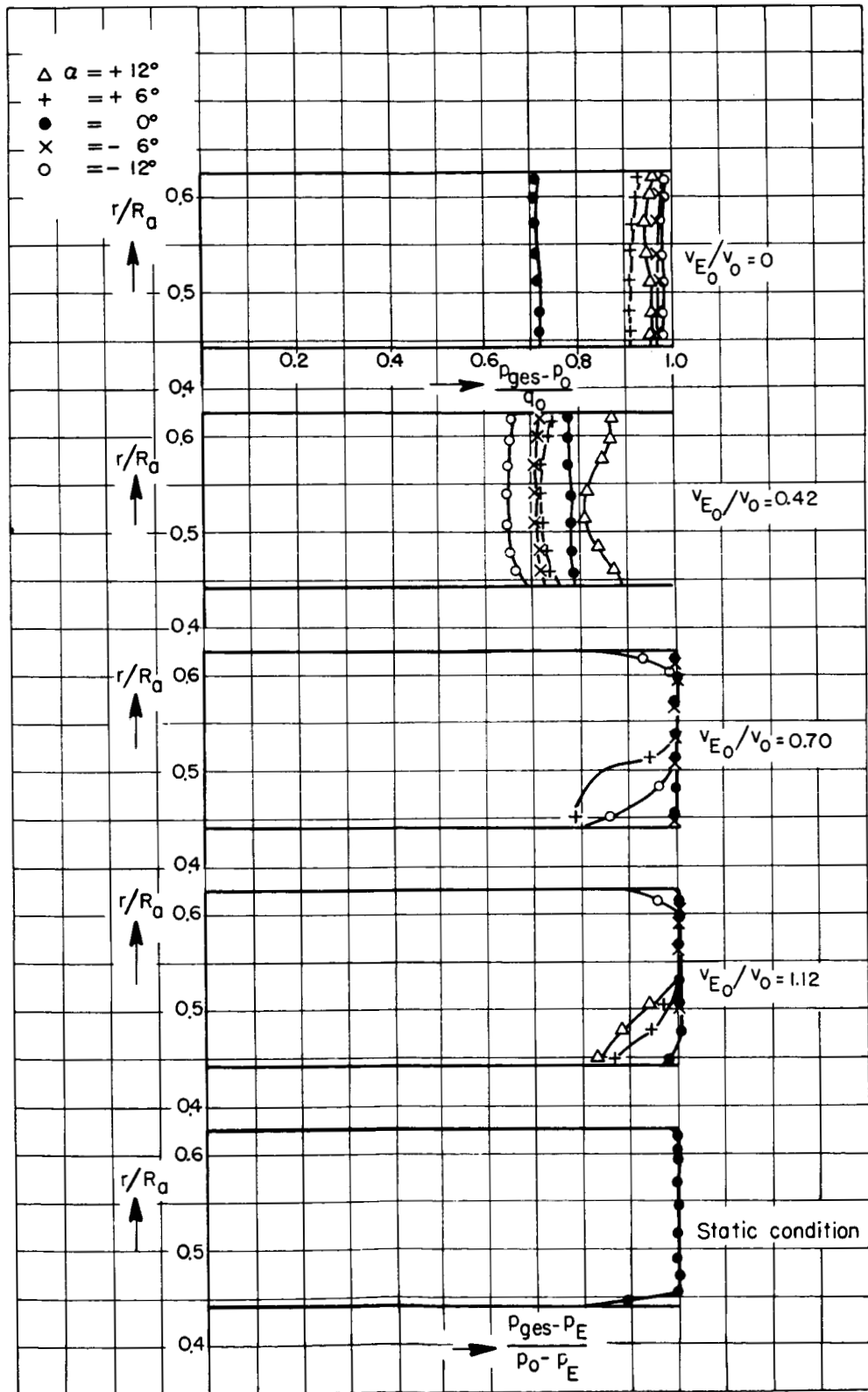


Figure 42.- Class IV of circular cowls (with hub); $F_{E'}/F_a = 0.4$.

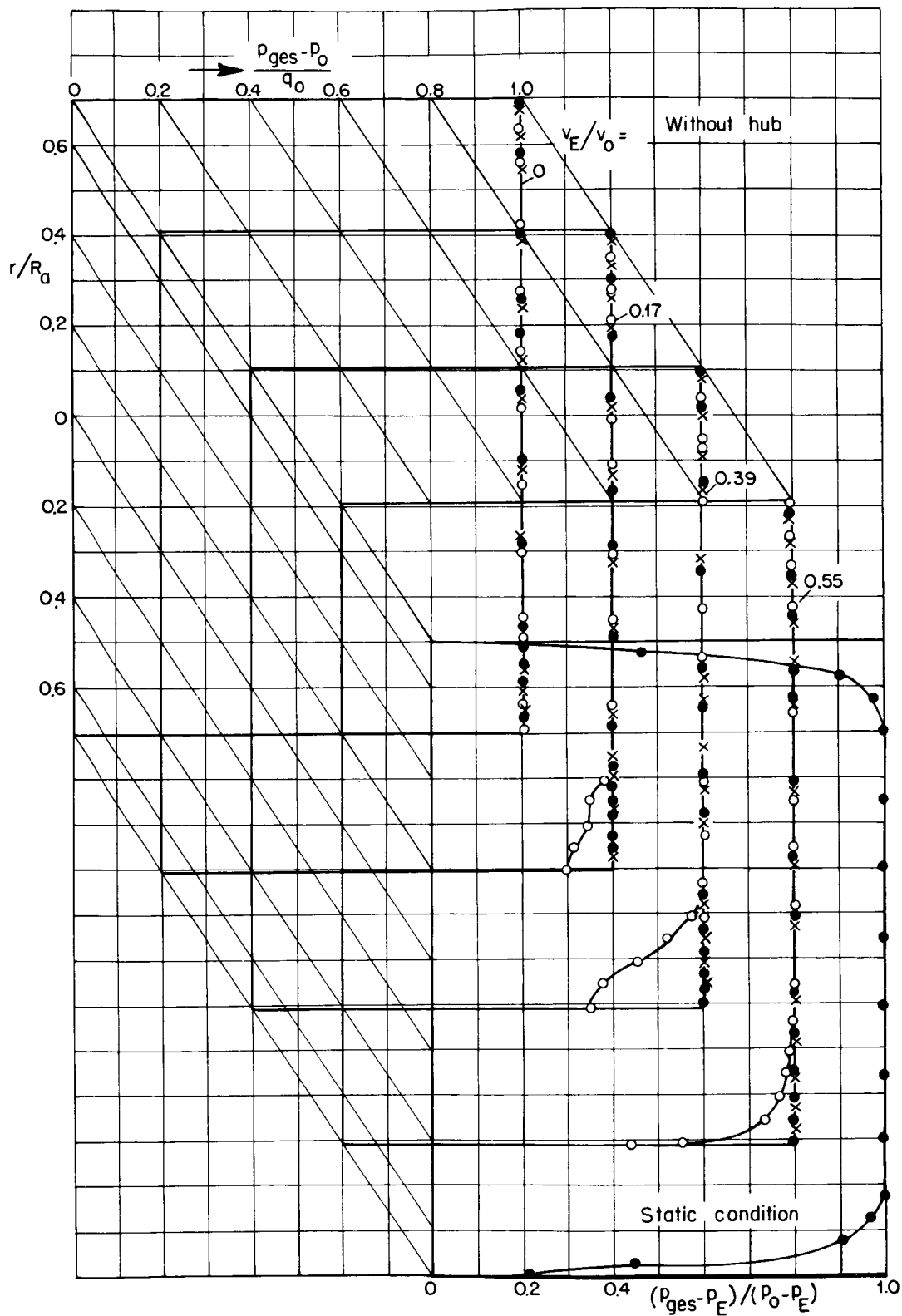


Figure 43.- Class IV of circular cowls; $F_E/F_a = 0.5$.

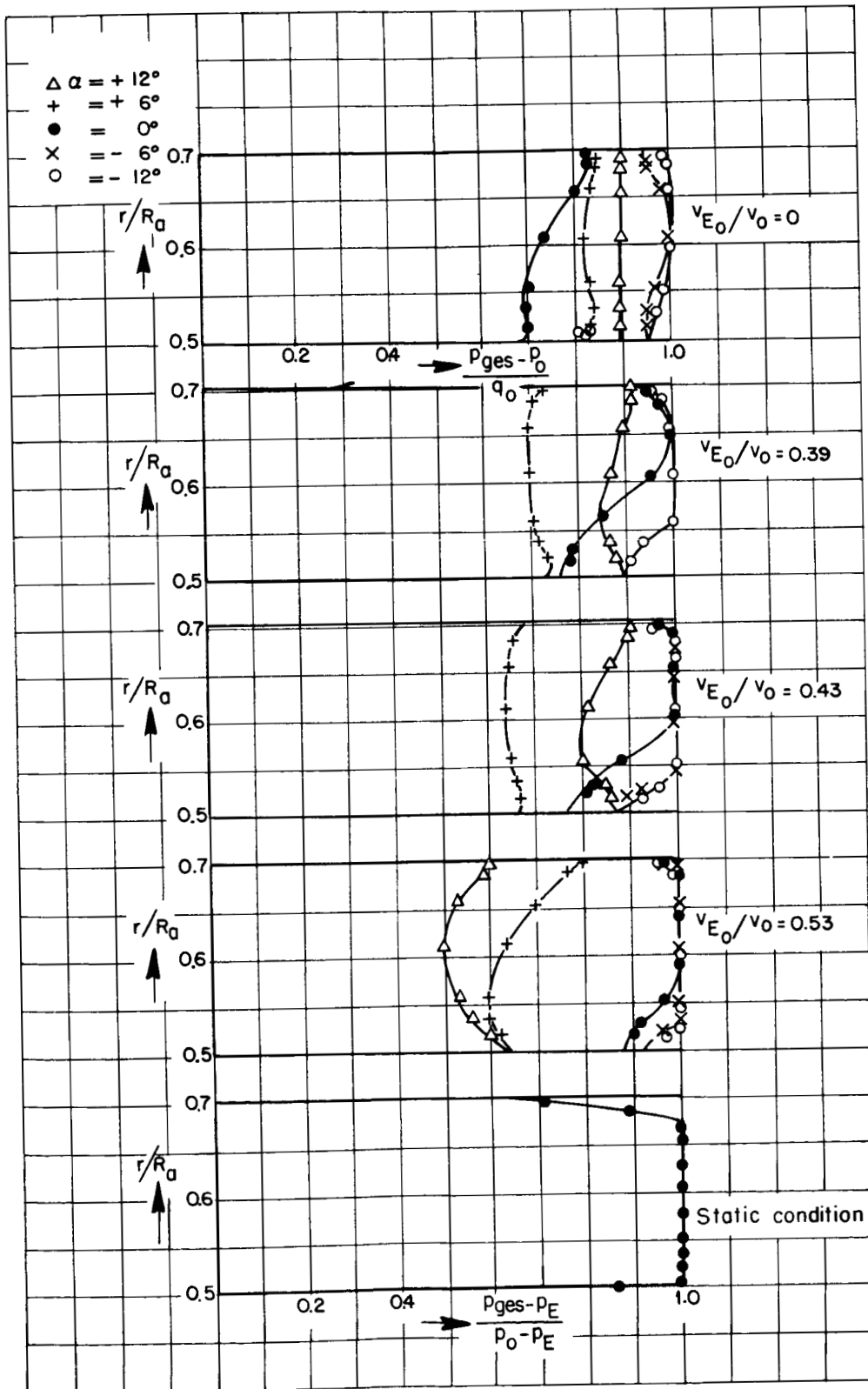


Figure 44.- Class IV of circular cowls (with hub); $F_{E'}/F_a = 0.5$.

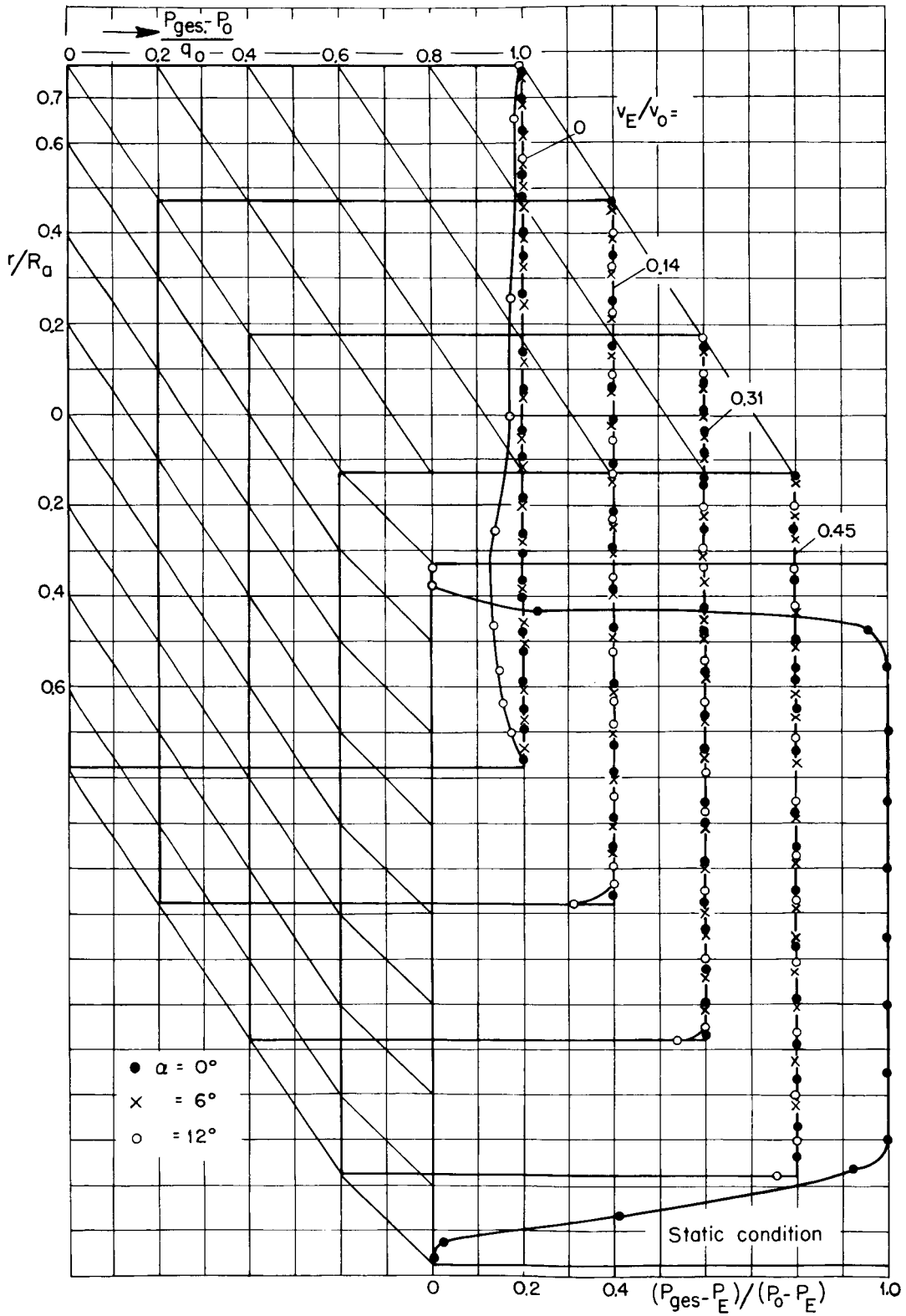


Figure 45.- Class IV of circular cowls (without hub); $F_E/F_a = 0.6$.

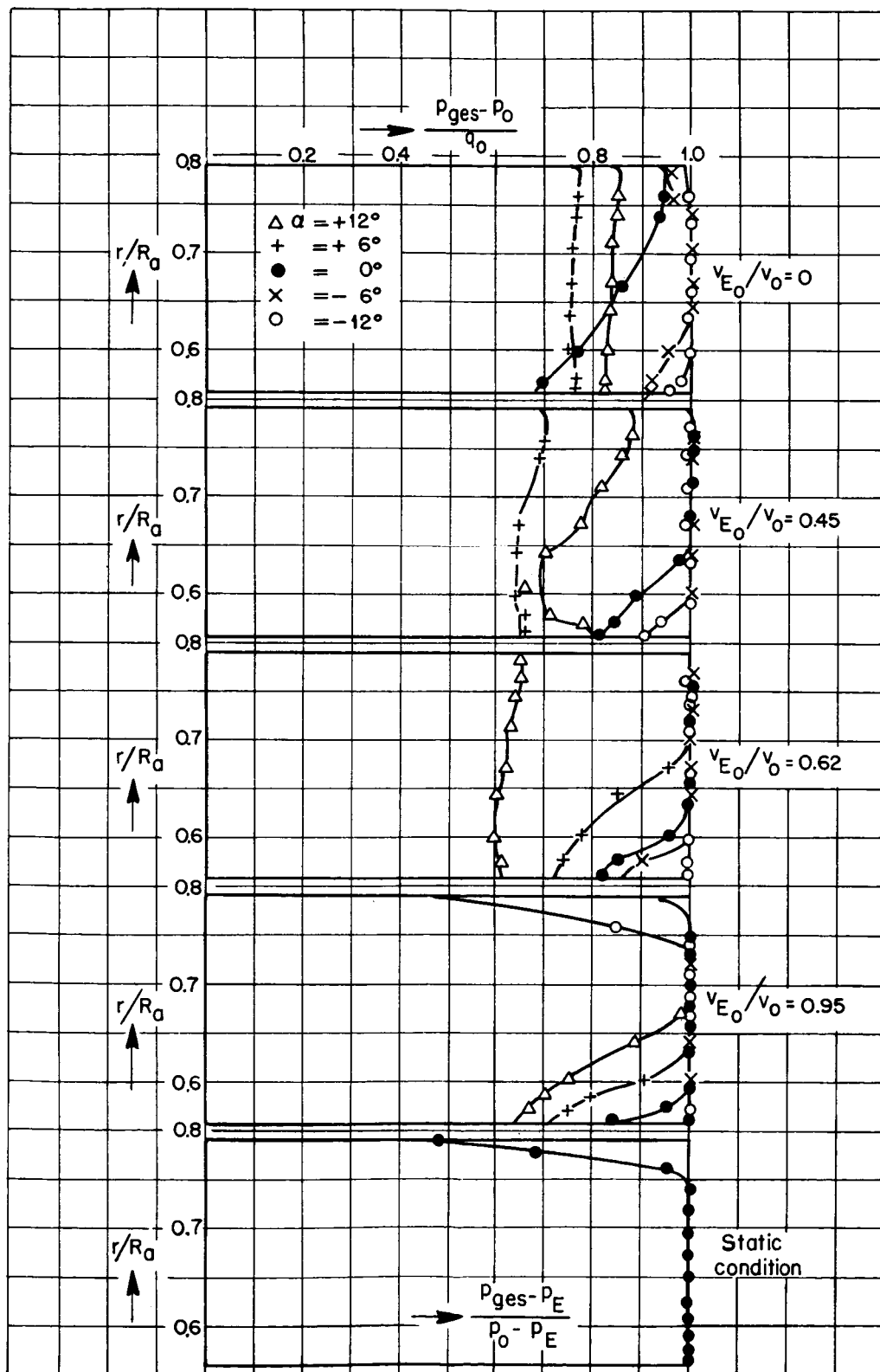


Figure 46.- Class IV of circular cowls (with hub); $F_{E'}/F_a = 0.6$.

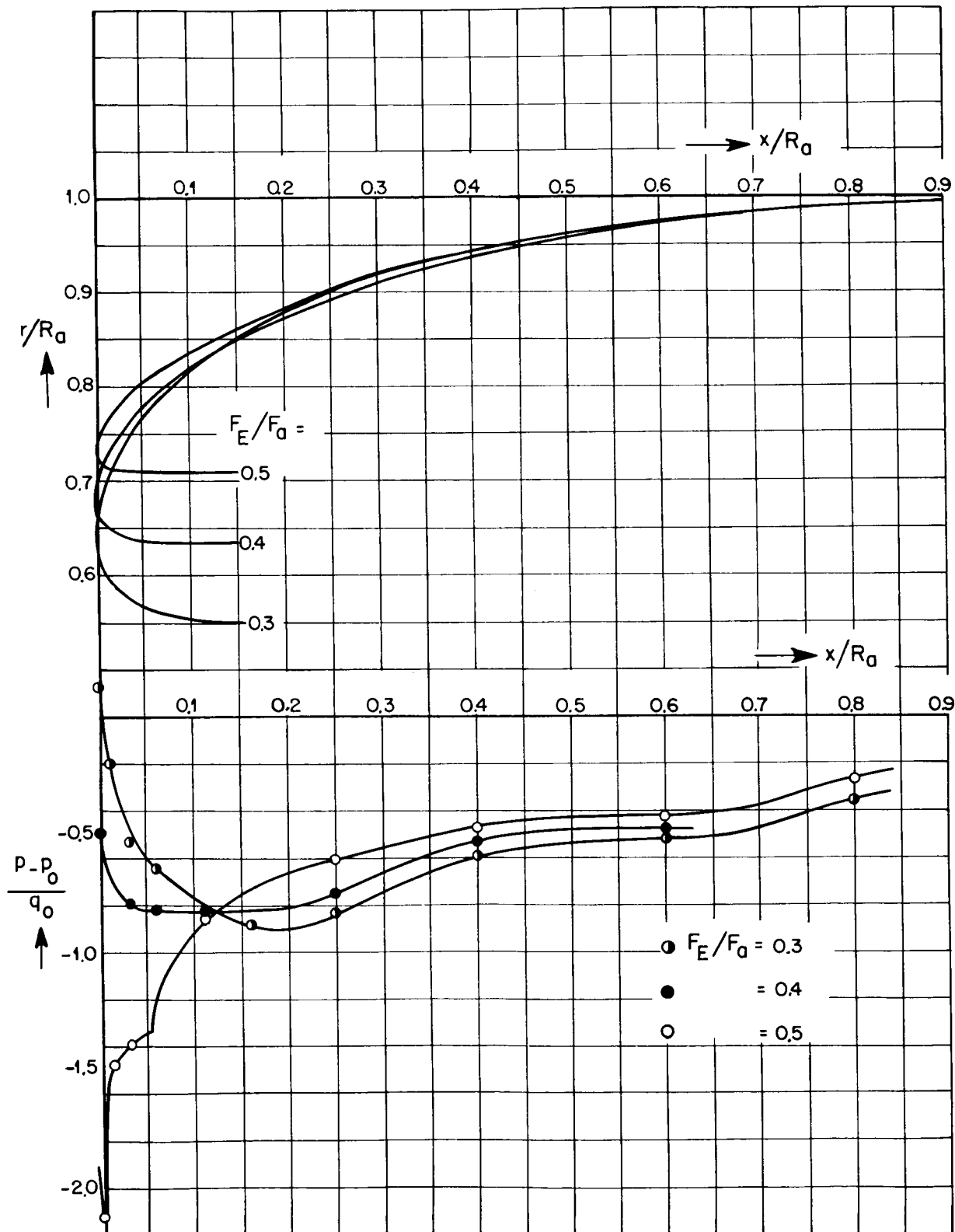


Figure 47.- Class III of circular cowls (without hub); $v_E/v_0 = 0$, $\alpha = 0^\circ$.

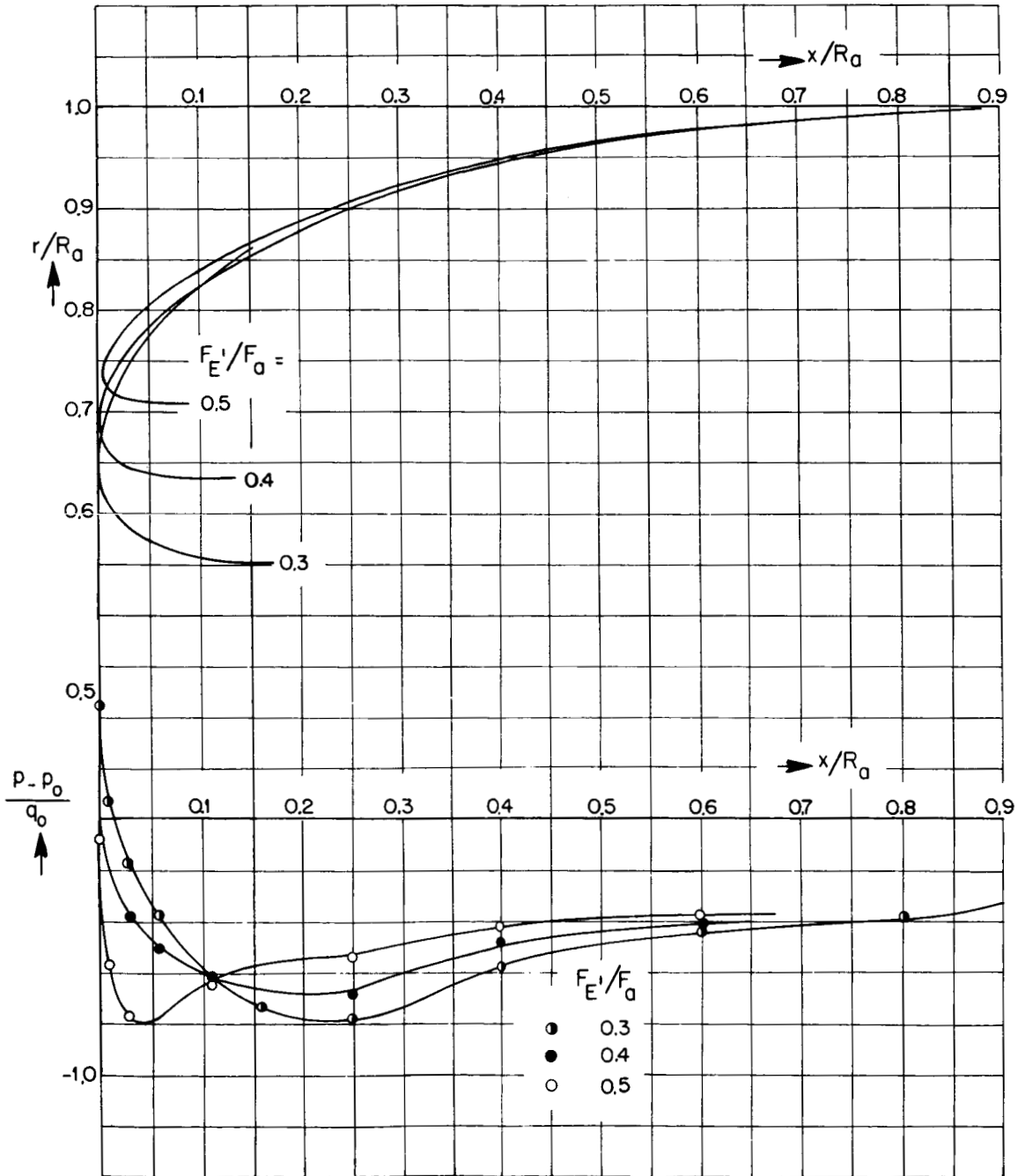


Figure 48.- Class III of circular cowls (with hub); $v_E/v_o = 0$, $\alpha = 0^\circ$.

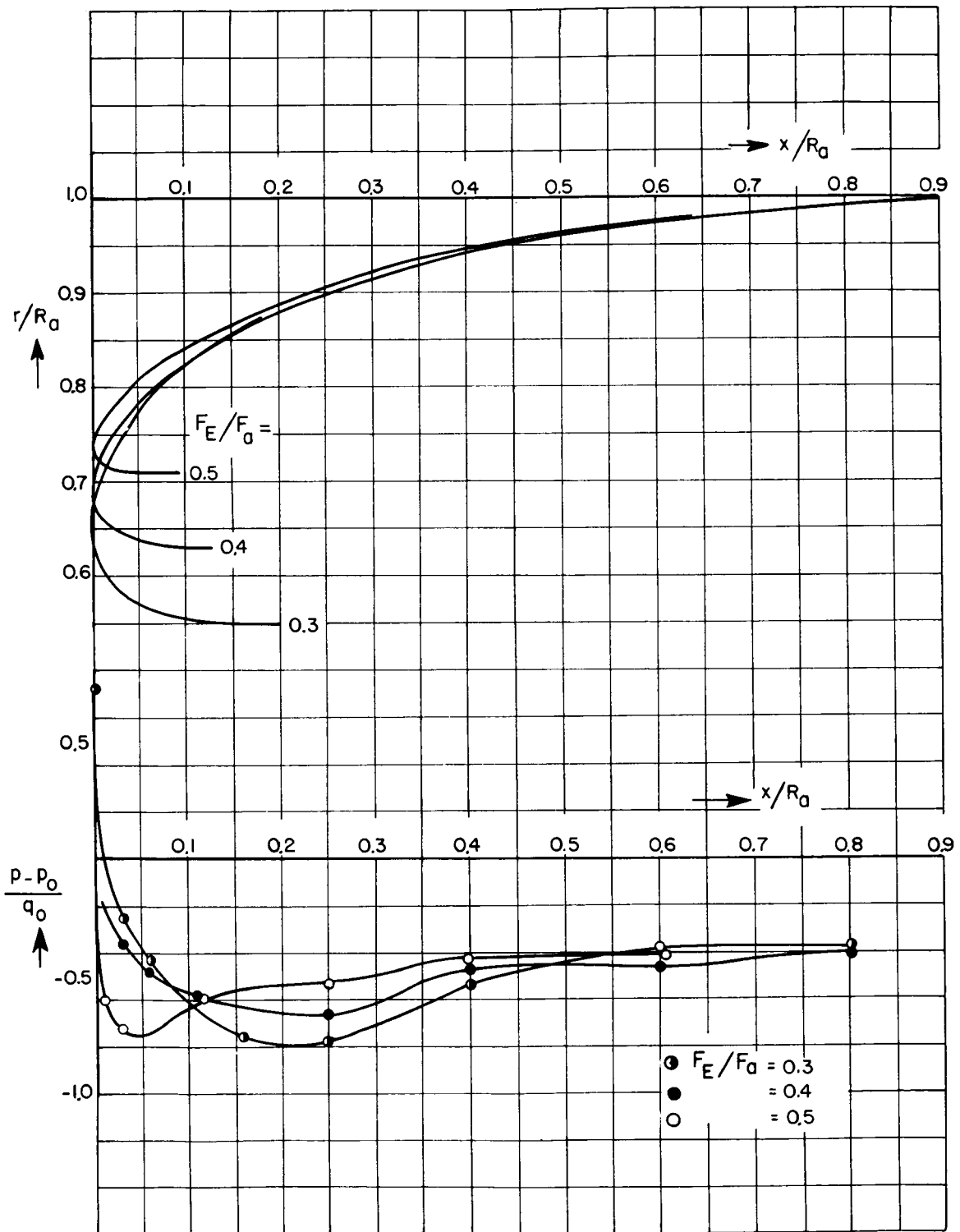


Figure 49.- Class III of circular cowls (without hub); $v_E/v_0 = 0.3$, $\alpha = 0^\circ$.

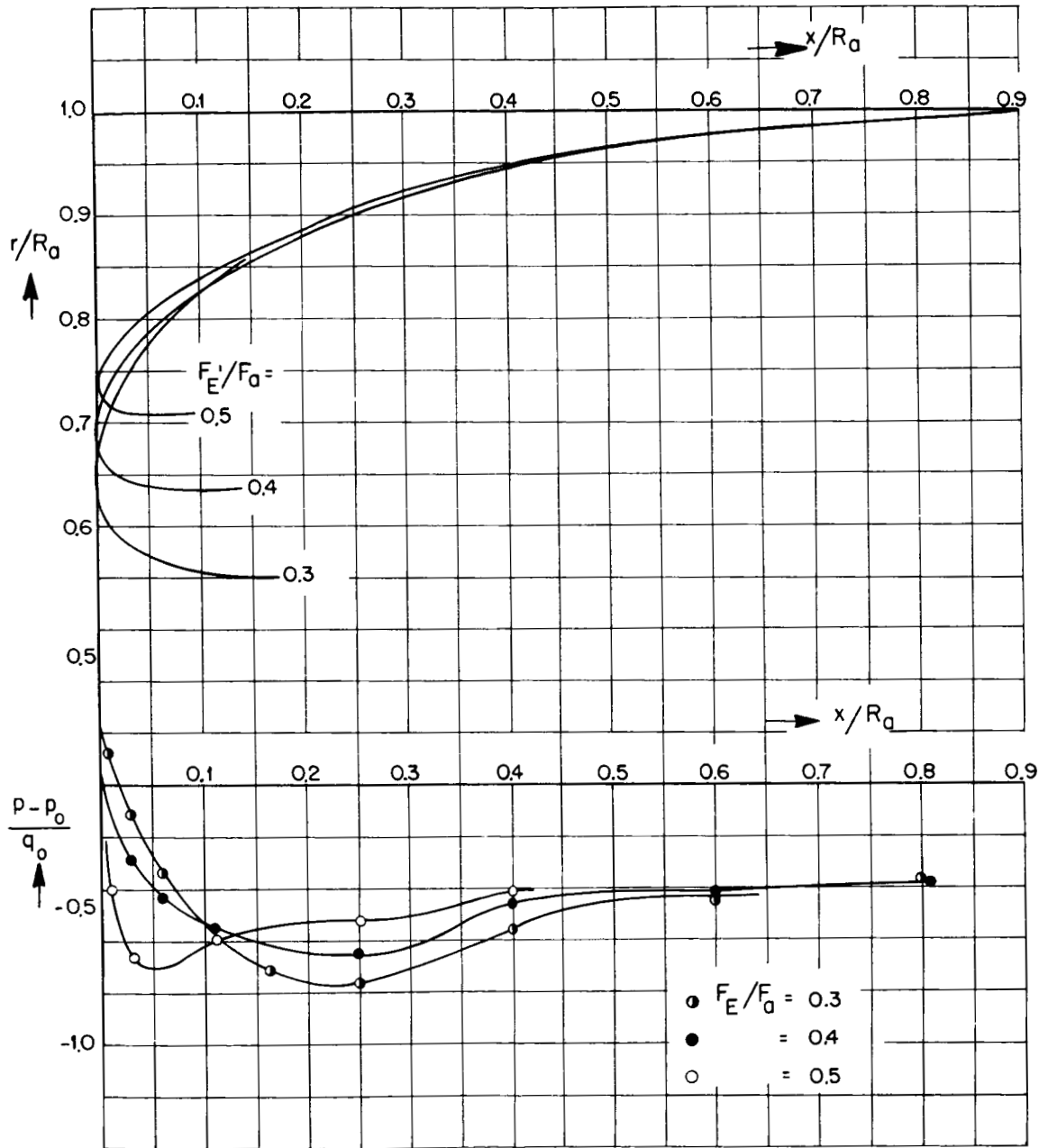


Figure 50.- Class III of circular cowls (with hub); $v_E/v_0 = 0.3$, $\alpha = 0^\circ$.

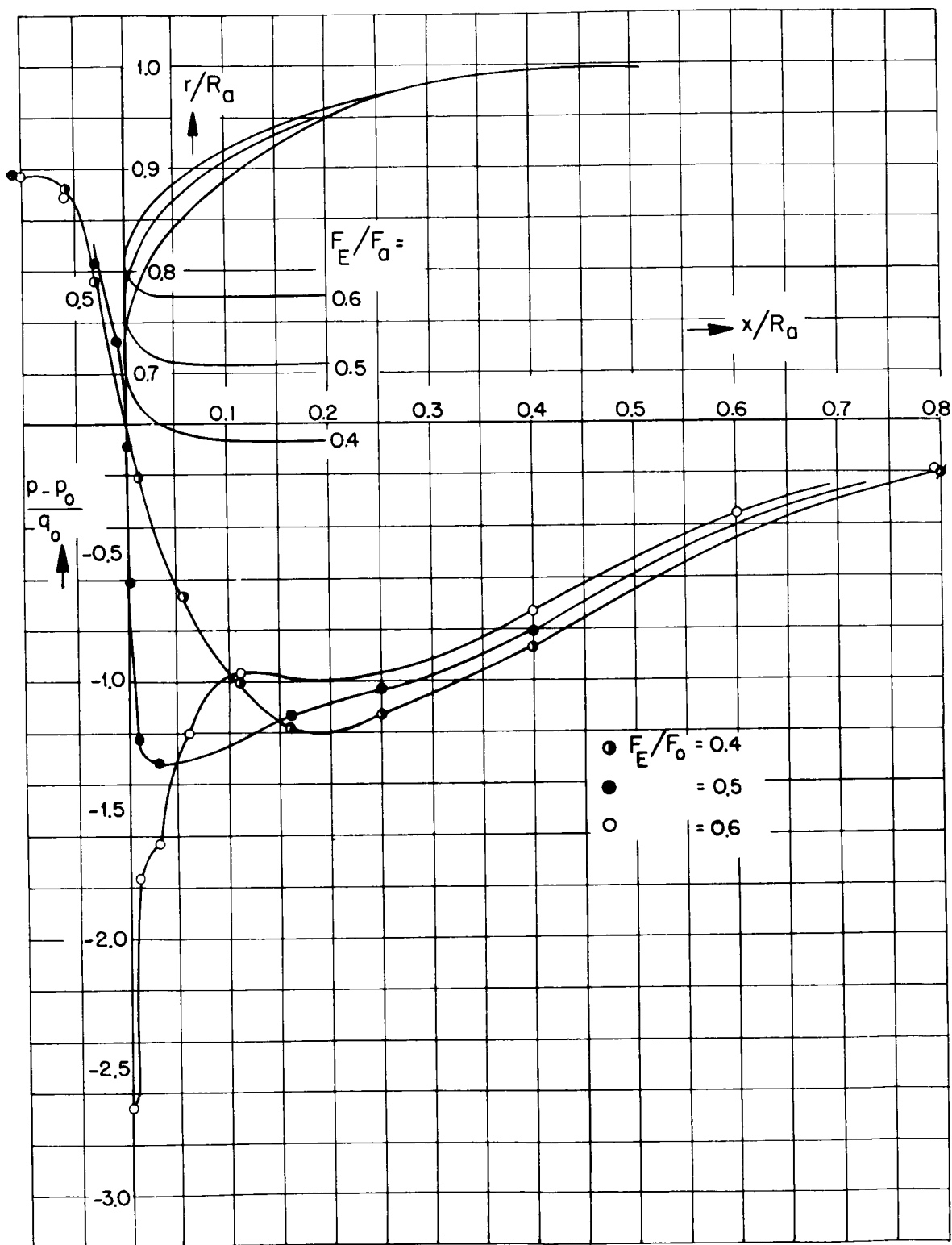


Figure 51.- Class IV of circular cowls (without hub); $v_E/v_0 = 0$, $\alpha = 0^\circ$.

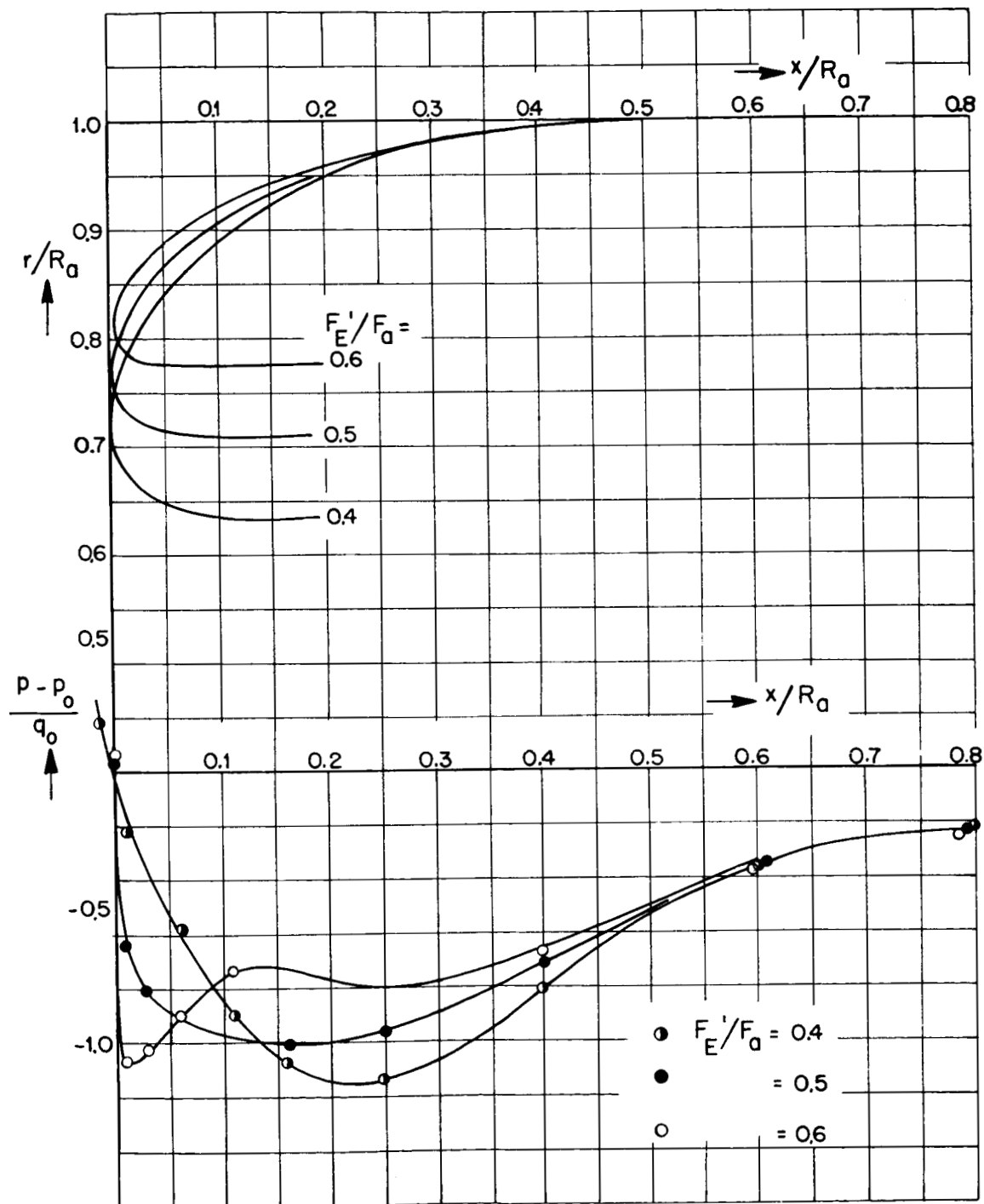


Figure 52.- Class IV of circular cowls (with hub); $v_E/v_0 = 0, \alpha = 0^\circ$.

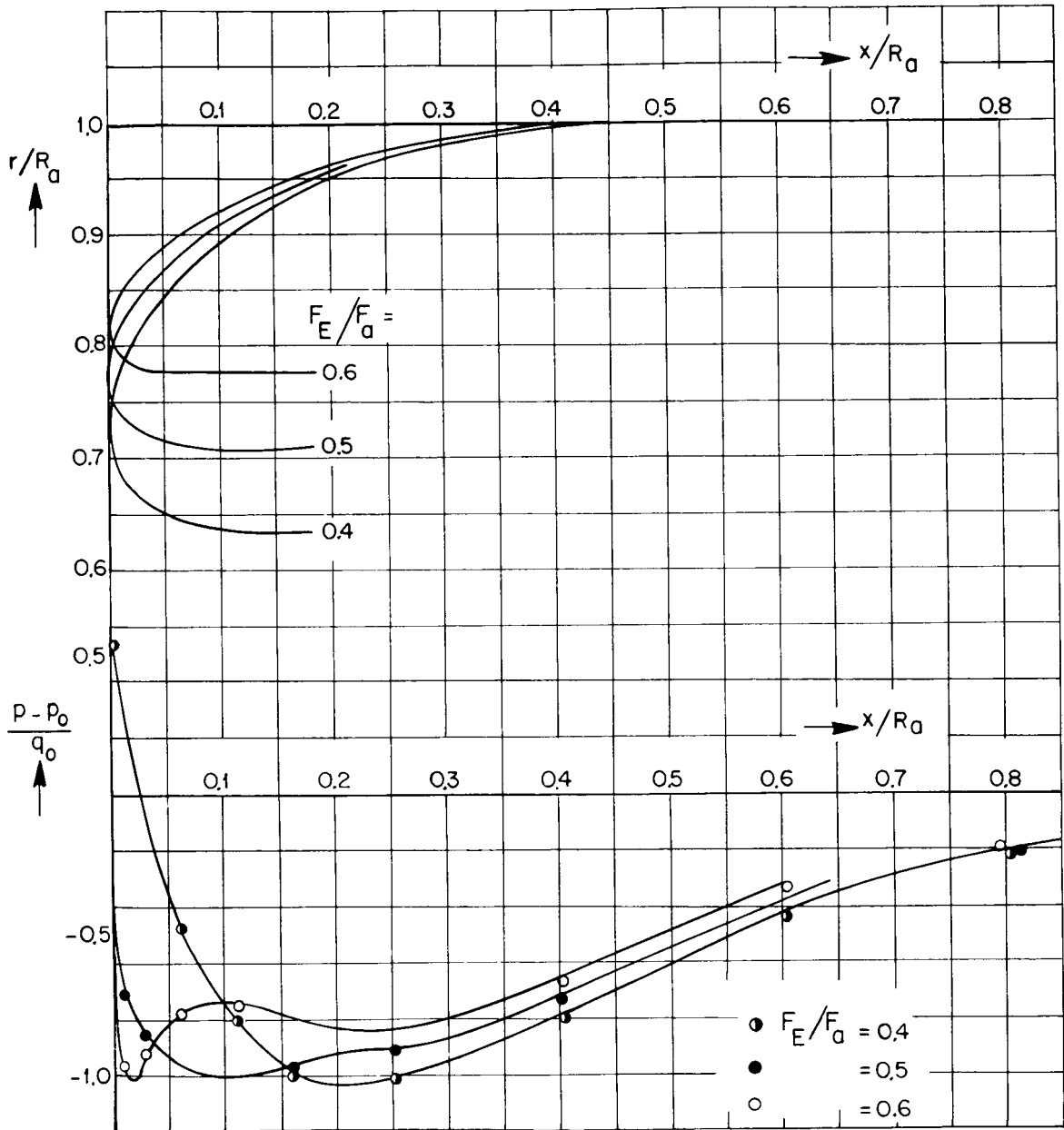


Figure 53.- Class IV of circular cowls (without hub); $v_E/v_0 = 0.3$, $\alpha = 0^\circ$.

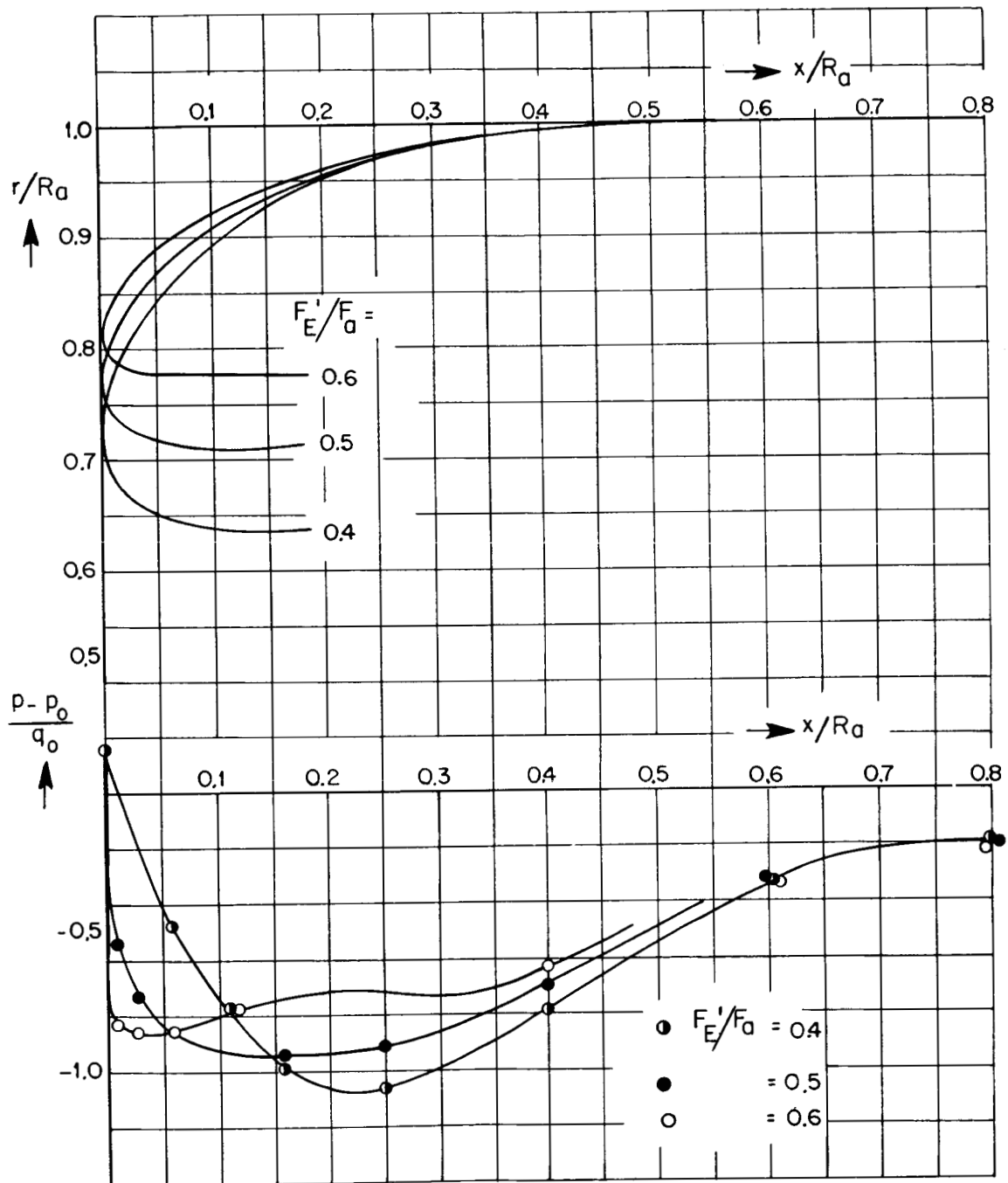


Figure 54.- Class IV of circular cowls (with hub); $v_E/v_0 = 0.3$, $\alpha = 0^\circ$.

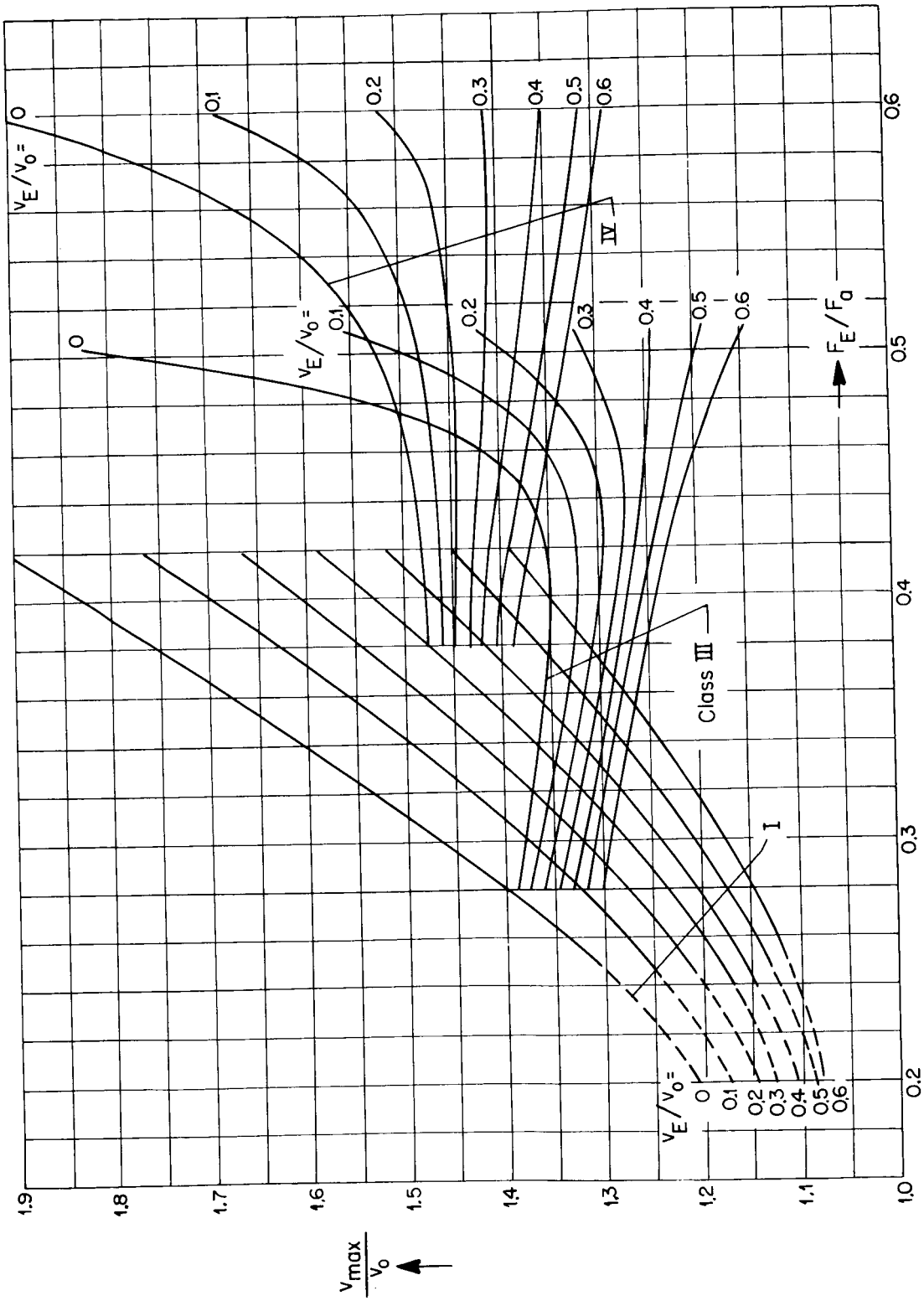


Figure 55.- Circular cowls (without hub); $\alpha = 0^\circ$.

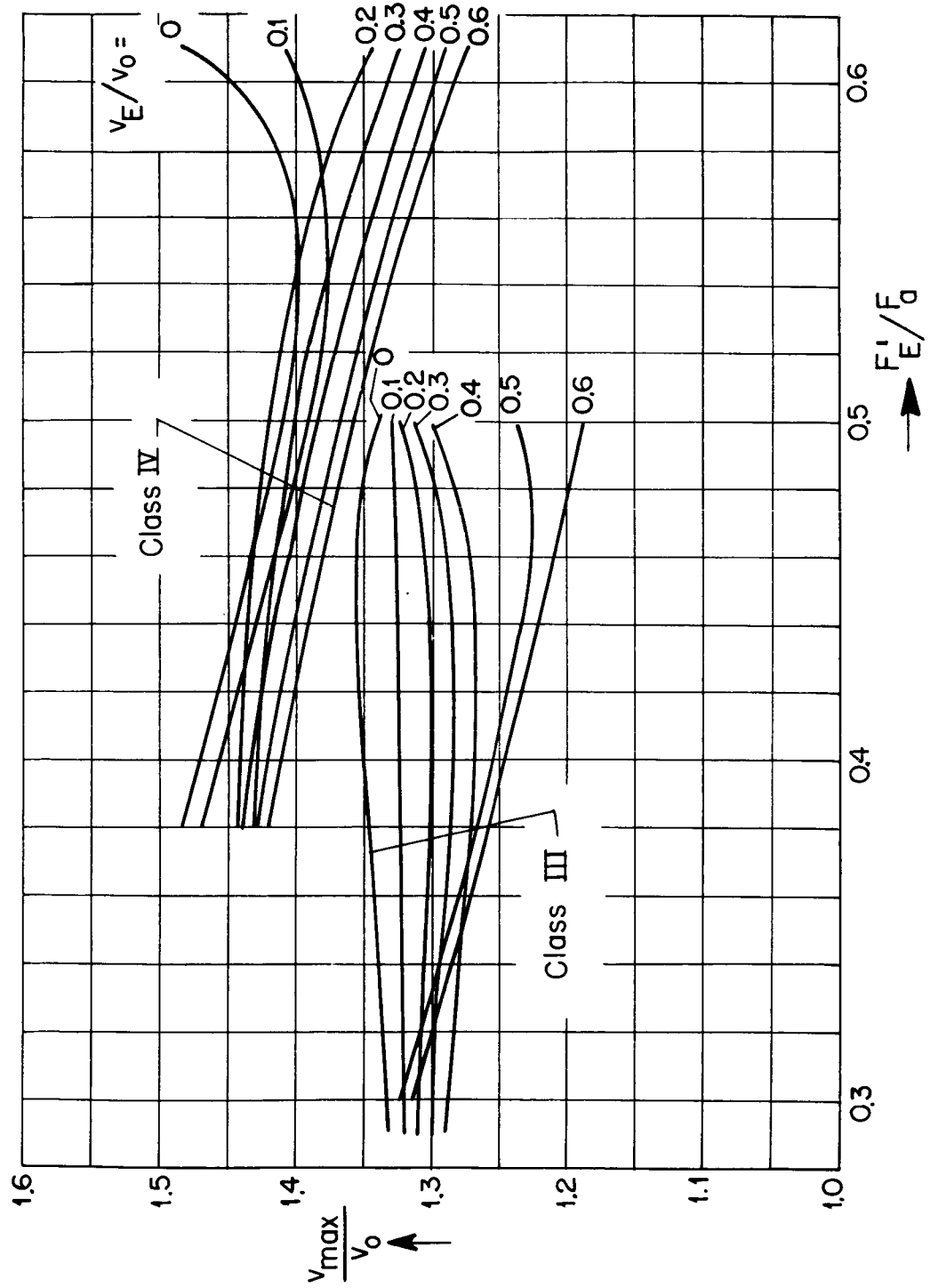


Figure 56.- Circular cowls (with hub); $\alpha = 0^\circ$.

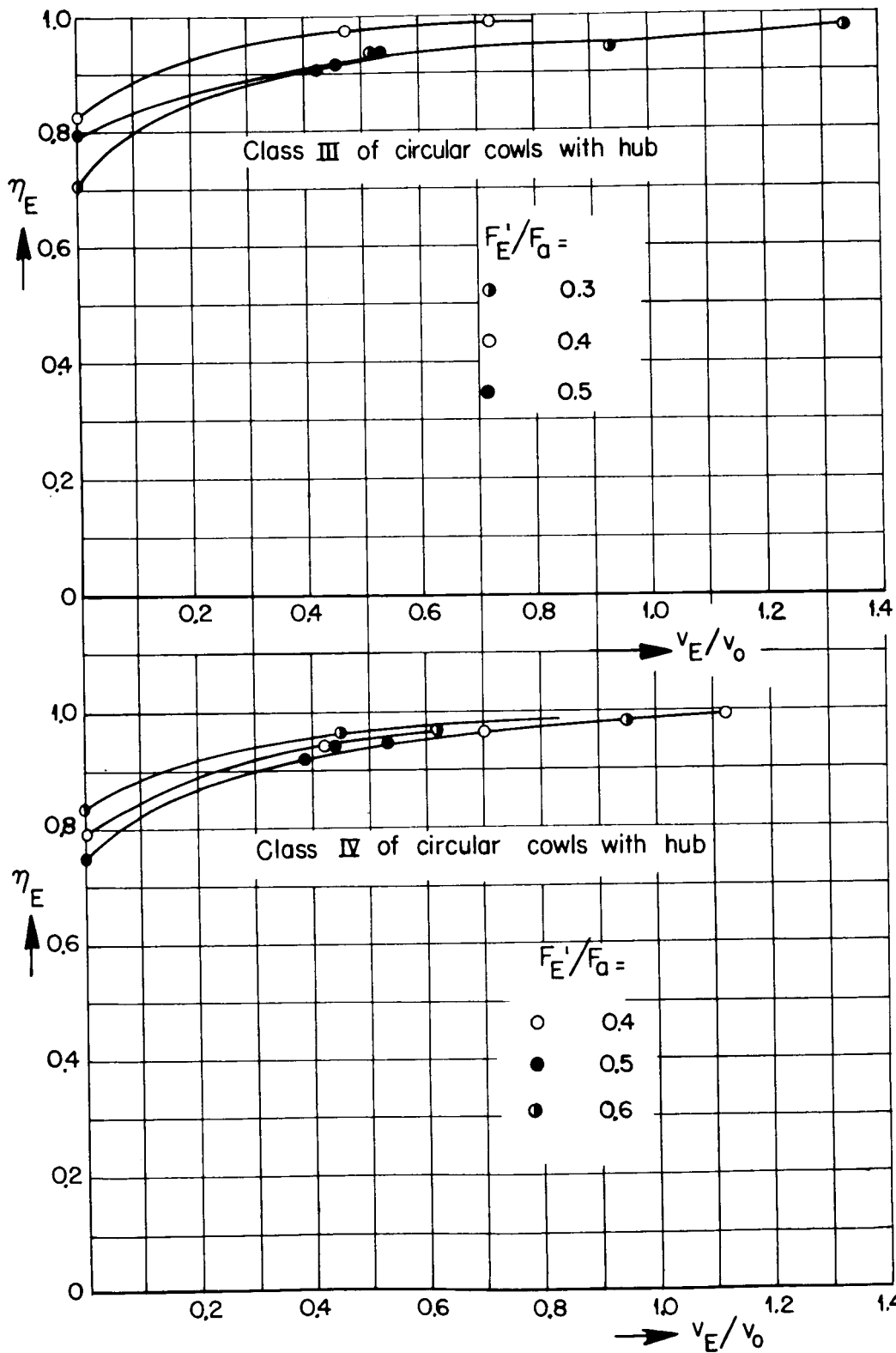


Figure 57.- Inlet efficiencies.

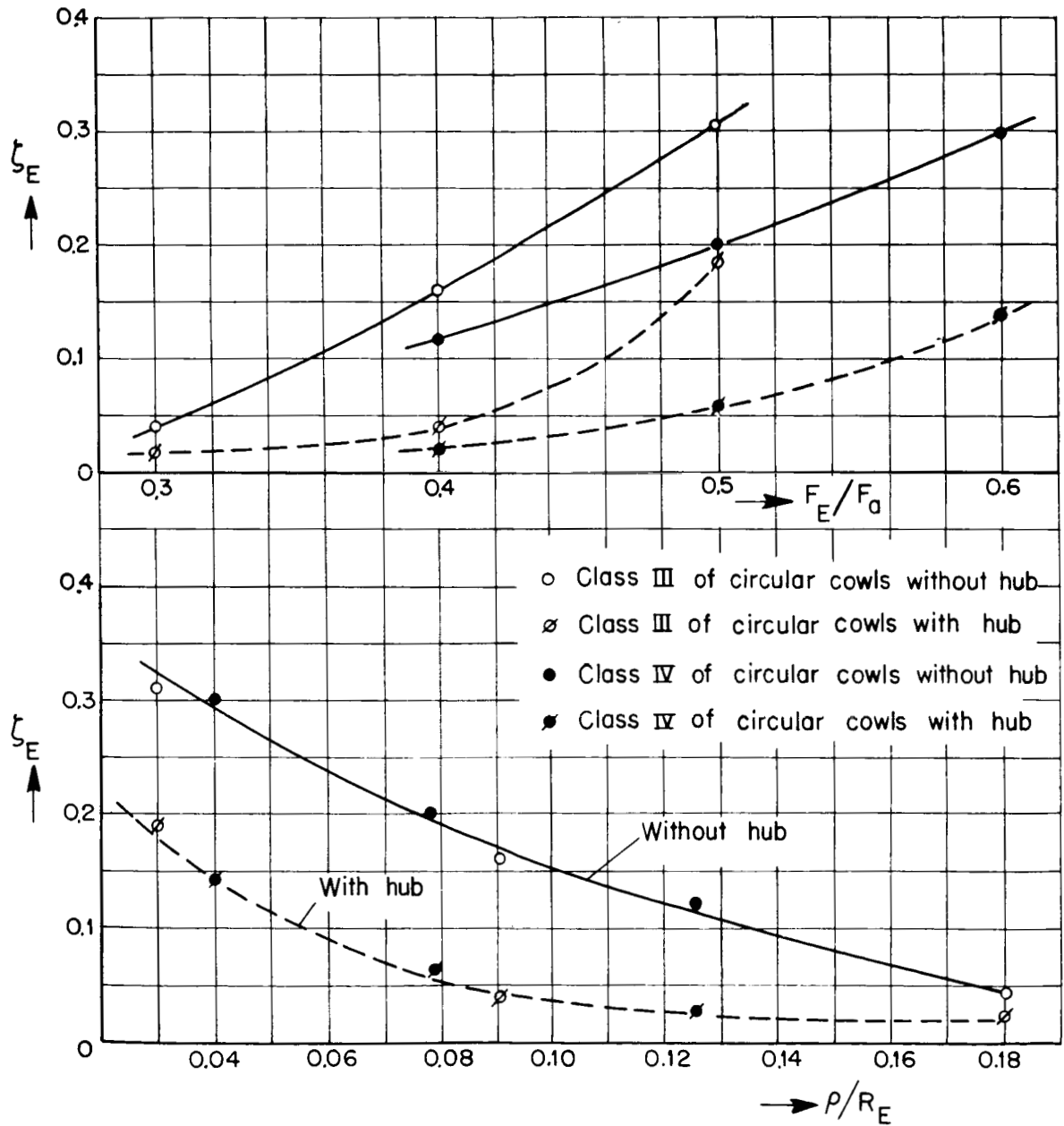


Figure 58.- Internal losses for static condition.

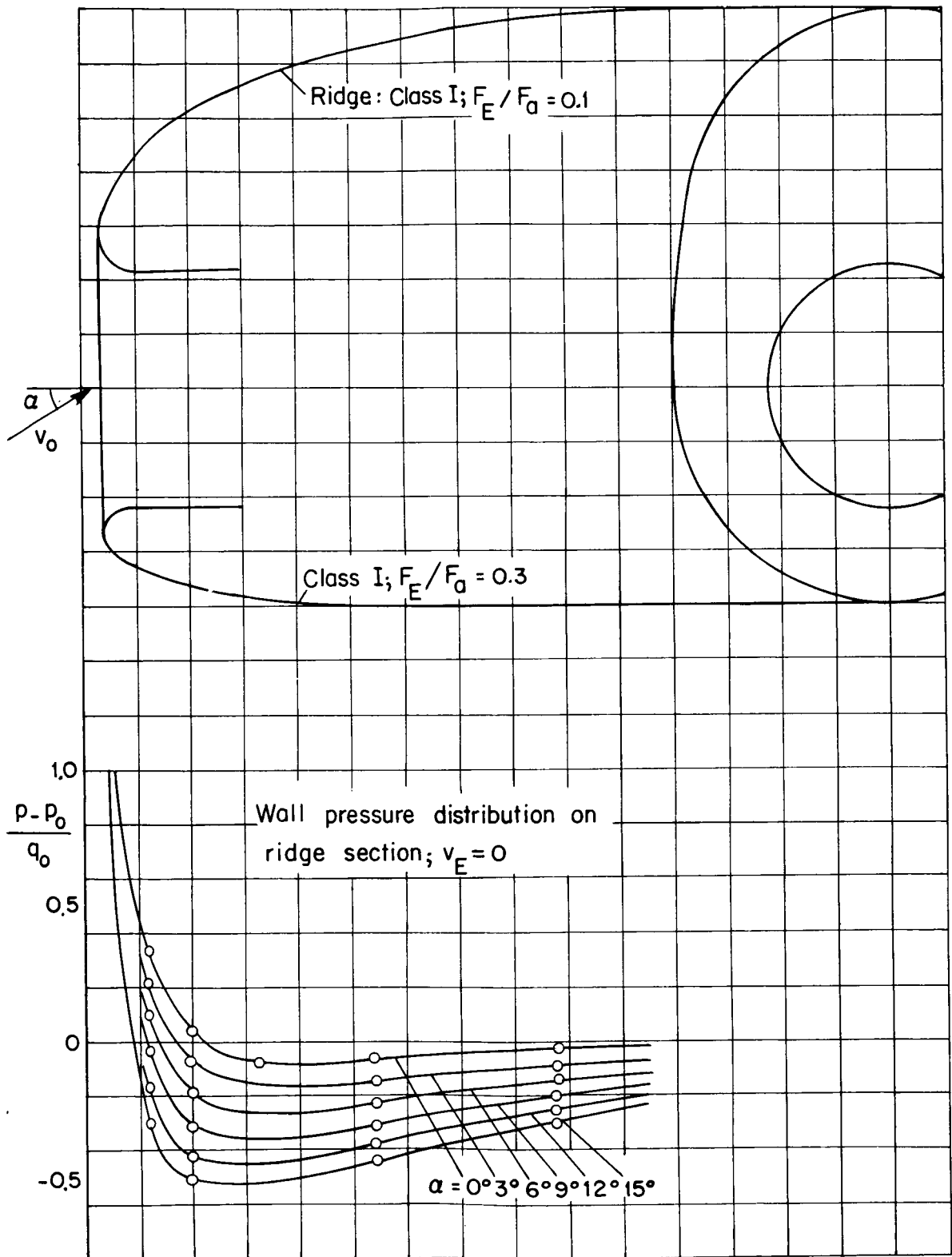


Figure 59